POTENTIAL USE OF SOLAR THERMAL AS AN ALTERNATIVE ENERGY SOURCE FOR ADAMA GENERAL HOSPITAL AND MEDICAL COLLEGE

M.Sc. Thesis

By

GEDLU SOLOMON

THERMAL AND AEROSPACE ENGINEERING PROGRAM
SCHOOL OF MECHANICAL, CHEMICAL AND MATERIALS ENGINEERING

ADAMA SCIENCE AND TECHNOLOGY UNIVERSITY

Adama, Ethiopia

January 2019

POTENTIAL USE OF SOLAR THERMAL AS AN ALTERNATIVE ENERGY SOURCE FOR ADAMA GENERAL HOSPITAL AND MEDICAL COLLEGE

M.Sc. Thesis

By

Gedlu Solomon

A Thesis Submitted to Thermal and Aerospace Engineering program of School of Mechanical, Chemical and Materials Engineering

Adama Science and Technology University in partial fulfilment of the requirement for the award of the degree of Master of Science in Thermal Engineering

Advisor: Dr. Chandraprabu Venkatachalam

Adama, Ethiopia

January 2019

Approval of Board of Examiners

We, the undersigned, members of the Board of Examiners of the final open defence by Gedlu Solomon have read and evaluated his thesis entitled "POTENTIAL USE OF SOLAR THERMAL AS AN ALTERNATIVE ENERGY SOURCE FOR ADAMA GENERAL HOSPITAL AND MEDICAL COLLEGE" and examined the candidate. This is, therefore, to certify that thesis has been accepted in partial fulfilment of the requirement for the award of the Degree of Masters of Science in Thermal Engineering.

____________________	________________	______________
Chairperson	Signature	Date
____________________	________________	______________
Internal Examiner	Signature	Date
____________________	________________	______________
External Examiner	Signature	Date

DECLARATION

I hereby declare that this M.Sc. Thesis entitled “POTENTIAL USE OF SOLAR THERMAL AS AN ALTERNATIVE ENERGY SOURCE FOR ADAMA GENERAL HOSPITAL AND MEDICAL COLLEGE” in partial fulfilment of the requirement for the award of the degree of Master of Science in Thermal Engineering is an authentic record of my own work carried out from September, 2017 to December, 2018 under supervision of Dr. Chandraprabu Venkatachalam Assistant Professor of Thermal and aerospace program, Adama Science and Technology University.

The matter embedded in this thesis has not been submitted for the award of a degree or diploma in any other university. All relevant resource information used in this paper has been duly acknowledged.

____________________________ ____________________________

Student Signature

This is to certify that the above statement made by the candidate is correct to the best of my knowledge and belief.

This has been submitted for examination with my approval.

____________________________ ____________________________

Advisor Signature

ACKNOWLEDGEMENT

First and for most I am very gratefully to appreciate Adama Science and Technology University for giving me Scholar to pursue my study. Next thank goes to my major Adviser Dr. Chandraprabu Venkatachalam who guides me to go in professional direction. I am also grateful to Assistant Professor, Dr. Addisu Bekele. Finally I would like to thank all staff member and class mates.

TABLE OF CONTENTS

LIST OF TABLES

LIST OF FIGURES

ABBREVATION

SHWS	Solar hot water system
LDC	Least developed country
HTF	Heat transfer fluid
PCM	Phase change material
HWLL	Hot water load for laundry
HWLK	Hot water load for kitchen
HWLR	Hot water load for restaurant
HWLS	Hot water load for shower
THWL	Total hot water load
CMS	Cost of mild steel
CHL	Cost of heat loss
TC	Total cost
CFG	Cost of fiber glass
LCS	life cycle saving of a solar water heating system
TAU, TLIN, SLOPE	Temporary variable in calculation
RISE	time of sunrise
SET	time of sunset
PV	photovoltaic cell
CI	Investment cost of solar water heating system
C_m	Annual maintenance and pumping cost
n	Number of Years
SHWS	Solar hot water system
T_{bt}	Water temperature at tank bottom

FPC	Flat plate collector
ETC	Evacuated tube collector
CPC	Compound parabolic collector
LFR	Linear Fresnel reflector
CTC	Cylindrical trough collector
PDF	Parabolic dish reflector
HFC	Heliostat field collector
CFD	Computational Fluid Dynamic
Birr	Ethiopian currency
DCV	Direction control valves
PCV	Pressure control valves
FCV	Flow control valves

NOMENCLATURE LIST

H	Daily global radiation [MJ/m^2/day]
H_b	Daily beam radiation [MJ/m^2/day]
H_d	Daily diffuse radiations [MJ/m^2/day]
R_b	Beam radiation factor [dimensionless]
R_d	Diffuse radiation factor [dimensionless]
Rr	Reflected radiation factor [dimensionless]
I	Hourly glodal radation [MJ/m^2]
F'	Collector efficiency factor [dimensionless]
FR	Collector heat removal factor [dimensionless]
η	Collector efficiency [dimensionless]
d	Diameter [m]
t	Thickness [m]
L	Length [m]
T_C	Total cost [Birr]
d_c	Direct cost [Birr]
id_c	Indirect cost [Birr]
f_a	Annual fraction of load supplied by Solar energy [dimensionless]
Q_a	Annual heating load [kWh]
i	Annual market discount rate [%]
i_e	Annual market rate of energy escalation [%]
f	Friction factor [dimensionless]

ABSTRACT

Solar energy is one of the widely used renewable energy that can be harnessed either by directly driving energy from the sunlight or indirectly. Solar water heating on the other hand is one of the applications of solar energy that has drawn great attention among researcher in this field. Solar collector and storage tank are the two core components in solar water heater application.

Hospitals and hospital buildings everywhere are large consumers of energy, which they use in many different ways. As large consumers of energy more than 50-60 % of energy is used for thermal energy application in the hospital have high bills for electricity and fuels, Ethiopia national energy agency (2013). This study aims is substituting electricity and fuel (diesel) assist energy source by solar-thermal system for hot water supply to Adama general hospital.

The load estimation technic applied by combine international and local water usage consideration, available radiation is calculated from sunshine hour duration in every 3 hours in the years of 2013 to 2017 G.C collected from nearby metrology agency also diurnal air temperature model is selected because of the parameter available to be used the equation used data for ambient temperatur (maximum and minimum) in the year of 2017.Optimization of storage tank and insulation thickness done by consider heat loss and cost of material. Transient performance of the system is computed using a numerical heat transfer model of U-Type evacuated tube solar collector with storage tank.

Sizing of solar collector and storage tank is based on amount of energy need to fulfil the daily water demand with required water temperature and the result from the analysis shows that the daily hot water demand of Adama general hospital is fulfil by the use of 52 collectors and two storage tank each with the capacity of 15.011 m^3 with initial investment cost 1,066,388.44 Birr and life cycle cost 2,003,254.14 Birr also unit cost per kWh equals to 0.24 Birr and the payback period of the project 67 months.

Keywords: Solar water heating system, evacuated tube solar collector, load estimation, Storage tank, solar radiation, ambient temperature, pressure drop, life cycle cost

CHAPTER 1

INTRODUCTION

Energy is one of the major inputs for the economic development of any country; in the case of the developing country the energy sector assumes a critical importance in view of ever-increase energy needs required huge investment to meet them, Maxi Brochure (2015). But a world are under stress on ongoing environmental damages by polluting the atmosphere and world demand for energy from non-renewable reserves run-out within some of our lifetimes (Estimated from international organization). Without an energy access, technologies that deliver modern life would cease to exist/function.

There are two types of energy renewable and non-renewable the difference is that some renew at faster rate than others making them more sustainable than those that do not renew very fast, Ministry of water irrigation and electricity (2017). Renewable energy obtained from sources that are essentially inexhaustible examples like solar power, wind power, geothermal energy, tidal power and hydroelectric power. The most important feature of renewable energy is that it can be harnessed without the release of harmful pollution, Maxi brochure (2015).

We are blessed with Solar Energy in abundance at no cost. The solar radiation incident on the surface of the earth can be conveniently utilized for the benefit of human society. One of the popular systems that harness the solar energy is solar hot water system (SHWS) Selvakumar et al., (2014).

For the first time, Renewables 2017 tracks off-grid solar PV applications more closely in developing Asia and sub Saharan Africa. Over the forecast period, off-grid capacity in these regions will almost triple reaching over 3000 MW in 2022 from industrial applications, solar home systems (SHSs), and mini-grids driven by government electrification programmes, and private sector investments. Figure 1.1 shows a brief review of forecasting off-grid capacity in developing Asia and sub Saharan Africa region.

Although this growth represents a small share of total PV capacity installed in both regions, its socio-economic impact is nonetheless significant. Over the next five years, SHSs the most dynamic sector in the off-grid segment are forecast to bring basic electricity services to almost 70 million more people in Asia and sub Saharan Africa.

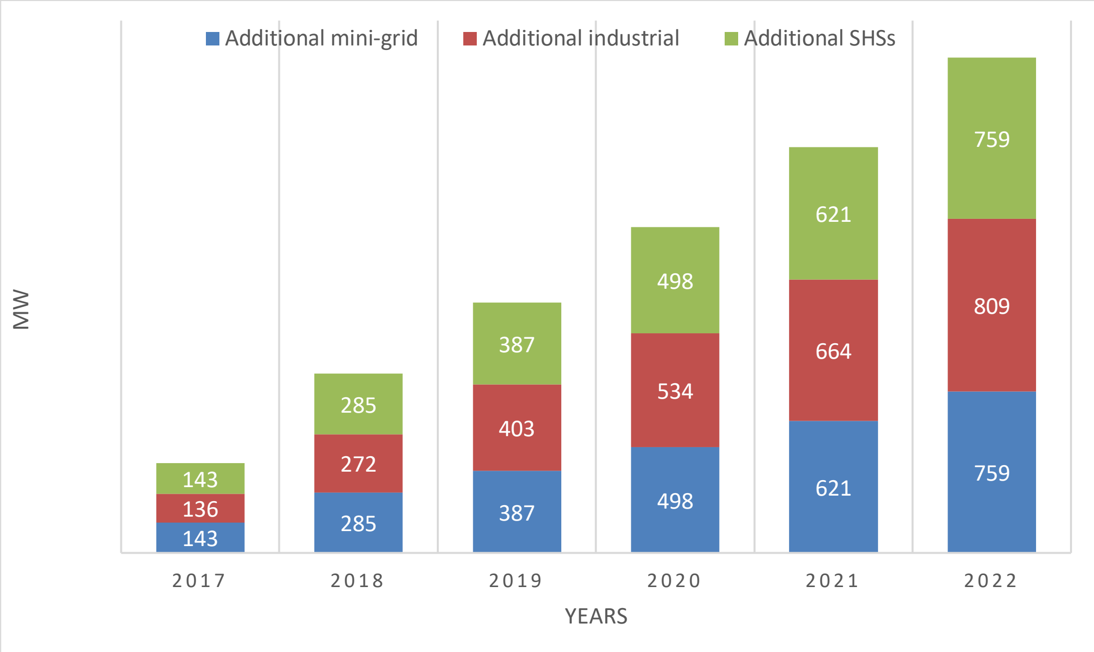

Figure 1.1: Cumulative growth of off-grid solar application in forecasting years, International energy agency (2017).

It will also lead to new business players bringing innovative payment solutions that allow low-income populations initial access to electricity services.

Solar heater is a device which is used for heating the water for production of hot water or steam for domestic and industrial purpose by utilizing solar energy. Solar is the energy which is come from sun in the form of solar radiations infinite amount, when the solar radiation falls on absorbing surface, then they gets converted into heat. Heat losses happen due to radiation and convection into environment, such losses increase rapidly as the temperature of the working fluid increase. Solar water heating systems have reached technical maturity and are used in many countries. After the first oil crisis in 1973, the strategies used by industrialized and developing countries to reduce their oil dependence have been numerous. A diversification of energy import, a structural change of the large domestic product (industrial development of activities using a low energy expenditure) or an increase of the national supply have been the essential measures taken by the countries with various degree of importance. Solar water heating system is one of essential process in hospital, residential, hotel industry and domestic services. Many services and processes in hospital need hot water for different applications such as washing and boiling medical equipment, washing clothes, for bath application, kitchen processes, etc.

1.1 The research problem

The Ethiopia population will continue to grow for several decades to come. Energy demand is likely to increase ever faster and the proportion of energy supplied by hydroelectricity and alternative energy source will also grow at the same rate for the last several years. Ethiopia electric power corporation the main provider of power has faced a critical power shortage, as part of ongoing fast economic development noted in the country many factories, hospitals, and hotels are established, adding that this had increased local energy demands.

Hospitals and hospital buildings everywhere are large consumers of energy which they use in many different ways. As large consumers of energy more than 50-60 % of energy is used for thermal energy application in the hospital, Ethiopia national energy agency [2013]. Have high bills for electricity and fuels, the cost of energy used in hospitals 100,000 birr/month as in other types of premises is subject to market force such as supply and demand, variation in prices and taxes and the form of energy used. It is anticipated that the cost of energy will generally increase over the long term.

1.2 Motivation for this work

For Ethiopia, green growth is a necessity as well as an opportunity to be seized. It is a necessity because it must arrest land degradation that threatens millions of our citizens with poverty. It is an opportunity because it motivates to use our country’s huge renewable energy potential in the development of our economy. That is why Ethiopia has developed its Climate Resilient Green Economy Strategy to transform it by 2025 from its present LDC status with agriculture as its main economic sector and annual per capita greenhouse gas emission of 1.8 tonnes to a lower middle income status with industry as its main economic sector and with zero net carbon emission, Tewolde B., (2016).

Fortunately Ethiopia is located in the part of world where the sun shines for maximum number of hours. It is therefore a matter of interest to assess the significance of solar thermal energy and its utilization in different fields of application. Solar thermal system which is environmental friendly and sustainable source of energy is the best alternative. But, this enormous amount of solar energy is not utilized as expected in the country, Ethiopia national energy agency (2013).

1.3 General objective: The general objective of this thesis is to substitute conventional hot water generation (diesel fuel and electrical heater assisted) with solar thermal heater (solar water heating system) for Adama general hospital and medical college hot water supply.

1.4 Specific objectives

- ✓ To estimate the amount of hot water load with corresponding water temperature for daily usages.
- ✓ To estimate the incidence solar radiation on inclined surface and diurnal cycle varation of ambient temperature.
- ✓ To determine storage tank capacity, optimization of thermal storage tank thickness and insulation material thickness.
- ✓ Modelling the transient thermal analysis of evacuated tube solar collector.
- ✓ Simulation of solar water heating system.
- ✓ Sizing of evacuated tube solar collector.
- ✓ Selection of system components like pumps, valves
- ✓ Financial analysis of the designed system.

1.5 Significances of the study

This thesis work focus on the solar thermal system for supply hot water demand to the Adama general hospital so the system will minimizes the dependence of electric and fossil fuel energy consumption of hospital in addition to this will form health environment.

1.6 Scope and Limitations

1.6.1 Scope of the study

This study mainly focuses on the solar thermal energy as a substitute for fuel and electric use for Adama general hospital and it is designed to work at Adama weather condition. This study also includes the economic analysis of a solar water heater system.

1.6.2 Limitations of the study

This study is limited to harvesting of energy so it does not go to heat distributions in difference appliance for hospital usages. All thermo-physical properties of the system are a function of temperature; this behaviour of a system more complicates the analysis, but in this study assumes that the thermo-physical properties are constant.

CHAPTER 2

LITERATURE REVIEW

2.1 Background on Solar water heating system:

Solar water heating systems are generally very simple and using only sunlight to heat water a working fluid is brought into contact with a dark surface exposed to sunlight which causes the raise in temperature of the fluid. This fluid may be the water being heated directly also called a direct system or it may be a heat transfer fluid such as a glycol/water mixture that is passed through heat exchanger and utilize the heat called an indirect system.

These systems can be classified into three main categories:

A. Active Systems

Active systems use electric pumps, valves, and controllers to circulate water or other heat transfer fluids through the collectors. So, the Active systems are also called forced circulation system and can be direct or indirect.

The active system is further divided into two categories:

Open-Loop Active Systems

Open-loop active systems use pumps to circulate water through the collectors this design is efficient and lowers operating costs but is not appropriate if the water is hard or acidic because scale and corrosion quickly disable the system.

These open-loop systems are popular in non-freezing climates.

Closed-Loop Active Systems

These systems pump the heat transfer fluids (usually a glycol-water antifreeze mixture) through collectors and heat exchangers transfer the heat from the fluid to the household water stored in the tanks.

Closed-loop glycol systems are popular in areas subject to extended freezing temperatures because they offer good freeze protection.

B. Passive Systems

Passive systems simply circulate water or a heat transfer fluid by natural convection between a collector and an elevated storage tank (above the collector). The principle is simple as the fluid heats up its density decreases and the fluid becomes lighter and rises to the top of the collector where it is drawn to the storage tank also the fluid which has low temperature settle down at the bottom of the storage tank then flows back to the collector. Passive systems can be less expensive than active systems but they can also be less efficient, thermosiphon system is the best example of passive systems.

Thermosiphon Systems:

In the thermosiphon system, water comes from the overhead tank to bottom of solar collector by natural circulation and water circulates from the collector to storage tank as long as the absorber keeps absorbing heat from the sun and water gets heated in the collector. The cold water at the bottom of storage tank run into the collector and replaces the hot water which is then forced inside the insulated hot water storage tank. This process will stop when there is no solar radiation and thermosiphon system is simple and requires less maintenance due to absence of controls and instrumentation. Efficiency of a collector depends on the difference between collector and ambient temperature and inversely proportional to the intensity of solar radiation.

C. Batch system

Batch System (also known as integral collector storage system) is simple passive system consist of one or more storage tanks placed in an insulated box that has a glazed side facing the sun. Batch systems have combined collection and storage functions depending on the system there is no requirement for pumps or moving part so they are inexpensive and have few components, less maintenance and fewer failures.

Reviews on system component

Pump selection:

Pumps transfer liquids from one point to another by converting energy from a rotating impeller into pressure energy. The pressure applied to the liquid forces the fluid to flow at the required rate and to overcome friction losses in piping, valves, fitting and process equipment, pumping system tips sheet # 2 (2005).

Most active solar system uses centrifugal pumps because Non-positive displacement pump used generally for low pressure and high volume flow application.

Pump selection depends on the following factors:

- System type(direct or indirect)
- Heat collection fluid
- Operating temperature
- Required fluid flow rates
- Heat or vertical lift requirement
- Friction losses

The most common pump used in solar system is the “wet rotor” type in which the moving part of the pump, the rotor, is surrounded by liquid. The liquid acts as a lubricant during pump operation.

Selection of Temperature Sensor:

Temperature is one of the most commonly measured Variables there are a wide variety of temperature sensors on the market today like Thermocouples, Resistance Temperature Detectors (RTDs), Thermistors, Infrared, Semiconductor Sensors and other.

The temperature sensor chosen for a particular process depends on the following consideration.

- Cost
- Range of operation
- Sensitivity
- Response time
- Repeatability
- Ability to survive environment

There is usually some measurement range overlap, and more than one sensor type may be suitable for an application. For example, biological systems can often be monitored with non-contact infrared (IR) detectors, thermistors, or silicon diodes. Occasionally the only practical way to monitor an internal temperature is to embed a temperature sensor into a product during the manufacturing process. An example is an electric motor with an embedded resistive temperature detector (RTD), or a thermistor on one of the motor’s copper windings.

Valve:

Different types Valves are used in hydraulic circuits to control pressure, flow direction and flow rate. They utilize mechanical motion to control the distribution of hydraulic energy within the system.

Directional control valves (DCV): For directing fluid flow to one or the other side of a cylinder or motor.

Pressure control valves (PCV): For controlling the fluid pressure at a point and

Flow control valves (FCV): For limiting the fluid flow rate in a line, which in turn limits the extension or retraction.

Actuators:

Pumps perform the function of adding energy to a hydraulic system for transmission to some remote point. Fluid power actuators do just the opposite. They extract energy from a fluid and convert it to a mechanical output to perform useful work. Fluid power can be transmitted through either linear or rotary motion by using linear actuators called hydraulic cylinders or rotary actuator called hydraulic motors.

Linear actuators/hydraulic cylinders: hydraulic cylinders extend and retract to perform a complete cycle of operation

Rotary actuator called hydraulic motors: rotary actuator can be of limited rotation or continues rotation type. Limited rotation motors are called oscillation fluid motors because they produce a reciprocation motion. Continues rotary hydraulic motors (or simply hydraulic motors) in reality are pumps that have been redesigned to withstand the different forces that are involved in motor applications. As a result hydraulic motors are of gear, vane or piston configuration.

Hydraulic motors: Are actuators that can rotate continuously and as such have the same basic configurations as pumps. However, instead of pushing on the fluids as pumps do, motors are pushed upon by the fluid. In this way hydraulic motors develop torque and produce continues rotary motion.

2.1.1 Review on Solar Collector

Solar collectors are devices that are used to harness the energy from the sun converting the incoming solar radiation into useful heat energy. Being the key element in solar energy utilization systems, solar energy collectors act as heat exchangers that converts the solar radiation energy into internal energy of the transport medium. The solar energy will be collected by absorbing the incoming solar radiation and converting it into heat, and transferring this heat to a fluid. Then, this heat energy will be transferred from the fluid to the heat application processes or the storage tank.

Soteris A. Kalogirou (2004) described various types of solar collector such as flat plate, compound parabolic, evacuated tube, parabolic trough, Fresnel lens, parabolic dish, and Heliostat field collector with their application. That was followed by optical, thermal, and thermodynamic analysis of the collector and the description of the methods used to evaluate their performance these include solar water heater, space heating and cooling, heat pump and refrigeration, industrial process heating, steam generation, desalination, thermal power system and chemical application. Various types of solar collector with efficient temperature range were listed in table 2.1

Table 2. 1: Comparisons the different types of Collectors

Collector type	**Absorber type**	**Concentration ratio**	**Temperature range** (℃)
(FPC)	Flat	1	30-80
(ETC)	Tubular	1	50-200
(CPC)	Tubular	1-5	60-240
(LFR)	Tubular	15-45	60-250
(CTC)	Tubular	10-50	60-300
(PDE)	Point	100-1000	100-500
(HFC)	Point	150-1500	150-2000

Siva et al. (2017) investigated on the performance of the evacuated tube solar collector with heat pipe heat extraction method numerically and experimentally analysis. And saw the duration of time required by the collector to gain the heat is less compared to other collector. Aman S. and Pathak A.K. (2016) explained the working model of evacuated tube solar collector, hybrid model and their application (solar water heater, solar cooker, solar dryer, solar desalination, air conditioning, heat engines, steam generation) and the authors reached on the conclusions that an evacuated tube collector was very efficient to be used at higher operation temperature and gave some suggestion to overcome obstacles. Chien et al. (2011) have worked on theoretical and experimental investigations of a two-phase thermo-syphon solar water heater and in this work the performance of this innovative solar water heater at different solar radiation intensities and tilt angles was experimentally discussed. The experimental results show that the best change efficiency of the two phase thermo-syphon solar water heater was 82% and the charge efficiency decreases no more than 5% when the tilt angle of the system was less than 15. Chong et al. (2012) have studied solar water heater with stationary V-trough collector using forced circulation system in this article experimental study and cost analysis of the stationary V-trough solar water heater system were presented in details. The performance test was carried out in two different cases: without glazing and thermal insulation and with glazing and thermal insulation installed to the prototype SWH including reflector, absorber and storage tank. With V-trough solar water heater, improve the thermal efficiency of the whole system. The main advantages of this type system were that easy to be fabricated, cost effective and high thermal efficiency. This prototype system had achieved the optical efficiency of 70.54% and the temperature of 85.9°C. Budihardjo and Morrison (2009) have studied the thermal performance of water-in glass evacuated tube solar water heaters and was evaluated using experimental measurements off optical and heat loss characteristics and a simulation model of the thermosiphon circulation in single-ended tubes. The performance of water-in-glass evacuated tube solar collector system were compared with flat plate solar collector shows that an evacuated tube system with 30 tubes has slightly lower energy saving than a two panel flat plate system. Xinyu et al., (2014) have worked on experimental investigation of the higher coefficient of thermal performance for water-in glass evacuated tube solar water heater in china. In this test, the performance of more than 1000 water-in-glass evacuated tube SWHs according to Chinese standards and found that the heat loss from the storage tank and capacity of the solar collector affected their thermal performance. In this study, they found that a shorter evacuated tube exhibited better thermal performance than longer tube. A shorter tube was also less likely to be damaged during transportation. The experimental results showed that the distance between the centres of the tubes will have an effect on the thermal performance of a water-in-glass evacuated solar water heater without diffuse reflectors. Luigi et al., (2016) have presented the comparison of mat-lab and TRYSYS 17 solvers to transient analysis of solar water heater using experimental input data for all model like irradiation, ambient temperature and wind velocity. A zero dimensional analytical model has been develop to evaluate the time-variation temperature of each collector component as well as the temperature of heat transfer fluid (HTF).A transient one dimensional model has been adopted for the evaluation of the temperature field of HTF flowing through the immersing coil heat exchanger also one dimensional model the water was consider divided into N tank isothermal node represent water layer of equal volume. The numerical simulation of the entire solar domestic hot water system component has been dealt with an iterative approach. Rokas et al., (2015) have studied the operation of solar water heater system in medium scale 60 m^2-166 m^2 solar collector panel by selected for the analysis both equipment used (flat plate collector, evacuated tube collector)and type of energy user (swimming pool building, domestic hot water heating , district heating) the result of analysis showed that measured annual efficiency of the analysed solar water heater system reached up 44% (design for domestic heater water and flat plate collector),39% (install in the swimming pool building and solar energy was used for hot water heating as well as a swimming pool heating) ,24% (was installed as a part of the district heating and consist of U-pipe evacuated tube collector. Zambolin and Del (2010) carried out thermal performance comparisons in two types of the flat plate and vacuum tubes solar collectors. They concluded that, in the steady-state conditions, the slope of the linear regression instantaneous efficiency with increasing heat losses in flat plate collector was greater than the water-in-glass ETCs. Xun et al., (2017) have studied on solar heating system in Lhasa (cold zone)in china: altitude 3650 m, a annual average temperature 8.1℃,cumulative solar radiation to 7.2 GJ/m^2per year and 2.56 GJ/m^2per year winter was investigated under the simulation under the simulation charging and discharging operation mode based on the solar heating system ,a numerical calculation method of the tank temperature distribution under the simulation charging and discharging operation mode was proposed and validated by experments.in addition to the numerical calculation method of the tank temperature distribute the system COP and the heating effect were also investigated. the calculate result showed that the system COP reached an average number 3.0 ,which was nearly equal to that of gas-boiler heating system and much higher than that of electrical heating system. Hernandez E. and Reguzman (2016) have tested three different types of solar water heaters two flat plate collector with two different material (stainless steel coil and copper coil) and vacuum tubes were analysis in the thermosiphon solar water heater system, the result showed that where stainless steel tube collector reached a maximum efficiency of 71.58%, the copper tubing collector a maximum value of 76.31% and vacuum tube heater collector a maximum efficiency of 72.33%. Adel et al., (2016) conducted an experimental study to compare the performance of both FPC and a heat pipe ETC for domestic water heating system application. The collector efficiencies were found to be 46.1% and 60.7% and the system efficiencies were found to be 37.9% and 50.3% for FPC and heat pipe ETC, respectively. Dagim K., (2016) have studied on solar thermal system for Hot water supply to Minilik II hospital to solve the derived system of equations, the implicit finite-difference scheme was suggested. The proposed method allows the transient processes occur in the flat-plate solar collector to be Simulated It was found that for Minilik II hospital of total daily hot water consumption of 30.475 m^3 a total of 108 collectors with two storage tanks of each capacity 18.3 m^3 were needed with initial capital cost of 1,006,865 Birr per project, which will cost a total of 1,864,054 Birr per project through-out its life time and the life cycle cost saving will be 1,869,571 Birr per project. The unit price of solar thermal energy was 0.033 Birr per kWh and the payback period of the project was 2.2 year. Since the unit cost of solar energy (0.033 Birr/kWh) was less than the unit cost of electricity (0.46Birr/kWh) in Ethiopia, therefore water heating by solar energy was a viable alternative to heating by electricity and fossil fuel (furnace oil). Addisu B., (2007) Have studied on the possible use of solar energy for large scale water heating system was conducted for the following sites in Ethiopia: Addis Ababa Tannery, Dire Tannery, Modjo Tannery, and Jimma Hospital. According to his study for addis abeba tannery of total daily hot water consumption of 32.6 m^3 a total of 261 collectors with four storage tanks of each capacity 6.5 m^3 were needed with initial capital cost of 3,183.05 Birr per collector, which will cost a total of 4,161.00Birr per collector throughout its life time and the life cycle cost saving will be 5,797.00 Birr per collector. For Dire tannery of total daily hot water consumption of 18.53 m^3 a total of 149collectors with two storage tanks of each capacity 7.4 m^3 were needed with initial capital cost of 3,206.62 Birr per collector, which will cost a total of 4,191.00 Birr per collector throughout its life time and the life cycle cost saving will be 5,610.00 Birr per collector. for Ethiopian tannery of total daily hot water consumption of 250 m^3 a total of 1667 Collectors with four storage tanks of each capacity 52.1 m^3 were needed with initial capital cost of 3,209.08 Birr per collector, which will cost a total of 4,194.00 Birr per collector throughout its life time and the life cycle cost saving will be 5,824.00 Birr per collector. For Jimma hospital of total daily hot water consumption of 119.24 m^3 a total of 795 collectors with four storage tanks of each capacity 24.8 m 3 were needed with initial capital cost of 3,216.77 Birr per collector, which will cost a total of 4,205.00 Birr per collector throughout its life time and the life cycle cost saving will be 6,197.00 Birr per collector. Dejene A., (2011) Have studied on the Technical performance of parabolic trough steam generation and oil fired boiler steam generation system for Black lion general hospital which was located in Addis Ababa. The hospital uses furnace oil for the generation of the steam, consumes 245 $m^3$and pays 1,593,087.41 Birr in the year, 2008/09. The result from technical feasibility study shows the parabolic trough can meet the steam demand of the hospital at the required time, more than 8 hour per day, as the hospital currently require steam for different activities during the day time for 8hour per day. During cloudy day the conventional back up steam generation system will meet the daily demand for few days of the year. Similarly the economic analysis shows that although the initial investment of concentrated solar steam generation was high as compared to convention steam generation system, the reverse was observed in operation and maintenance cost, resulting concentrated solar steam generation break even (payback) to occur early, after 7 year the system let to operate over the conventional steam generation.

2.1.2 Review on Energy storage

Due to the intermittent nature of solar energy, storage of energy is required for different application (use later). Energy storage is a medium that stores all forms of energy to perform useful function after sometimes is known as energy storage. Tiwari et al., (2016) Storage tank classification listed below in Figure 2. 1

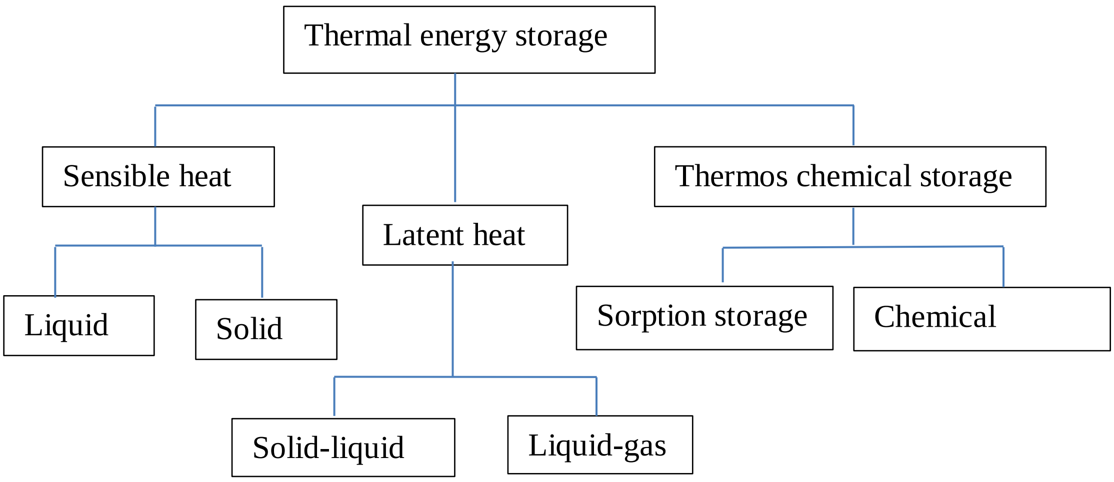

Figure 2.1: Solar thermal energy storage classification

2.1.2.1 Sensible heat storage:

The level of sensible heat-storage system depends on the heat capacity $m * C_p$ and temperature difference during charging and discharging.

Liquid media storage:

Many liquid can be used for thermal storage. However the water is most economical free available with higher capacity in abundant liquid for the short term storage of thermal energy less than 100 ℃.

Three main benefits are

- It is nontoxic and non-combustible.
- It has low thermal conductivity and viscosity
- The charging and discharging of energy can occur simultaneously.

Solid media storage:

Thermal energy can be stored in loosely packed rock-bed material either in insulation box or underground for a temperature range of 100 ℃.

2.1.2.2 Latent heat storage:

Latent heat is thermal energy either absorber or released by substance during a phase change at constant temperature. Most phase change material has high thermal energy storage density compared with sensible heat storage Martials.

2.1.2.3 Thermo-Chemical storage:

Chemical energy is a form of potential energy. The storage capacity depends on its source.in this concept; energy is stored in the form of heat from chemical reactions. It is often of a large magnitude than latent-heat storage. The idea of storage solar energy by the use of chemical reactions is not a new concept.

Delfine et al., (2015) Simulated the existing design of domestic solar water heater and the system performance modelled by mat-lab programming language for difference design parameter with difference storage tank volumes and the results observe that effect of storage volume on solar fraction. Solar fraction increase when increase storage volume this increase the relative high for small volume and moderates for large volume, remain near constant for higher volumes in all simulation independent of other consideration. Zahedi et al., (2007) performed the computer simulation program on variation of tank volume (collector area 2

m^2) on solar fraction for different tank height and effect on $\frac{V_L}{A_c}$ on the solar fraction for the difference T(set). and get the result increasing the storage tank height above 1.0 m has no significant effect on solar fraction and reach on the best optimum ratio of tank volume to collector area ($\frac{V_L}{A_c}$) when Ac=2 m^2 was 50-70 $\frac{L}{m^2}$. Doerte and Dorothea., (2008) Performed experimental analysis of sensible heat storage system using concrete as storage materials, a major focus was cost reduction of heat exchanger and the high temperature concentred storage material was proved that concrete storage technology was a suitable option for storing sensible heat application for solar trough system, industrial waste heat combined heat and power system so far storage in concrete has been tested and prove in the temperature range up-to 400 °C. Lingkai et al., (2015) investigated the influence of the inner cylinder design and operation parameters and on the water flow characteristics. Used 3D transient CFD simulation to optimized thermal storage tank parameter at the early design stage, the result showed as the cylinder inside the tank plays a role of uniform diffuser, so that the water in the tank was formed better thermal stratification.

2.2 Conventional steam Generation (boiler)

Boiler (Convectional steam generation) is an enclosed vessel that provides a means for combustion heat to be transferred into water until it becomes heated water or steam. When water is boiled into steam its volume increase about 1600 times, producing a force that is almost as explosive as gunpowder.

Convectional steam generation system uses boiler system which consist feed water tank, boiler, end use devises (it may be turbine or other steam driven devices) and condensates pump. The feed water tank supplies treated water for boiler (evaporation) and regulated by automatic valves with the steam demand. The steam generation will be distributed via steam pipelines to the point of use. Along the pipeline the steam pressure is regulated as per the demand. The water supplied for the boiler comes from feed water tank where condensate from process and treated make up water were mixed and collected. To improve boiler efficiency, feed water is heated in pre heaters using waste heat in the flue gas.

Generally we have two types steam generation system (boiler), fire tube and water tube. Fire tube boilers, feed water is converted into steam in the shell side where as hot flue gas passes through the tubes and this type of boilers are used usually for low steam demand at low pressure. In case of water tube boilers, flue gases passes over the tube and water is converted to steam inside the tube. (Reverse of fire tube system). Adama general hospital uses one three pass (3p) wet back fire tube boiler, 3000 kg/hr steam generation capacity at a pressure of 12bar, with another one standby to satisfy the daily steam demand of different services in the hospital.

2.2.1 Boiler feed water the boiler feed water comprises mainly of a feed water system, fuel system and steam system. The feed water system provides water to the boiler and regulates it automatically to meet the steam demand. The water supplied to the boiler that is converted into steam is called feed water.

The two sources of feed water are

- Condensate return from the processes and

- Make-up water (treated raw water)

2.3.2 Water treatment

Proper treatment of makeup and feed water is necessary to prevent scale, other deposits and corrosion in pre-boiler, steam and condensate systems, and to provide the required steam purity. Absence of adequate treatment can lead to operational upsets or unscheduled outages; it is also ill advised from the point of view of safety, economy, and reliability.

2.3.3 Fuel supply system

The fuel used for boiler is usually light oil or furnace oil, for better combustion usually the fuel is pre-heated to a temperature of 120 ℃ using exhaust gas. Adama general hospital uses diesel fuel used.

CHAPTER 3

DATA COLLECTION FOR ADAMA GENERAL HOSITAL AND MEDICAL COLLEGE

One of the main building types with a great potential to apply measures of energy is hospitals. Below, some of the most important reason why hospitals consume a lot of energy, guideline for energy efficiency in hospital (2007)

- 24 hours operation (lighting, heating, air-conditioning, electricity consumption): the non-stop function of the hospitals is an important factor why there is such big energy consumption.
- Big surface of the buildings: Rooms with big volume, long corridors and the need for satisfactory ventilation are factors that increase energy consumption in hospital.
- Needs for hot water: Hot water use, which is very energy Consuming is high in hospitals. Also, because of the big size of the building there is important loss of heat in the pipeline. That’s why the needs in hot water must be determined with accuracy, since they differ from one hospital to another, in order to avoid -unnecessary energy consumption for water heating.
- Needed for thermal comfort: obtaining high quality of the inside climate and assuring the thermal comfort for the patients are very helpful for the improvement of their health.
- Sterilization supplies: the great needs for sterilization in hospitals.
- Energy consuming machines and equipment: medical machines with are necessary for a hospital’s operation also contribution to the high energy consumption of hospitals.

3.1 Hot water load estimation for Adama general hospital

This chapter deals about calculating hot water demand for Adama general hospital with required water temperature by visiting hospital data and international experience. In Ethiopia most of hospitals requires hot water for the appliance including laundry facilities, showering purpose, food service to the patient and hospital restaurants, kitchen equipment washing, sterile processing, boilers and radiology.

Few private hospitals like Adama general hospital have higher standard which riches to the typical standard hospital hot water demand and appliance used.

Figure 3. 1: Adama General Hospital

The hospital was attempted to occupy 230 beds, and had modern planned, accommodate and facilitated without patient department.

Unfortunately in the hospital like any other developing country due to lack of recording data malfunction of measuring instruments recorded data of the hospital is unavailable.

In the absence of recorded data amount of hot water demand is calculated by assumption and estimation are made on the standard hot water delivery system of hospital. Different appliance for energy usage in hospital are listed in Table 3.1 and Standard hot water demand for different appliance and usage in hospital are given on Table 3.2

Table 3. 1: Data from Adama general hospital.

Loads	**quantity**	**Occupancy (%)**	**Person per room**	**Energy source**
	Patient 82	95 %	3	
	Stuff 12	65 %	7	
	Student 18	15 %	10	
laundry	3	100 %	10	
restaurant	1	90 %	15	
kitchen	2	100 %	12	

Table 3.2 : Standard hot water demand for different appliance and usage in hospital, International energy agency [2017].

Demand	**Standard hot water demand for different uses**			
	kitchen	**shower**	**restaurant**	**laundry**
Hot water	320 L/kitchen	60 L/person	160 L/restaurant	530 L/laundry
temperature	48 ℃	43 ℃	48 ℃	60 ℃

Laundry service is a large energy consumption process, which includes all types of linen for children, bed linen for patient, cafeteria lines for patients and guests, surgery room's lines, staff uniform and others.

The laundry has constantly schedule operating morning and evening in the adama general hospital.

Hot water load for laundry (HWLL)

Hot water load for laundry like cloth washing at 60 ℃ temperatures.

HWLL = 3*503 $\frac{Lts}{day}$ = 1509 $\frac{Lts}{day}$

Hot water load for kitchen (HWLK)

Hot water load for kitchen like equipment (cooking) washing set temperature up-to at 48 ℃.

HWLK = 2* 320 $\frac{Lts}{day}$ = 640 $\frac{Lts}{day}$

Hot water load for restaurant (HWLR) Hot water load for restaurant like cooking goods, hand water, soon at set temperature of 48℃ HWLR = 1 * 160 $\frac{Lts}{day}$ = 160 $\frac{Lts}{day}$

Hot water load for shower (HWLS)

Hot water load for shower include patient, medical stuff, student, kitchen worker, laundry worker, restaurant works are the main user at 45℃.

Patient Shower load (PSL) = 82 * 0.95 *60 $\frac{Lts}{day}$ * 3 = 14022 $\frac{Lts}{day}$

Medical stuff load (MSL) = 12 * 0.4 * 60 $\frac{Lts}{day}$ * 7 = 2016 $\frac{Lts}{day}$

Student load (SL) =18 * 0.15 * 60 $\frac{Lts}{day}$ * 10 = 1620 $\frac{Lts}{day}$

Kitchen worker shower load (KSL) = 2 * 12 * 60 $\frac{Lts}{day}$ * 1 = 1440 $\frac{Lts}{day}$

Laundry worker shower load (LSL) = 3 * 10 * 60 $\frac{Lts}{day}$ * 1 = 1800 $\frac{Lts}{day}$

Restaurant worker shower load (RSL) = 1* 15 * 60 $\frac{Lts}{day}$ * 0.90 = 810 $\frac{Lts}{day}$

Total hot water load (THWL) summation of the above loads as follows

THWL=HWLL + HWLK + HWLR + HWLS………………………………………… 3.1

HWLS=PSL + MSL + SL + KSL + LSL + RSL……………………….………..…….. 3.2

From equation (3.2) and (3.1)

HWLS = 21,708 $\frac{Lts}{day}$

THWL = 24,017 $\frac{Lts}{day}$

To compensate any unexpected need of hot water at night time and any wastage of water since it is public service multiplies the value by the facture of one fourth of the total calculation. Figure 3.2 Shows amount of hot water demand for each appliance

So the updated result as follows

HWLL=1.25 *1509= 1,886.25 $\frac{Lts}{day}$

HWLK=1.25 *640= 800 $\frac{Lts}{day}$

HWLR=1.25 *160= 200 $\frac{Lts}{day}$

HWLS=1.25 *21708= 27,135 $\frac{Lts}{day}$

Then THWL=30,022 $\frac{Lts}{day}$

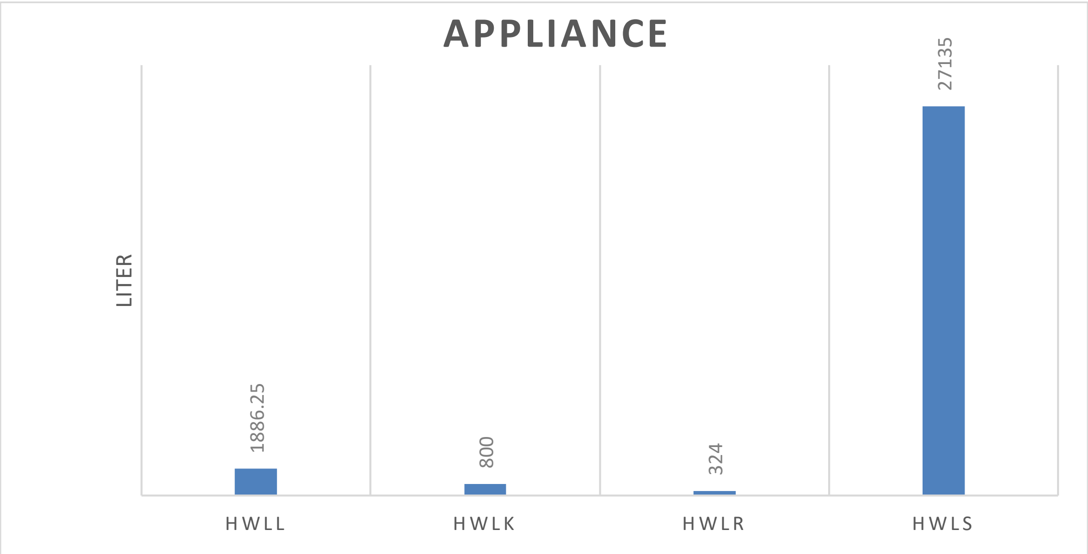

Figure 3.2: Variation of hot water load for different appliances

3.2 Daily Hot water load pattern

In the Adama general hospital 2 times a day launder of cloths, also workers have 2 shifts so most shower happen in morning and evening. Figure 3.3 Shows daily hot water load pattern.

MSL = 2016/2 =1008 (morning and evening) 3.344 % morning, 3.344 % evening

SL = 1620 (20% morning (324), 60% mid-day (972), 20% evening (324)) 1.1% morning, 3.2 % mid-day, 1.1 % evening.

KSR = 1440/2 = 720 (morning and evening) 2.4% morning, 2.4% evening

LSL = 1800/2 = 900 (morning and evening) 3 % morning, 3 % evening

RSL = 810/2 = 405 (morning and evening) 1.4 % morning, 1.4 % evening

Let sum up the percentile value

Morning load= (3+.9+.4+15.51+3.334+1.1+2.4+3+1.4) % = 31.044 % + 10 % = 41.044 %

Mid-day load = (0.9+0.4+15.51+3.2) = 20.01 %

Evening load= (3+0.9+0.4+15.51+3.334+1.1+2.4+3+1.4) % = 31.044 %

Over the day distribute = 7.902 %

Morning 41.044 % (30,022) = 12,309.02 $\frac{Lts}{day}$

Mid-day 20.01% (30,022) = 6,004.4 $\frac{Lts}{day}$

Evening 31.044% (30,022) = 9,306.8 $\frac{Lts}{day}$

Over the day 7.902 % (30,022) = 2,371.74 $\frac{Lts}{day}$

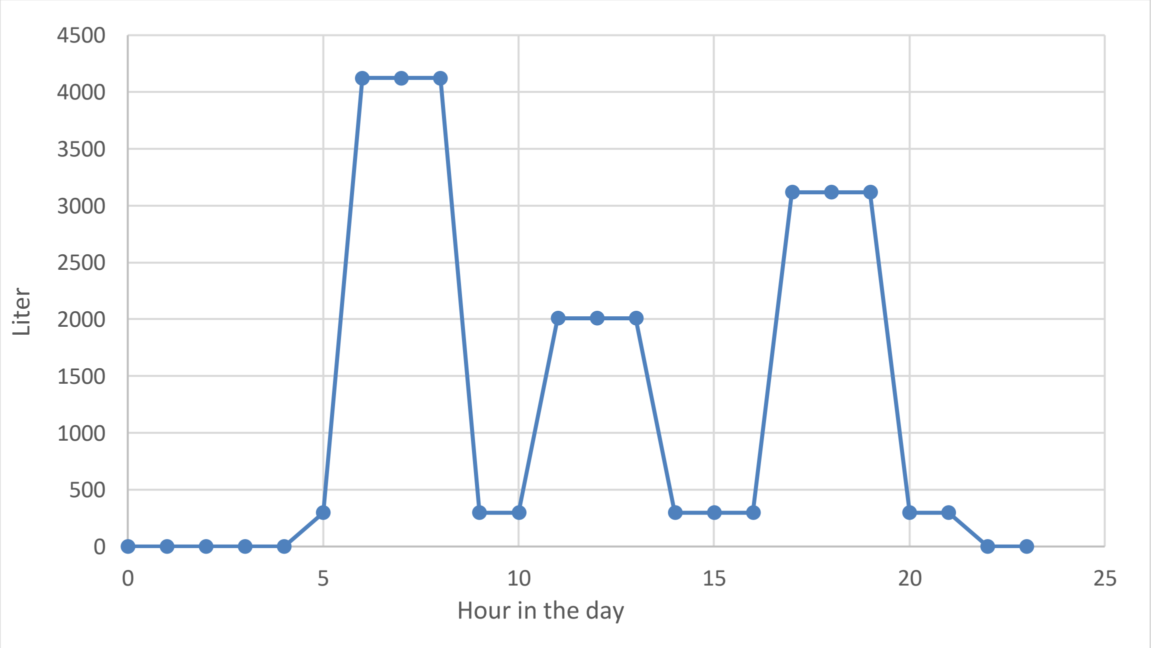

Figure 3.3: Daily hot water load pattern in a day

HWLL

$m = \rho * v = 997\frac{kg}{m^3} * 1.89\ m^3 = 1880.6\ kg$

Q = $mc_p(T_{fo} - T_{fi})$ =301,723,464 J

HWLK

$m = \rho * v = 997\frac{kg}{m^3} * 0.8\ m^3 = 797.6\ kg$

Q = $mc_p(T_{fo} - T_{fi})$ = 87,767,904 J

HWLR

$m = \rho * v = 997\frac{kg}{m^3} * 0.2\ m^3 = 199.4\ kg$

Q = $mc_p(T_{fo} - T_{fi}) =$ 21,941,976 J

HWLS

$m = \rho * v = 997\frac{kg}{m^3} * 27.135\ m^3 = 27{,}053.595\ kg$

Q = $mc_p(T_{fo} - T_{fi})$= 2,408,852,099 J

$Q_T = 2820.3\ MJ$

CHAPTER 4

SOLAR POTENTIAL ASSESMENT FOR ADAMA CITY

Solar energy from the sun gives life to human beings and all living organism on planet earth and generated by several fusion reaction; two hydrogen molecules combine to form one helium nucleus at approximately at 10^7K. The mass of helium nucleus is less than that of four protons, the mass have been lost in the reaction is converted into energy by the relation gives by Einstein, i.e. E= MC^2.

Solar radiation treated as an electro-magnetic wave with wavelength between 0.30 - 3 um as well as visible photons in a visible wave length, Shelkel et al., (2014) Solar radiation data are available in several forms. Whether they are instantaneous (irradiance) or value integrated over some period of time (irradiation) usually hours or days. Most radiation data available are for horizontal surface, include both direct and diffuse radiation, and were measured with thermopile pyrometers.

Radiation data are the best source of information for estimating average incident radiation. Lacking data from nearby location, of similar climate, it is possible to use empirical relationships to estimate radiation from hours of sunshine or cloudiness. Data on average hours of sunshine or average percentage of possible sunshine hours are widely available (Campbell-stokes instrument).

The original angstrom-type regression equation related monthly average daily radiation to clear-day radiation at the location in equation and average fraction of possible sunshine hours, Duffie and Beckman (2013).

$$\frac{H}{H_C} = a' + b' * \frac{n_s}{N_s} \qquad 4.1$$

The basic difficult in above equation 4.1 lies in the ambiguity of the terms $\frac{n_s}{N_s}$ and H_C. And other has modified the method to base it on extra-terrestrial radiation on a horizontal surface rather than clear day radiation.

$$\frac{H}{H_O} = a + b * \frac{n_s}{N_s} \qquad 4.2$$

Cloud cover data are also widely available but are based on visual estimates. And are probable less useful than hours of sunshine data. Data are also available on mean monthly cloud cover C, expressed as tenths of the sky obscured by clouds.

$\frac{H}{H_O}$ = a''+ b''C 4.3

Thus these may not be as good a statistical relationship between $\frac{H}{H_O}$ and C as there is between $\frac{H}{H_o}$ and $\frac{n_s}{N_s}$ many surveys of solar radiation data have been based on correlations of radiation with sunshine hour's data.

4.1 Available solar radiation

Available solar radiation on the tilt surface for a day as the sum of three terms like global radiation (H), beam radiation (H_b), diffuse radation (H_d).

H_t= $H_b R_b$ +$H_d R_d$ + H p R_r 4.4

Global radiation (H) is the sum of beam and diffuse radiation and available in two ways first data from nearby metrology and the second by empirical relation. Under this empirical relation average hours of sunshine or average percentage of possible sunshine hours are widely available. Data available from Adama metrology agency measuring sunshine duration every 3 hours in the 2013-2017 G.C is as follows. (Adama metrology agency)

Sunshine hours is a climatological indicator, measuring duration of sunshine in given period(usually, a day or a year) for a given location on earth, typically expressed as an averaged value over several years. It is a general indicator of cloudiness of a location, and thus differs from insolation, which measures the total energy delivered by sunlight over a given period. Table 4.1 shows Sunshine hour duration for five (5) years and Table 4.2 shows five years average Sunshine hour duration from nearby metrology agency.

Adama Station - Latitude (ϕ) =8 33' 23.8'' N = 8.558

- Longitude = 39 17' 2.5'' E = 39.28

- Altitude = 1648 m above sea level

- Dominating climate of the city is hot/arid climate type

Table 4. 1: Sunshine hourly duration

Year	Jan	Feb	mar	Apr	may	Jun	Jul	Aug	Sep	Oct	Nov	Dec
2013	8.9	10.05	8.4	8.12	8.35	7.89	5.3	6.8	7.7	8.3	8.78	10.10
2014	9.46	8.7	8.6	9.0	8.6	8.6	6.4	6.9	6.6	8.7	9.1	8.85
2015	9.7	10.1	9.5	8.7	8.8	7.5	9.3	8.0	8.3	9.0	9.07	8.8
2016	7.7	8.5	9.3	6.7	7.6	7.8	6.4	6.7	7.2	9.8	10.05	9.7
2017	7.9	8.9	9.2	9.5	7.8	8	6.6	5.9	6.8	8.7	9.9	9.3

Table 4. 2: Five years average sunshine hour duration.

Years	Jan	Feb	mar	Apr	may	Jun	Jul	Aug	Sep	Oct	Nov	Dec
Average (2013-2017)	8.7 32	9.25	9.0	8.4	8.23	7.96	6.8	6.86	7.32	8.9	9.38	9.35

Figure 4.1 shows Sunshine hour duration for Adama city in previous five years (2013-2017) averages.

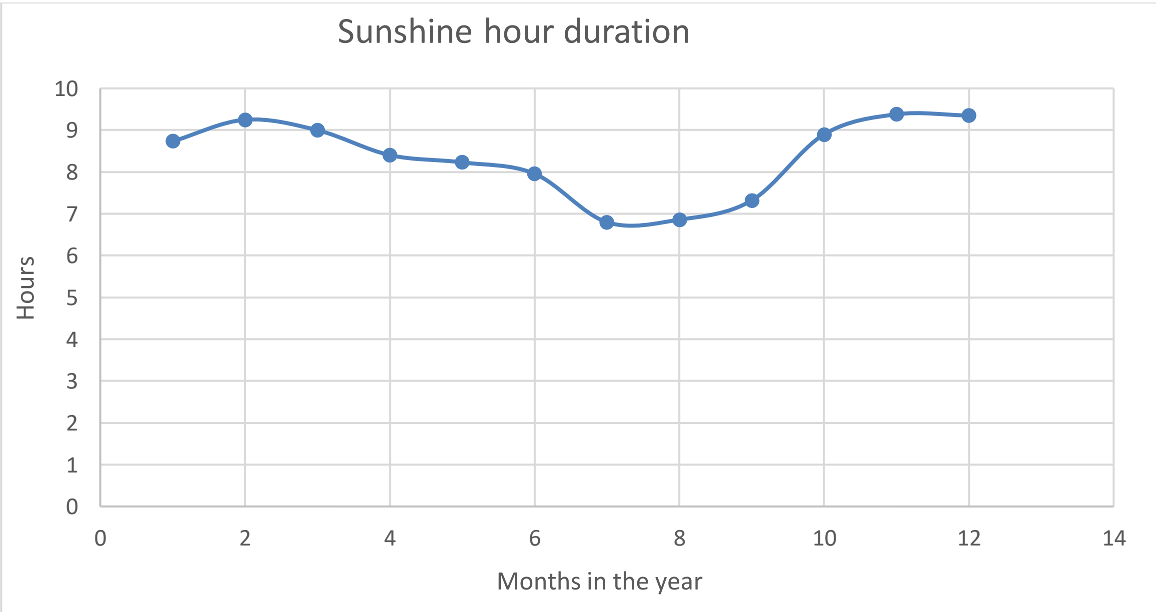

Figure 4. 1 : Sunshine hour duration Verse months of the year

From equation 4.2, modified angstrom-type regression equation

H= Monthly average daily radiation on horizontal surface

H_O=monthly average radiation at extra-terrestrial region for the same location

H_O=24*3600*$\frac{I_{sc}}{\pi}$ (1+0.033cos ($\frac{360*n}{365}$))* (cos ϕ cos δ sin ωs + π * $\frac{\omega s}{180}$(sin ϕ* sin δ))……………4.5

Solar constant, I_{sc} =1367 $\frac{W}{m^2}$

Declination angle (δ) = $23.45 * \sin(\frac{360}{365} * (284n))$……………………………………….4.6

Sunset hour angle (ωs) = cos^{-1}(-tan ϕ tanδ) …………………………………….....4.7

a, b=empirical constant

a = -0.110 + 0.235 cos ϕ + 0.323*($\frac{n_s}{N_s}$)………………………………………………. 4.8

b = 1.449 - 0.533 cos ϕ - 0.694*($\frac{n_s}{N_s}$)………………………………………………....4.9

Ns=2/15(ωs)…………………………………………………………………………....4.10

n_s= hours of sunshine duration

Detain MS-EXIL Calculation for radiation data available in appendix 3. Monthly Average daily global radiation on horizontal surface are listed on Table 4.3

Table 4.3: Monthly Average daily global radiation (MJ/m^2/day) in horizontal surface.

Months	**Jan**	**Feb**	**mar**	**Apr**	**may**	**Jun**	**Jul**	**Aug**	**Sep**	**Oct**	**Nov**	**Dec**
Average (2013-2017)	21.7	23.6	24.7	24.6	23.9	23.2	21.8	22.5	23.1	23.6	22.4	21.5

Diffuse radiation (H_d) is type of radiation come from sun after scattering in the atmosphere. and amount obtain from global radiation by empirical relation. Monthly Average daily diffuse radiation on horizontal surface are listed on Table 4.4

$\frac{H_d}{H}$ = 0.931 – 0.814 *$\frac{n_s}{N_s}$……………………………………………………………….... 4.11

Table 4. 4: Monthly Average daily diffuse radiation (MJ/m^2/day) on horizontal surface

Months	Jan	Feb	mar	Apr	may	Jun	Jul	Aug	Sep	Oct	Nov	Dec
Average (2013-2017)	6.9	6.8	7.9	9.1	9.3	9.5	10.6	10.7	10.1	7.5	6.1	5.8

Beam radiation ($\boldsymbol{H_b}$) radiation directly come to the object without scattered obtained by subtract diffuse radiation from global radiation as follows. Monthly Average daily beam radiation on horizontal surface are listed on Table 4.5

Table 4. 5: Monthly Average daily beam radiation (MJ/m^2/day) on horizontal surface

Months	Jan	Feb	mar	Apr	may	Jun	Jul	Aug	Sep	Oct	Nov	Dec
Average (2013-2017)	14.9	16.8	16.8	15.5	14.6	13.6	11.2	11.8	13.1	16.2	16.3	15.7

Figure 4. 2 shows beam, diffuse and global solar radiation on horizontal surface in meter quarter Verse months of the year.

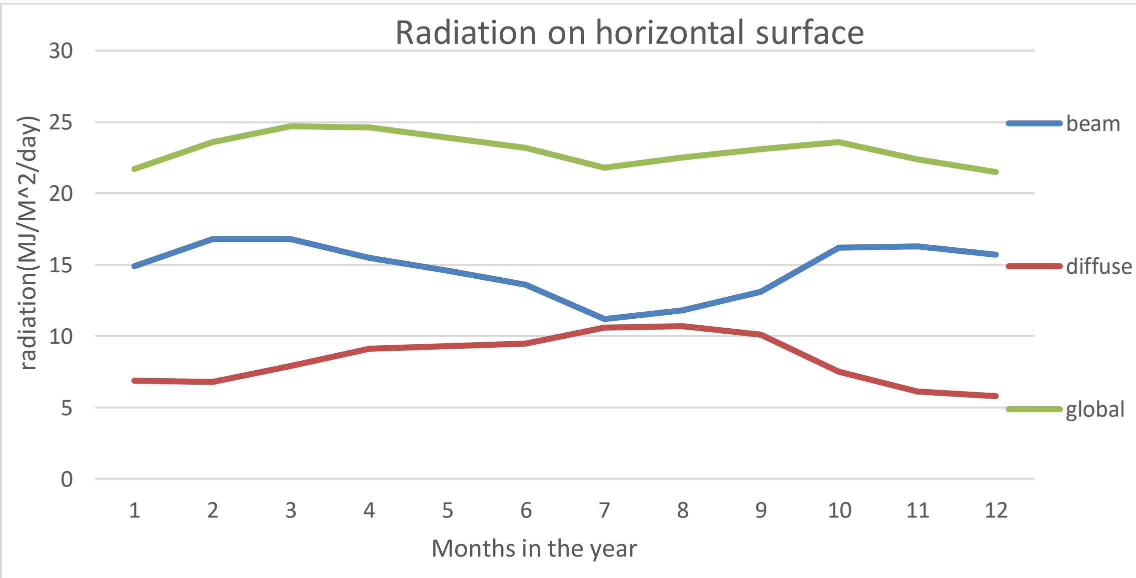

Figure 4. 2: Daily solar radiation Verse months of the year

4.2 Conversion factors

There are three conversion factors namely beam radiation factor (R_b), diffuse radiation factor (R_d) and reflected (Rr) solar radiation.

Beam radiation factor (R_b) the ratio of the average daily beam on the tilted surface to that on a horizontal surface for the month is R_b, which is equal to $\frac{H'_b}{H_b}$. For surface that are sloped toward the equator in the northern hemisphere that is for surface with surface azimuth angle y=0^o.

$$R_b = \frac{\cos(\phi - \beta) \cos \delta \sin \omega's + (\pi/180)\, \omega's \sin(\phi - \beta) \sin \delta}{cos\phi \cos\delta \sin\omega s + \left(\frac{\pi}{180}\right)\omega s \sin\phi \sin\delta} \text{………………… 4.12}$$

Where ω's is the sunset hour angle for the tilted surface for the mean day of the month, which is given by

$$\omega's = \min [cos^{-1} (-\tan \phi \tan \delta) \text{ or } cos^{-1} (-\tan (\phi - \beta) \tan \delta)] \text{……………….. 4.13}$$

Sunset hour angle 1 and Sunset hour angle 1 are listed in Table 4.6 and Table 4.7 respectivily. The minimum value from Table 4.6 and Table 4.7 are listed in Table 4.8

Collector tilt (β) the optimum tilt angle is different for each month of the years. The collector solar energy amount is higher if the optimum tilt angle for each month is chosen. The yearly optimum slope angle of solar collector as βopt = ϕ + (10-15)° at a location with latitude, Soulayman and Sabbagh., (2015)

$$\beta = \phi + 15° = 8.558 + 15 \cong 24 \text{…………………………………………….. 4.14}$$

ω's = cos^-1 (-tan ϕ tan δ)………………………………………….………. 4.15

Table 4. 7: Sunset hour angle 1

Months	Jan	Feb	mar	Apr	ma y	Jun	Jul	Aug	Sep	Oct	Nov	Dec
Sunset hour angle	86.7	88.0	89.63	91.43	92.93	93.67	93.3	92.0	90.3	88.5	87.0	86.3

Or ω's = cos^-1 (-tan (ϕ – β) tan δ)……………………………..…………4.16

Table 4. 8: Sunset hour angle 2

Months	Jan	Feb	mar	Apr	ma y	Jun	Jul	Aug	Sep	Oct	Nov	Dec
Sunset hour angle	96.1	93.6	90.7	87.4	84.6	83.23	83.8	86.21	89.4	92.7	95.4	96.74

Table 4. 9: Minimum value from table 6 and table 7(degree)

Months	Jan	Feb	mar	Apr	ma y	Jun	Jul	Aug	Sep	Oct	Nov	Dec
Minimum value	86.7	88.0	89.6	87.4	84.6	83.2	83.8	86.2	89.6	88.5	87.0	86.3

Diffuse radiation factor (R_d)

$R_d = \frac{1+\cos\beta}{2}$…………………………………………………………………………4.17

Reflected radiation factor (Rr)

Rr = $\frac{1-\cos\beta}{2}$…..……………………………………………………….………. 4.18

The ground reflectance is 0.2 for all months except December and March (p = 0.4) and January and February (p = 0.7) using the isotropic diffuse assumption, Xinyu et al., (2014). Global solar radiation reach on tilt surface are listed in Table 4. 10

Table 4. 11: Total solar radiation (MJ/m^2/day) reach on tilt surface

Months	Jan	Feb	mar	Apr	may	Jun	Jul	Aug	Sep	Oct	Nov	Dec
Global radiation on tilt surface	36.8	37.9	33.7	29.4	27.5	25.3	25.2	27.7	29.6	31.1	31.0	33.1

Global solar radiation on tilt surface in meter quarter Verse months of the year are shows in Figure 4. 3

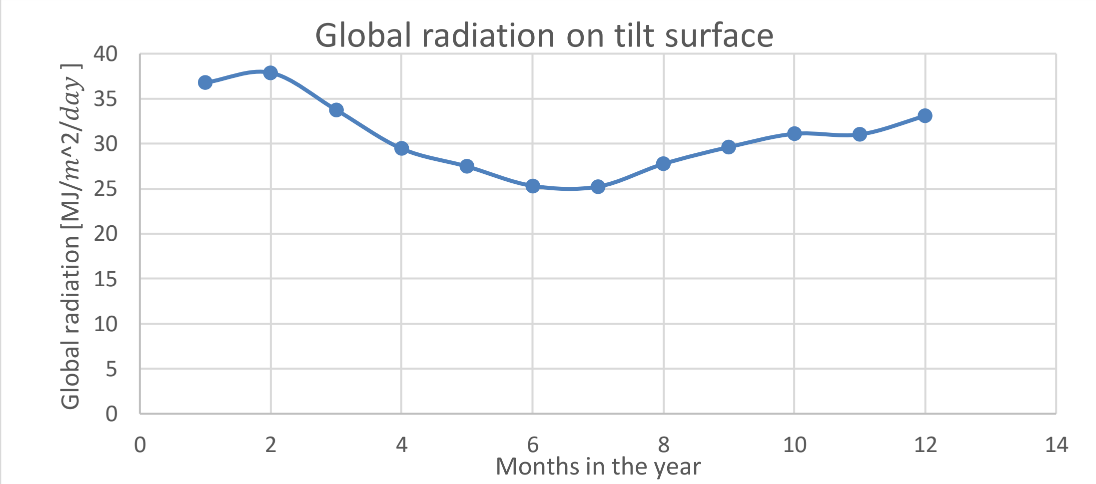

Figure 4. 3: Daily solar radiation Verse months of the year

4.3 Prediction of hourly global radiation: the hourly glodal radation can be calculated from the knowledge of the daily global radiation. Monthly Averages of daily global radiation are shown in Figure 4.4

$$\frac{I}{H} = \frac{\pi}{24}(a + b\cos\omega)\frac{\cos\omega - \cos\omega_s}{\sin\omega_s - \frac{\pi}{180}\omega_s\cos\omega_s} \quad \text{4.19}$$

Where

a=0.409+0.5016sin($\omega_s - 60$)

b = 0.6609-0.4767sin($\omega_s - 60$)

$\omega = 15(t - 12)$

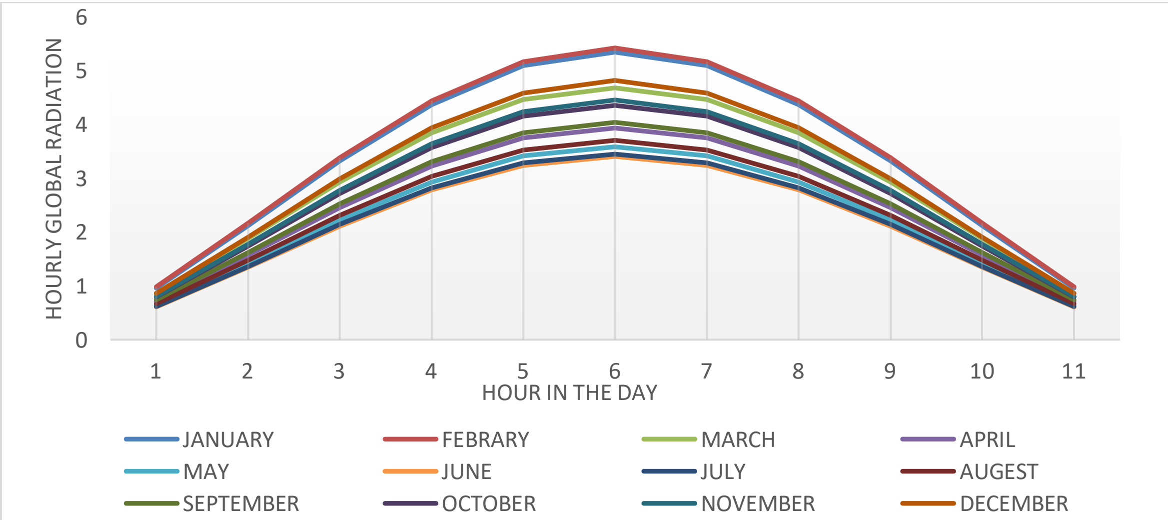

Figure 4. 4: hourly global radiation (MJ/m^2) reach on tilt surface Verse hours of day

4.4 Prediction of hourly diffused radiation: the hourly diffuse radation also can be calculated from the knowledge of the daily radation. Monthly Averages of daily diffuse radiation are shown in Figure 4.5

$$\frac{I_d}{H_d} = \frac{\pi}{24} \frac{\cos\omega - \cos\omega_s}{\sin\omega_s - \frac{\pi}{180}\omega_s\cos\omega_s} \quad \ldots\ldots\ldots\ldots\ldots\ldots\ldots\ldots\ldots\ldots\ldots\ldots\ldots\ldots\ldots\ldots\ldots \; 4.20$$

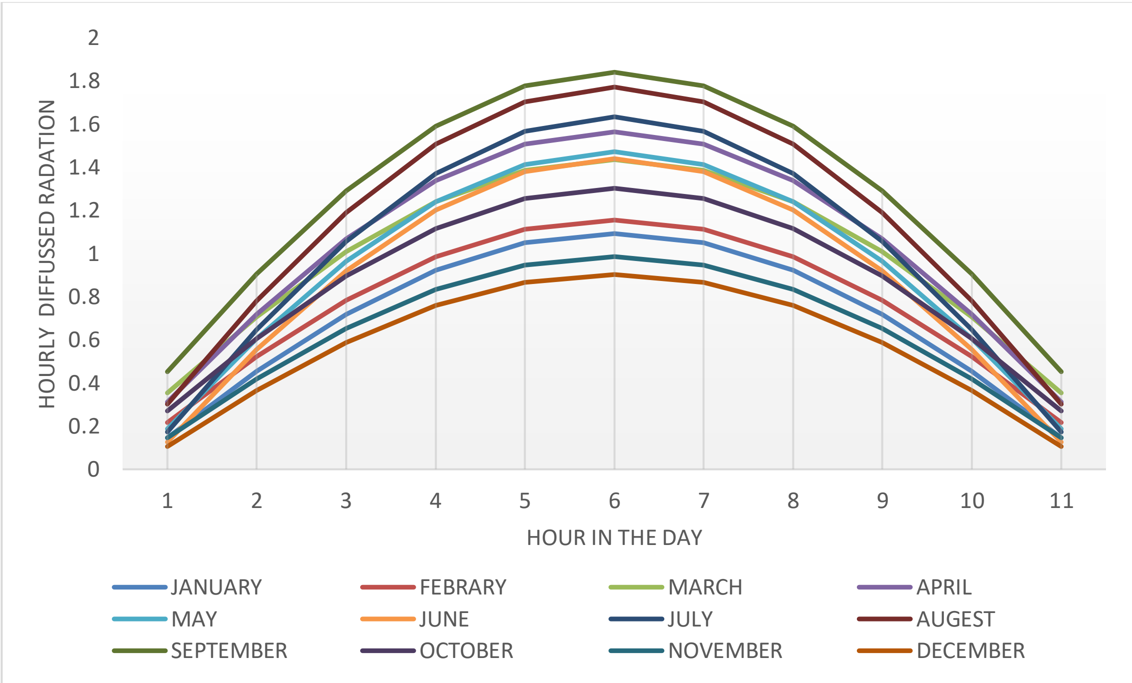

Figure 4. 5: hourly diffused radation (MJ/m^2) reach on tilt surface verse hours of day

4.5 Estimation of diurnal cycle varation of temperature

Temperature is one of the critical variable,there are different models of calculating diurnal temperature in literature out of this model one is selected because of the parameter available to be used the equation. used data for ambient temperatur (maximum and minimum) in the year of 2017 from near by methdology station. Figure 4.6 shows ambient air temperature varation in a day.

Model : presented by Wilk-Erson et al (1983)

In this model the day is divided into three segment

- Midnignt to sunrise+2 h
- Day light hours

- Sunset to midnignt

This model assumes a change from nignt to day temperature at sunrise +2 h and the night temperature are linear with time in addition to the current day's Tmax and Tmin, the method required Tmax and Tmin of the previous day's and Tmin of the following day.The hourly temperatures are given by the following equation.(ploted graph in appendix B-3)

1, Midnignt to sunrise+2 h

TAU= $\frac{\pi(SET_{n-1}-RISE_{n-1}-2)}{(SET_{n-1}-RISE_{n-1})}$

TLIN=$TMIN_{n-1} + (Tmax_{n-1} - Tmin_{n-1})\sin(TAU)$

SLOPE= $\frac{(\text{TLIN}-Tmin_n)}{(24-SET_{n-1}+RISE_n+2)}$

T(H)=TLIN-SLOPE (H+24-SET_{n-1})…………………………………………………. 4.21

2, Sunset to midnignt

TAU=$\frac{\pi(SET_n-RISE_n-2)}{(SET_n-RISE_n)}$

TLIN=$Tmin_n + (Tmax_n - Tmin_n)\sin(TAU)$

SLOPE=$\frac{(\text{TLIN}-Tmin_{n+1})}{(24-SET_n+RISE_{n+1}+2)}$

T(H)=TLIN-SLOPE(H-SET_n)………………………………………………………… 4.22

3, Daylight hours

TAU=$\pi(H - RISE_n - 2)(SET_n - RISE_n)$

T(H)=$Tmin_n + (Tmax_n - Tmin_n)\sin(TAU)$……………………………………… . 4.23

Where n=current day of the year(1-365)

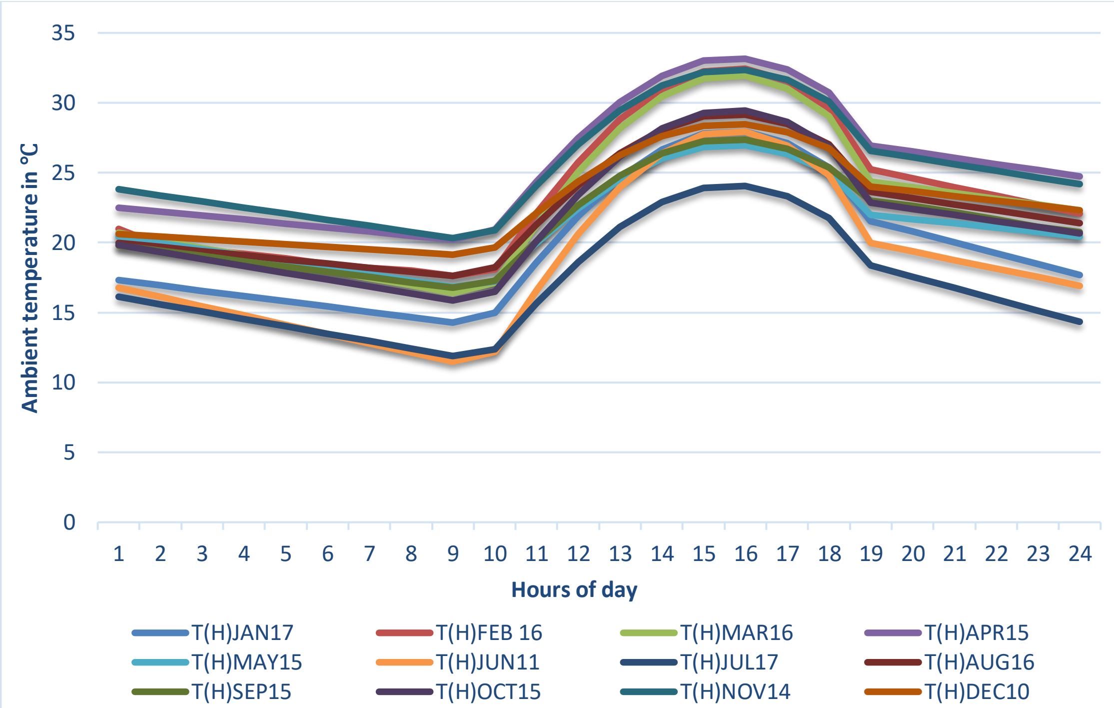

Figure 4. 6: Ambient air temperature (°C) Verse hours of day

CHAPTER 5

MODELLING AND THERMAL ANALYSIS OF EVACUATED TUBE SOLAR COLLECTOR

5.1 Introduction to evacuated tube solar collector

The evacuated tube solar collectors are common and can achieve higher temperature than flat plate collector ranging from 50-130 ℃. They are made up of vacuum glass tubes. The absence of air highly reduces convection and conduction thermal losses. They also have barium getter component in common, the main role of getter is to maintain the vacuum inside the tube and to give a visual indicator of the vacuum status. The silver colour of the barium will turn while in case of presence of air indicating the bad functioning conditions of the evacuated tubes can be identified, Soteris A. Kalogiros (2004).

Heat extraction from long thin absorber is the main problem with evacuated tube solar collector. Following methods are used to extract heat from evacuated tubes, Sabiha M.A (2016).

- Heat pipe
- Flow through absorber
- All glass tube
- Storage tubes

Two **main categories** of evacuated tubes can be identified.

1) Direct flow principle different arrangements are possible; the working fluid passing through the collector tubes.
   - Water in glass evacuated tube collector
   - Evacuated U-tube collector
2) Heat pipe evacuated tubes the heat carried fluid is not connected to the solar loop. The pipes must be angled at a specific degree above horizontal so that the process of vaporizing and condensing can work properly. there are two types of collector connection to the solar circulation system, either the heat exchanger extends directly into the manifold (wet connection) or it is connected to the manifold by a heat conduction material (dry connection)

Advantage of evacuated tube collector

- ✓ It can be used in any climate, from extremely hot to extremely cold weather.
- ✓ Its high level of vacuum ensures the operation under cold weathered conditions.
- ✓ Evacuated tube solar collectors require lesser space and it is very easy to install.
- ✓ It can absorb the solar radiation from multiple angles, due its tubular design.
- ✓ Wind and low temperature have less of effect on the function of evacuated tubes.
- ✓ Since no water is flowing through the collector tubes and the tubes are hermetically sealed it does not suffer from corrosion problems as in the case with other solar collector types.(Heat pipe evacuated tubes solar collector)

Limitation of evacuated tube solar collector

- ✓ Initial cost is high as compared to other collector
- ✓ Construction of evacuated U-tube collector is little bite complicated as compare to other collectors and thus proper handling required
- ✓ Some-times due to improper handling and maintenance temperature become very high due to lack of water in the tube and hence it causes a thermal shock so tube may crack and resulting vacuum to loose.

Water in glass evacuated tube collector

Evacuated tubes are the absorber of the solar water heater and they absorb solar energy converting it into heater and they absorb solar energy converting it into heat for use in heating water.

Evacuated tube consists of two glass tubes made from extremely strong borosilicate glass. The outer glass is transparent to allowing light rays to pass through with minimal reflection and the inner tube is coated with a special selection coating (Al-Nickel/Al) which features excellent solar radiation absorption and minimum reflection characteristics. The free end of tubes is fused together with each other and the air contained in the space between the two layers of glass is pumped out to expose the tube to high temperatures. This vacuum play an important role in the performance of the direct flow evacuated tubes.

Evacuated tube solar collector with U-tube

Evacuated tube collector receiver consists of a copper U-tube inside a glass vacuumed tube. The copper tube is surrounded by a cylindrical aluminium fin pressed on it. The fin enhances the heat transfer area between the inner glass absorber surface and the U-tube. The working fluid enters the collector inlet pipe, then it is evenly distribution to the U-tubes, absorbs heat and at the end, it is returned to the outer manifold pipe. The outer cylindrical glass transmits the rays to the inner glass tube, which conducts the energy to the absorber fin. The energy transformed into heat is conducted by the fin to the copper U-tube and finally absorbed by the working fluid which is water in this case.

5.1.1 Applications of U-pipe evacuated tube solar collector are as listed below, Dilip Mishara and Saikhedkar N.K., (2014)

- ✓ In industrial field e.g. power plant, steam power plant, in school and hospital
- ✓ In laundries, in space heating. Generally used in northern country for heating purpose of water like swimming pool as per the season
- ✓ It is used for domestic purpose e.g. electricity, water heating and in kitchen stuff

Detailed schematic diagram of the U-type evacuated tube solar collector are shown in Figure 5.1

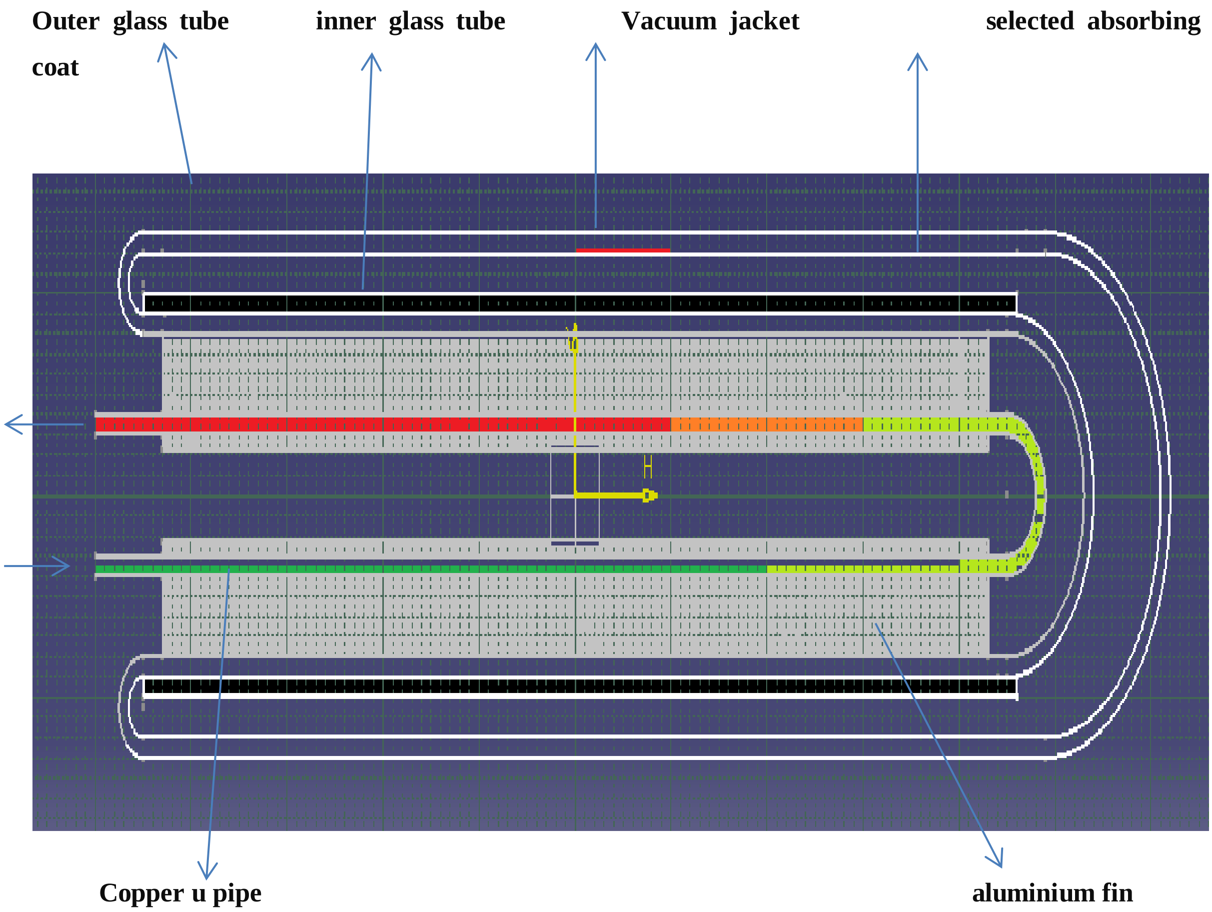

Figure 5.1: Evacuated tube with U-type heat extraction (CATIA V5 R19)

Table 5.1: Specification and nomenclature of evacuated tube solar collector and manifold (150 LPD).

Material	Parameter	Dimension and other properties	Units
Outer glass tube	Thickness	2	mm
	Diameter	58	mm
	Conductivity	0.74	W/m*K
	Transmissivity	0.92	-
	Refractive index	1.474	-
	length	1800	mm
Inner glass	Diameter	48	mm
	Thickness	2	mm
	Conductivity	0.74	W/m*K
Copper tube	Diameter	10	mm
	Conductivity	398	W/m*K
	Thickness	0.7	mm
	length	3500	mm
Absorbing coating	Absorptivity	0.96	-
	Emissivity	0.08	-
Number of tubes		15	-
Distance between center to center		80	mm

5.2 The heat transfer correlation

Radiation from the outer glass tube: The radiation loss from the outer glass tube surface accounts for radiation exchange with the sky; the radiation heat transfer coefficient from the outer glass tube surface can be written in following equation.

$$h_{rad,og} = \varepsilon_{og}\sigma * \frac{(T_{og}+273)^4-(T_s+273)^4}{T_{og}-T_a} \quad \ldots\ldots 5.1$$

Where

ε_{og} = is the emissivity of the outer glass,

σ = Stefan Boltzmann constant = $5.6697 * 10^{-8} \frac{W}{m^2K^4}$

T_{og} = temperature of outer glass (K)

T_a = ambient temperature (K)

$T_s =$ Equivalent sky temperature as a function of the ambient air temperature (K)

Sky temperature to the local air temperature in the simple relationship shown below

$T_{sky} = 0.0552 * {T_a}^{1.5}$

Outer glass convection: the wind loss coefficient or the adjusted convection heat transfer coefficient h_{wp} of the outer glass tube surface is approximated by heat transfer coefficient around the outer glass tube, Mishara D., (2014).

h_{wp}= $\frac{A_{og}}{A_{ig}}$ * 0.6 * h_w ………………………………………………………….… 5.2

h_w = 5.7 * 3.8 V_W…………………………………………………….……...….. 5.3

$h_w =$ Convection heat transfer coefficient around the outer glass tube

$V_W =$ Average wind speed (m/s)

h_{wp} = adjusted convection heat transfer coefficient

Radiation between absorber glass tubes to the outer glass tube: the coefficient of radiation heat transfer between the absorber tube and outer glass tube can be written as:

$h_{rad,p} = \varepsilon_{ig} * \sigma * \frac{(T_p+273)^4-(T_{og}+273)^4}{T_p-T_{og}}$………………………………………………… 5.4

Where

T_p = temperature of absorber tube

ε_p = emissivity of plate

T_{og} =Temperature of outer glass tube

5.3 Thermal analysis

In this section we outline the manner in which convection coefficient may be obtained theoretically for laminar flow in a circular tube. For short tubes the developing thermal and hydrodynamic boundary layers will result in a significant increase in the heat transfer coefficient near the entrance.

Where h_f is fluid convective heat transfer coefficient inside the U Pipe copper Walls, Soulayman S. and Sabbagh W., (2015).

$$h_f = \frac{N_{UD} * K}{D_i} \qquad \text{5.5}$$

$$N_{UD} = N_{UD\infty} + \frac{a1 * (R_{ew} * P_{rw}\left(\frac{D_h}{L_t}\right))^m}{1 + b1((R_{ew} * P_{rw}\left(\frac{D_h}{L_t}\right))^n} \qquad \text{5.6}$$

$N_{UD\infty}$= Nusselt number at infinity.

N_{UD}= present local nusselt number at constant heat rate.

Where $a1$, b1, m, n, $N_{UD\infty}$ are constant and the value from annex A table A-4.

$flow\ area(A_{cu}) = \pi * (r_{cu})^2$ =0.0000785m^2

Wetted perimeter = $2 * \pi * r = 0.0314$ m

hydraulic diameter$(D_h) = \dfrac{4(flow\ area)}{wetted\ perimeter} = 0.01\ m$

Reynolds number $(R_{ew}) = \frac{\rho * Vav * D_h}{\mu} = 249.15$

$P_{rw} = \frac{\text{v}}{\alpha} = \frac{v * \rho * C_p}{K} = 3.374784$

V = Kinematic viscosity$(\frac{m^2}{s})$

Few assumptions made to simplify the analysis are

- The heat flux along only the radial direction.
- The heat transfer process is assumed to be steady

- The conduction from the glass tubes through the structure that supports them is very small thus effect has been assumed to be neglected.
- Ambient air temperature 21.8 °C.
- No convective and conduction loss from absorber tube.

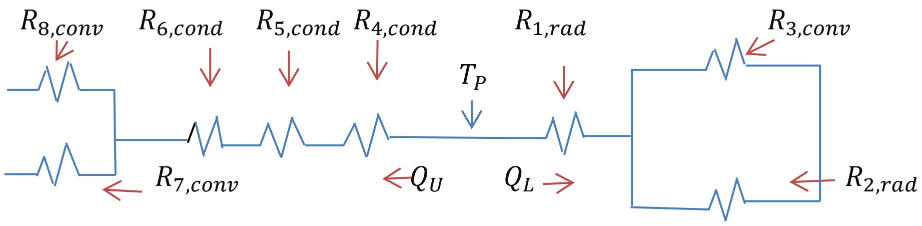

Figure 5.2: Thermal resistance network

The heat loss coefficient U_L is calculated from thermal resistance (Figure 5.3) between the absorber tube and the outer glass tube and between the outer glass tube and the surrounding air such that:

$$U_L = \frac{1}{\frac{1}{h_{rad,og}+h_{wp}}+\frac{1}{h_{rad,ig}}} \quad \text{5.7}$$

The heat lost coefficient is calculated in iterative form, with inner glass initialization temperature of 120°C. Detail calculation available in Mat-lab M-file Appendix B: **1** and the result become U_L= 0.1068 $\frac{W}{m^2K}$.

5.3.1 Collector efficiency factor F': is defined as the ratio of the actual rate of useful heat collection to the rate of useful heat collection when the collector's absorbing plate is at the local fluid temperature, Tiwari et al., [2016].

$$F'=\frac{Q_u}{Q_{u\; T_p=T_f}} \quad \text{5.8}$$

$$F' = \frac{1}{1+\frac{U_L P_l}{U_{ith} P_{ith}}} \quad \text{5.9}$$

$$U_{ith} = \frac{1}{\frac{1}{U_L}+\frac{r_1}{K_{ig}}ln\frac{r_4}{r_3}+\frac{r_1}{K_{Al}}ln\frac{r_3}{r_2}+\frac{r_1}{K_C}ln\frac{r_2}{r_1}+\frac{1}{h_f}} \quad \text{5.10}$$

$$pL_{cu} = 2*(\pi*D_{cu}+L_{cu})$$

$$pL_{al} = 2*(\pi*D_{al}+L_{al})$$

$$pL_{ig} = 2*(\pi*D_{ig}+L_{ig})$$

$$pL_{cs} = 2*(\pi*D_{cs}+L_{cs})$$

$pL_{og} = 2 * (\pi * D_{og} + L_{og})$

U_L = Over all heat loss coefficient

U_{ith} = Heat transfer coefficient at the n surface

P_{ith} = Perimeter of the n surface

5.3.2 Collector heat removal factor (FR): is defined as the ratio of the rate actual useful energy gain to the rate of useful energy gain if the entire collector were at the fluid-inlet temperature in forced circulation mode.

$$F_R = \frac{m_f c_p}{A_{ig} U_L} *(1- \exp(\frac{-\ U_l A_{og} F^-}{m_f c_p}))\ldots\ldots 5.11$$

5.3.3 Useful heat gain (Qu): the useful heat gain by working fluid is given as follows

$$\text{Qu} = A_{ig} * F_R\left[I\left(\tau_g * \alpha_p\right) - U_L\left(T_{f,i} - T_a\right)\right]\ldots\ldots 5.12$$

5.3.4 Collector efficiency (η): The thermal performance of evacuated tube collector can be estimated by the solar collector efficiency which is defined as the ratio between the net heat gain and the solar radiation energy.

$$\eta = \frac{\text{Qu}}{I*A_c} = \frac{\dot{m} c_p (T_o - T_i)}{I*A_c}\ldots\ldots 5.13$$

$$T_o = \frac{\eta * I*A_c}{\dot{m} c_p} + T_i\ldots\ldots 5.14$$

Apply equation 5.14 with mass flow rate range of 0.005:0.001:0.03 detail Mat-lab code present in Appendix B:2 Relation between mass flow rate and collector outlet water temperate shows in Figure 5.4

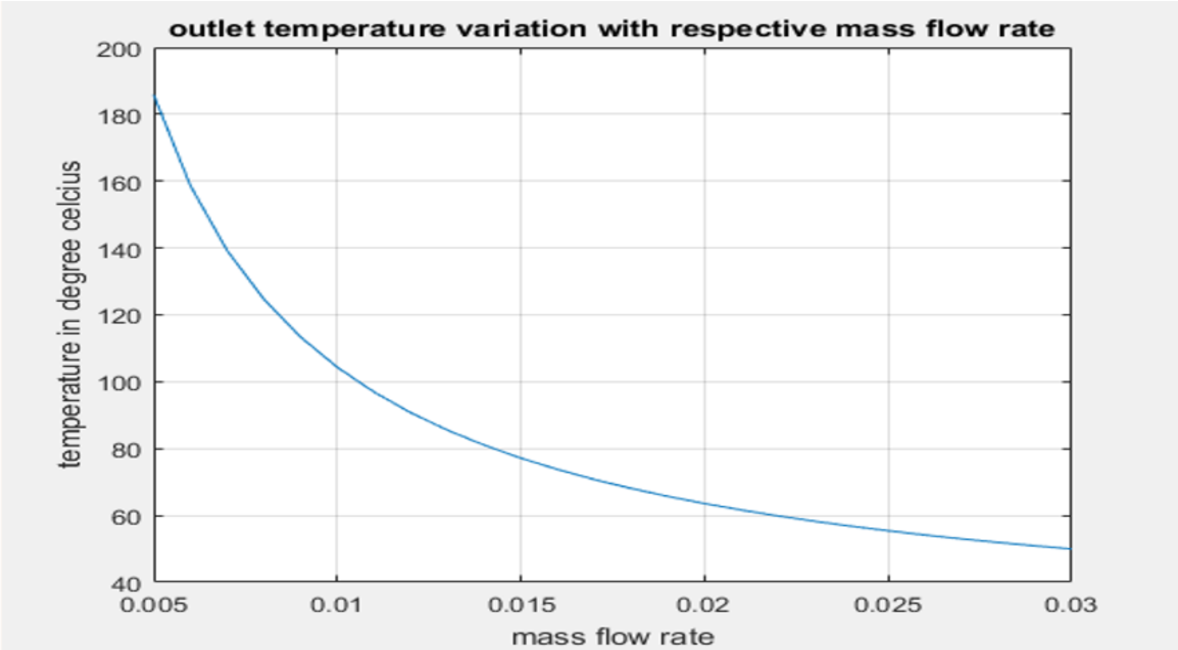

Figure 5.4: Mass flow rate Verse Collector outlet water temperate

5.4 Transient model and analysis of evacuated tube solar collector and Storage tank

Collector models can be subdivided into three categories empirical models rely on experimental or testing data, single-capacitance models, consider only one temperature node, which is very often the spatial mean fluid temperatures and Distributed models that consist to the division of the collector into a number of nodes perpendicular to flow direction, and the number of nodes along flow direction are better in minimizing errors. The most complex models lead to better result, but require more computing time, in minimizing errors and in terms of compromise between precision and computing time, the 3-node model seeds to be the most appropriate. This type of model considers the respective temperatures of the glass envelope, the absorber, and the fluid, Demba N. [2014].

Collector modelling the collector is modelled by considering 3 isothermal regions: those of the glass envelope, of the absorber, and of the fluid. The governing equations were derived by applying the energy balance for each zone as follows. The development of the numerical heat transfer model will be discussed; the derived differential equations are solved using the explicit finite difference method with first order accuracy forward difference scheme replaced time derivation.

5.4.1 Glass Envelope Tube

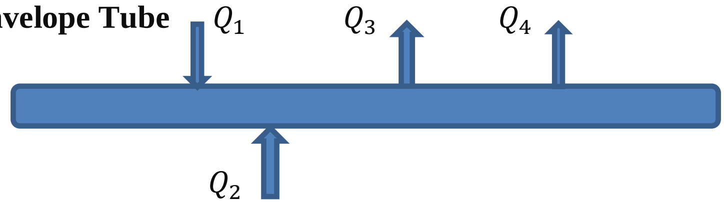

Figure 5.5: heat energy balance of glass tube

$Q_1 = \alpha_{og} A_{og} I$: Solar energy absorbed by the glass envelope

$Q_2 = A_{og} \sigma \varepsilon_p ({T_p}^4 - {T_{og}}^4)$: Radiation heat exchanger between absorber to glass envelope

$Q_3 = A_{og} \sigma \varepsilon_g ({T_{og}}^4 - {T_s}^4)$: Heat radiation toward the sky

$T_s = 0.0552 {T_a}^{1.5}$: Sky temperature according to Swanbank equation

$Q_4 = A_{og} hwp \left(T_{og} - T_a\right)$: Heat losses to the environment

Heat Energy balance equation

$$m_{og} C_{pg} \frac{dT_{og}}{dt} = Q_1 + Q_2 - Q_3 - Q_4 \ldots\ldots\ldots\ldots\ldots\ldots\ldots\ldots\ldots\ldots \quad 5.15$$

$$m_g C_{pg} \frac{dT_{og}}{dt} = \alpha_g A_{og} I + A_{og} \sigma \varepsilon_p \left({T_p}^4 - {T_{og}}^4\right) - A_{og} \sigma \varepsilon_g \left({T_{og}}^4 - {T_s}^4\right) - A_{og} hwp \left(T_{og} - T_a\right)$$

$$\mathrm{T_{g1}} = \mathrm{T_g} + \frac{\alpha_g A_{og} I \Delta t}{m_g c_{pg}} + \frac{A_{og} \sigma \varepsilon_p {T_p}^4 \Delta t}{m_g c_{pg}} + \frac{A_{og} \sigma \varepsilon_g {T_s}^4 \Delta t}{m_g c_{pg}} + \frac{A_{og} hwp T_a \Delta t}{m_g c_{pg}} - (A_{ig} \sigma \varepsilon_p + A_{og} \sigma \varepsilon_g + A_g hwp / {T_{og}}^3) \frac{{T_g}^4 \Delta t}{m_g c_{pg}}$$

5.4.2 Absorber tube

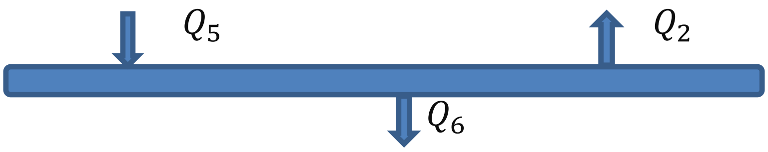

Figure 5.5: heat energy balance of absorber tube

$Q_5 = \tau_g \alpha_p A_{ig} I$: Energy transmitted by the glass envelope and absorbed.

$Q_6 = Aw * h_f * \left(T_p - \frac{T_{wo} + T_{wi}}{2}\right)$: Energy carried away by the fluid.

A_w Is the inner lateral area of copper tube, $A_w = 0.1099\ m^2$

Heat Energy balance equation

$$m_p C_{pp} \frac{dT_p}{dt} = Q_5 - Q_2 - Q_6 \ldots\ldots\ldots\ldots\ldots\ldots\ldots\ldots\ldots\ldots\ldots\ldots\ldots\ldots\ldots\ldots\ldots\ldots\ldots\ldots .. \; 5.16$$

$$m_p C_{pp} \frac{dT_p}{dt} = \tau_g \alpha_p A_{ig} I - A_{ig} \sigma \varepsilon_p \left({T_p}^4 - {T_g}^4\right) - Aw * h_f * \left(T_p - \frac{T_{wo}+T_{wi}}{2}\right)$$

$$\text{Tp1=Tp0+}\frac{\tau_g \alpha_p A_{ig} I \,\Delta t}{m_p C_{pp}} + \frac{A_{ig} \sigma \varepsilon_p {T_g}^4 \Delta t}{m_p C_{pp}} + \frac{Aw * h_f * \left(\frac{Two+Twi}{2}\right)\Delta t}{m_p C_{pp}} - \frac{A_{ig} \sigma \varepsilon_p {T_p}^4 \Delta t}{m_p C_{pp}} - \frac{Aw * h_f * T_p \Delta t}{m_p C_{pp}}$$

5.4.3 Working Fluid

Figure 5.6: Energy balance of working fluid

The energy balance in a control volume of the working fluid in evacuated tube solar collector taking into consideration the change in total energy with time and the total heat transferred into the fluid control volume, the heat energy balance under transient properties of the working fluid can be written as…

Heat Energy balance equation

$$(mc_p)_w \frac{dT_{wo}}{dt} = Aw * h_f * \left(T_p - \frac{T_{wo}+T_{wi}}{2}\right) - m_f c_{pw}(T_{wo} - T_{wi}) \ldots\ldots\ldots\ldots\ldots\ldots\ldots\ldots \; 5.17$$

$$\text{Two1=Two} + \frac{\text{Aw}*h_f*\text{Tp}*\Delta t}{m_w C_{pw}} + \frac{m_f C_{pw} T_{wi} \Delta t}{m_w C_{pw}} - \frac{A_w \; h_f}{m_w C_{pw}} \left(\frac{T_{wo}+T_{wi}}{2}\right) \Delta t - \frac{m_f C_{pw} T_{wo} \Delta t}{m_w C_{pw}}$$

5.4.4 Storage tank

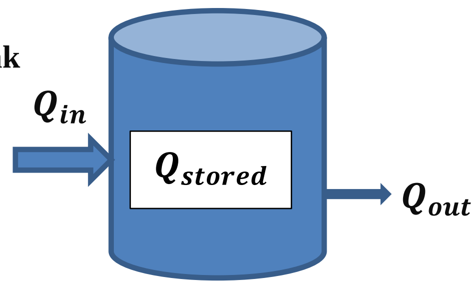

Figure 5.7: Energy balance in control volume of storage tank

The energy balance of the water in the storage tank is evaluated by taking the hot water extracted from the solar collector and the heat losses across the storage tank to the ambient into account. In the model, the level of water in the storage tank is to be controlled by a float valve keeping the mass of water in the storage constant.

Apply the thermal energy balance of the storage tank.

$Q_{storage} = Q_{in} - Q_{out}$ …………………………………………………………..…..…. 5.18

$Q_{stored} = (\rho c_p)_w V_s \frac{dT_s}{dt}$: Net energy gain of storage tank

$Q_{in} = m_f c_{pw}(T_{wo} - T_{wi})$: input energy to storage tank

$Q_{out} = U_{Ls} A_s (T_s - T_a)$: Heat energy loss to the ambient

V_s = storage tank volume (m^3)

U_{LS} = is the heat transfer coefficient of the storage tank

A_S= is the storage tank heat transfer area.

$(\rho c_p)_w V_s \frac{dT_s}{dt} = (m_f c_p)_w (T_{wo} - T_{wi})$ - $U_{Ls} A_s (T_s - T_a)$

$$T_{s1} = Tso + \frac{m_f C_{pw} T_{wo} \Delta t}{\rho_w C_{pw} V_s} + \frac{U_{ls} A_s T_a \Delta t}{\rho_w C_{pw} V_s} - \frac{m_f C_{pw} T_{wi} \Delta t}{\rho_w C_{pw} V_s} - \frac{U_{ls} A_s T_s \Delta t}{\rho_w C_{pw} V_s}$$

CHAPTER 6
OPTIMIZATION OF HOT WATER STORAGE TANK

Hot water storage tank is one of the major components in the solar thermal system because solar energy is a time-dependent so hot water storage tank used as thermal inertia. The primary task of the storage tank is to contain the hot heat transfer fluid without heat losses and must withstand the pressures involved. Figure 6.1 shows hot water load pattern from chapter 3 (Figure 3.3) and available solar radiation variation from chapter 4 (Figure 4.4) in a day.

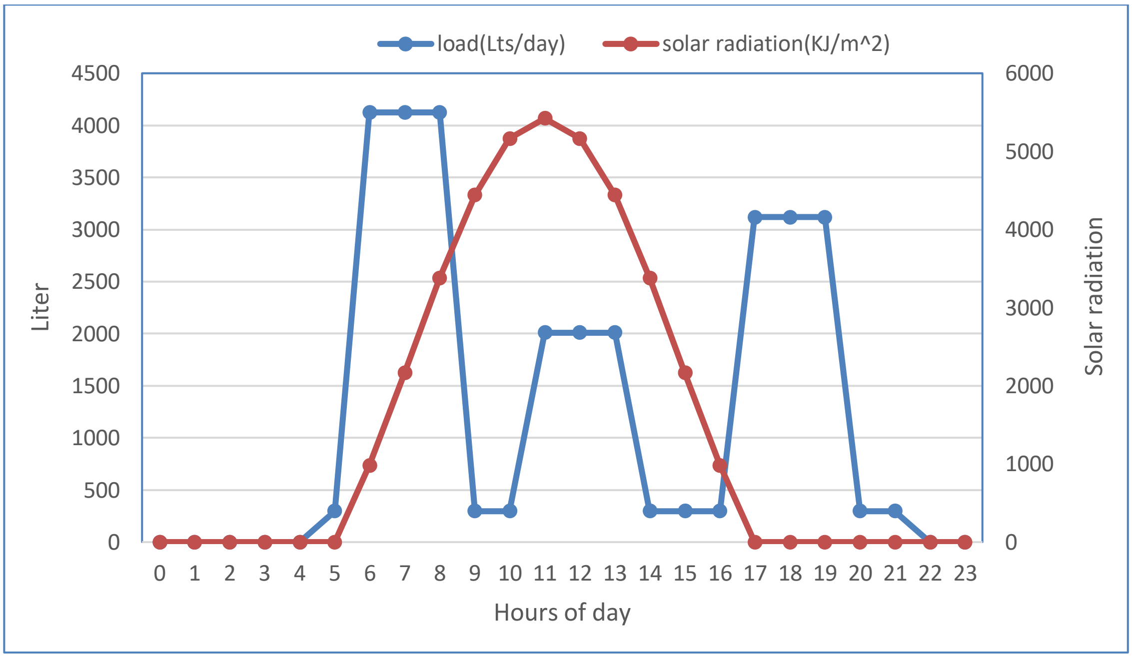

Figure 6.1: variation of load and solar radiation (February) in a day

Different materials are available, Copper is the most common material used for storage vessels because of its high corrosion resistance. The corrosion resistance of the copper is good but its disadvantage lies in its high thermal conductivity leading to heat losses.

Stainless steel has much the better corrosion resistance but is more expensive. The thermal conductivity of steel is lower than copper and therefore less insulation material is required.

Polymerise such as polypropylene and GRP can be used for storage vessels. Corrosion and degradation resistance are adequate and polymerises have the major advantage of thermal conductivity values reducing the need for insulation, Selvan Bellan et al., (2015) Property of selected thermal storage tank materials is listed in appendix (1).and from the wide rank of selected material mild steel is selected because of the following reasons

- Higher melting point
- Lower cost of heat loss per cost of thickness
- Low thermal conductivity
- Higher performance

6.1 Sizing of hot water storage tank volume:

The optimum size of a solar energy storage tank depends on the expected time dependence of solar radiation, the nature of the loads to be expected on the process, the manner in which auxiliary energy is supplied and cost of material, Duffie and Beckman (2013).

The total volume of the storage tank can be specified by multiply the daily hot water demand by 0.8-1.2 in high solar radiation Climate and by 2.2 - 2.5 in lower solar radiation climate, (www.aee-intec.at)

The volume of storage tank (V_s)

V_s =THWL*1.0…………………………………………………………………….……. 6.1

V_s= 30.022 m^3

For circular cylinder recommended storage tank height and radius, $H = 4 * R$ two storage tank each with the capacity of 15.011 m^3

V_s= 4*$\pi * r^3$………………………………………………………………………….... 6.2

$H = 4 * R$………………………………………………………………………....... 6.3

$V_s = 15.011\ m^3$

$V_s = 4 * \pi * r^3$

r ≈ $1.1\ m$

h ≈ 4.25 m

6.2 Optimization of hot water storage tank thickness

Cost of mild steel: the cost of mild steel plate gather from market 315 Birr / thickness (mm) per unit area (m^2). Figure 6.2 shows the relationship between storage material cost and cost of heat loss.

CMS = (cost/mm)*(t_t mm)……………………………………………………………..6.4

Heat loss

$Q_l = U_l * A_s * \Delta T$……………………………………………………………………6.5

The overall heat transfer coefficient (U_l)

$U_{lms} = \frac{K}{t}$………………………………………………………………………………6.6

Surface area of thermal storage tank

$A_s = 2 * \pi * r * h + 2 * \frac{\pi Di^2}{4}$…………………………………………….…….….....6.7

Assume the temperature difference between fluid temperature and ambient temperature around 55 K.

$Q_l = 129.8882/t(mm)\ kWh$

Cost of heat loss

From Ethiopia electric power tariff the cost of energy 1.674 Birr per kWh

CHL = (Cost/kWh) * ($Q_l(kWh)$……………………………….…………….……..…. 6.8

Total cost = CHL+ CMS....…………………….…………….……………..…....….. 6.9

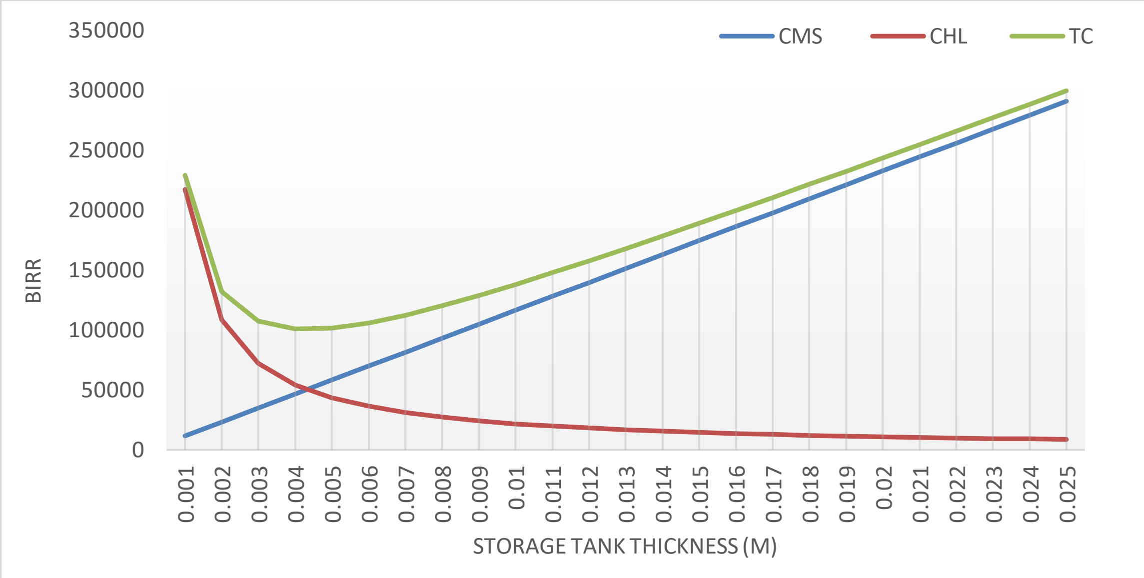

Figure 6.2: Cost of Heat loss V_s storage material thickness (m)

Differentiating the total cost equation 6.9 with respect to the thickness and setting the value equal to Zero, is given as :

$11641.707 - \frac{217432.85}{t^2} = 0$……………………………………………………….. 6.10.

The optimum thickness of mild steel is 4.322 mm so for safety we take 5 mm.

6.3 Optimization of Insulation material thickness, Glass Fiber

Heat losses from the storage tank are reduced by use of insulation. Property of various insulation materials are listed in appendix (2). Out of this Fibre glass is selected because of the following reason.

- Higher temperature resistance
- Lower thermal conductivity
- Lower cost per unit area
- Higher durability in the presence of moisture
- Higher resistance to the water

Cost of fibre glass: the cost of fibre glass plate gather from market 10.5 Birr/thickness (mm) per unit area (m^2) Figure 6.3 shows the relationship between insulation material cost and cost of heat loss.

CFG = (cost/mm)*(t_t mm)…………………………………………………….. 6.10

Heat loss

$U_l = U_{cond,fg} + U_{conv,fg}$ ……………………………………………………….....6.11

$A_{s1} = 2 * \pi * (r + t) * h + 2 * (\frac{\pi Do^2}{4})$ ……………………….……………..…. 6.12

$$U_{lfg} = \frac{K}{t} = \frac{0.032}{t}\ W/Km^2$$

$U_{lcfg} = 2.8 + 3\,Vw$ ……………………………………………………………….... 6.13

but $Vw = 3.5\ m/sec$

$Q_l = (\frac{0.0651}{t} + 27.05)$ kWh

The rate of heat loss from the tank in 24 hours

Cost of heat loss

From Ethiopia electric power tariff the cost of energy 1.674 Birr per kWh

CHL = (Cost/kWh) * ($Q_l(kWh)$ …………………………………………………..... 6.14

Seen from equation 6.8 the cost verses heat loss related linearly decreasing.

Total cost = CHL+CMS…………………………………………………………….…. 6.15

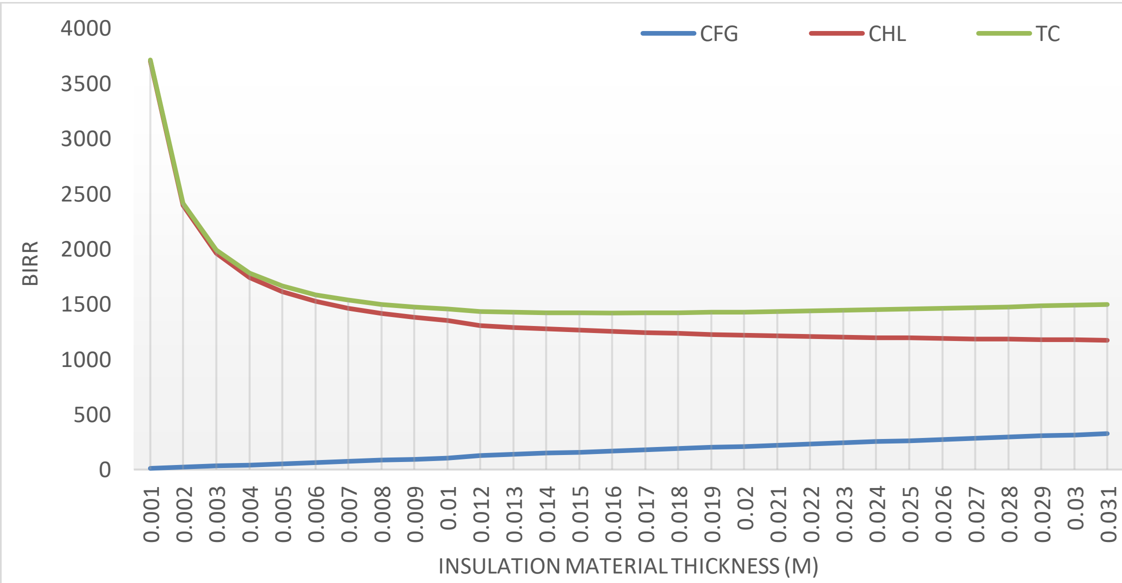

Figure 6.3: Insulation material thickness (m) Verse Heat loss

Differentiating the total cost equation 6.15 with respect to the thickness and setting the value equal to Zero, is given as:

$$10.5 - \frac{2615.4576}{t^2} = 0 \qquad \text{……… 6.16}$$

The optimum thickness of fibre glass is 15.783 mm so for safety we take 16 mm.

CHAPTER 7

PROGRAMMING AND SIMULATION

Simulations are numerical experiments and can give the near the same kinds of thermal performance information as can physical experiments. They are, however, relativity quick and inexpensive and can produce information on effect of design variable changes on system performance by series of numerical experiments all using exactly the same loads and weather.

Simulation can be used to predict the way in which the system will evolve and respond to its surroundings, so that you can identify any necessary changes that will help make the system perform the way that you want it to.

There are different types of software used to code mathematical model for numerical problem solution; which are MATLAB, C, C++, FORTRAN, etc. This study use MATLAB version R2017a, mathematical model programing for U-type evacuated tube solar collector with storage tank. The mat-lab code numerically solves the derived model and computes the transient temperature distributions at any time start from (t=0) with the following initialized assumption; Tgo=Ta0+0.5, Tpo=Ta0 +1.0, Twi0= Ta0, Two0= Ta0+1 and Ts0= Ta0+0.75 appendix B-3 shows detail mat-lab code.

All physical dimensions of the collector, storage tank and the thermos-physical properties can be entered as inputs also solar radiation and ambient temperature for every hour of the day, and daily hot water consumption.

Detail simulation flowchart (Figure 7.1) entailing the various steps to solve the mathematical model developed in the previous chapter.

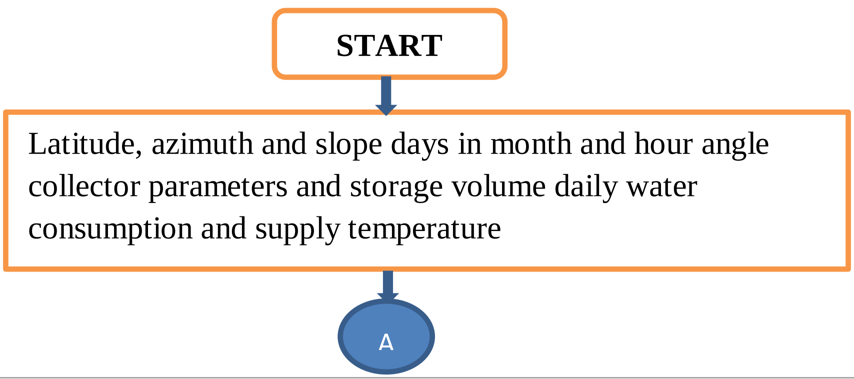

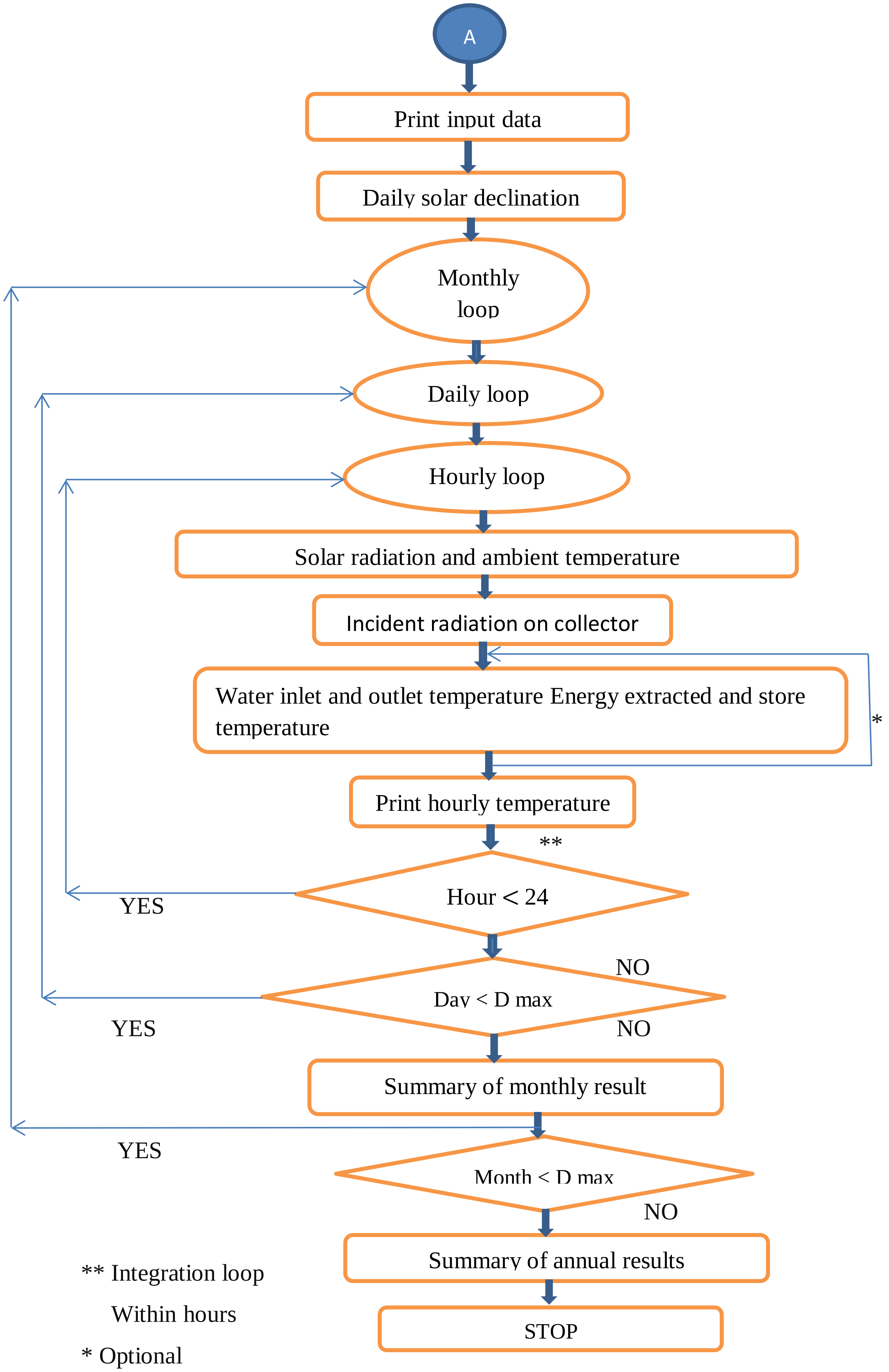

Figure 7. 1: Flowchart of simulation programme

7.1 Procedure for simulation of solar thermal water heater

The simulation program is used to predict the monthly and annual performance of the solar water heating system includes the following procedures:

I. Properly writing the programming code of input parameters; basic angles (latitude, slope angle…) the solar collector parameter and solar radiation data.

II. The fraction of the total daily hot water load that occurs in the hours should also be specified in the simulation process.

III. Determining sun basic angle (declination, hour, zenith, and incident), total and incident solar radiation for each hour of the day

IV. Starting the system simulation by assuming the following initial temperatures for the various components of the solar-collector model.
   - Ambient temperature: Tao= read from January 1 at 01:00 AM.
   - Glass temperature: Tgo=Tao+0.25,
   - Plate temperature: Tpo=Tao+1.0,
   - Temperature of water at collector inlet: Twio=Tao,
   - Temperature of water at collector outlet Two0=Tao+0.5,
   - Storage tank temperature: Tso=Tao+0.5,

V. Evaluate temperature of the plate, of the glass, of the water at outlet from the collector and of the storage tank at time (t+Δt) apply equation 6.15, 6.16, 6.17 and 6.18.

VI. Since the assumed temperature for the various components of the collector are too crude, they have to be refined by taking average values of the assumed temperatures and the evaluated temperature at time (t+Δt) and substituted for temperature values at time t.

VII. Temperature variation (Tp1),(Tg1),(Two1) and (Ts1)during a period of 24 hours over the years are then estimated by substituting the new values of (Tp1),(Tg1),(Two1) and (Ts1) respectively, for (Tp0),(Tg0),(Two0) and (Tso),for the next time interval.

VIII. Evaluate the possible performance of solar collector.

IX. Finally the expected output of the MATLAB simulation displayed using graph.

CHAPTER 8

RESULT AND DISCUSSION

8.1 Outlet water temperature from collector: The output water temperature from the collector strongly depends on solar radiation and mass flow rate; means higher available radiation means higher outlet temperature and higher mass flow rate means lower out let water temperate, the result of outlet water temperature distribution for different season of the year are plotted in below Figure 8.1 and shows maximum outlet water temperature in winter season (February) and minimum water temperature in summer season (July).

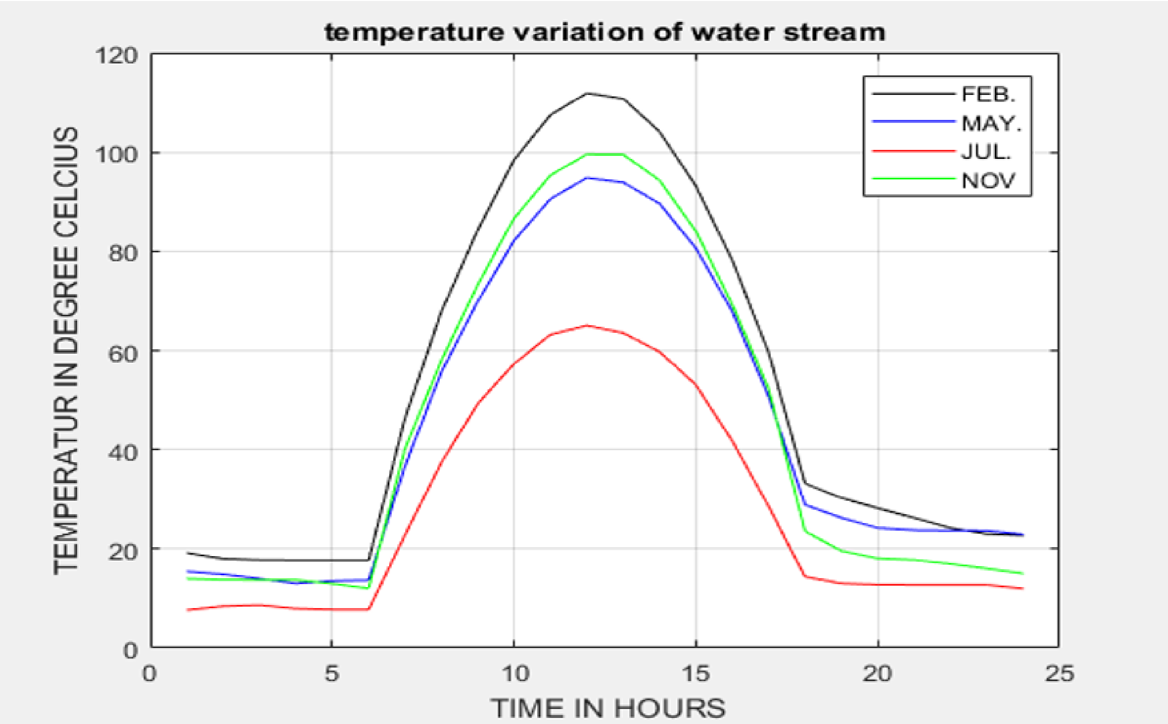

Figure 8.1: Simulated hourly outlet water temperature for various seasons

8.2 Storage tank water temperature: Water temperatures in storage tank depend on temperature of water in the collector and ambient condition. Water temperatures in the tank are plotted in Figure 8.2 for the representative days of selected month at various seasons of a year. Maximum temperate achives in winter season, Febrary month and minimum achives in summer season, July month.

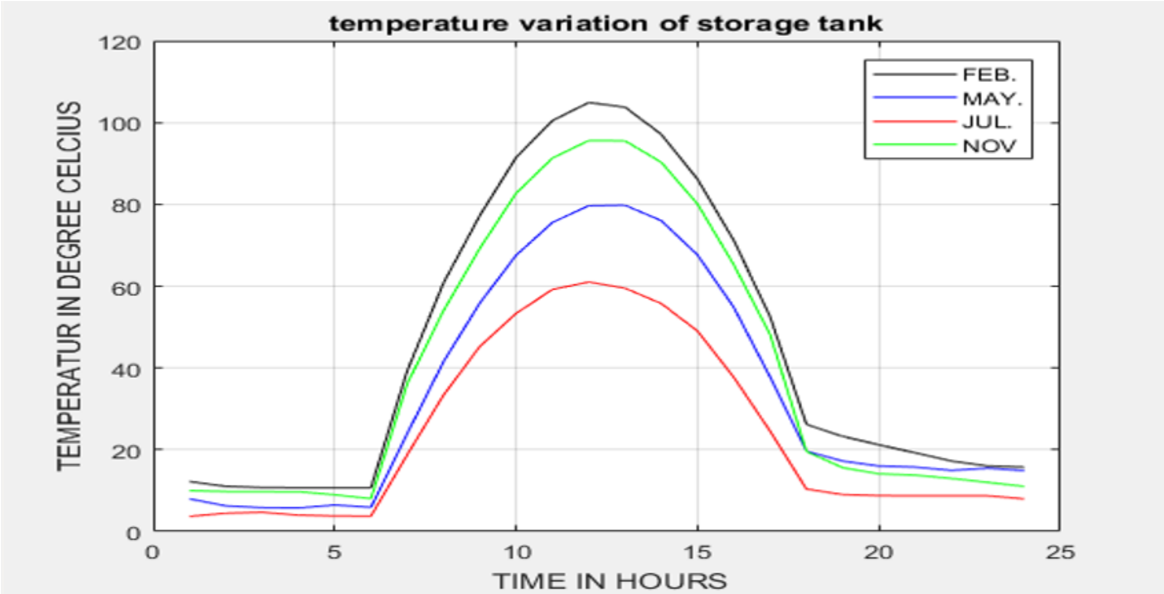

Figure 8.2: Simulated hourly storage tank temperatures for various seasons

8.3 Hourly useful heat gain: The amount of useful energy gained by the water flowing though collector is strongly depends on solar radiation and mass flow rate and according to Figure 6.4 selected mass flow rate 0.0227 Kg/sec and Figure 8.3 shows useful heat gain collected from unit collector for different season of the year and maximum heat energy harvested in winter season month of Febraury 54.717603 MJ/day and the least one energy harvested in summer season month of July 34.724741 MJ/day.

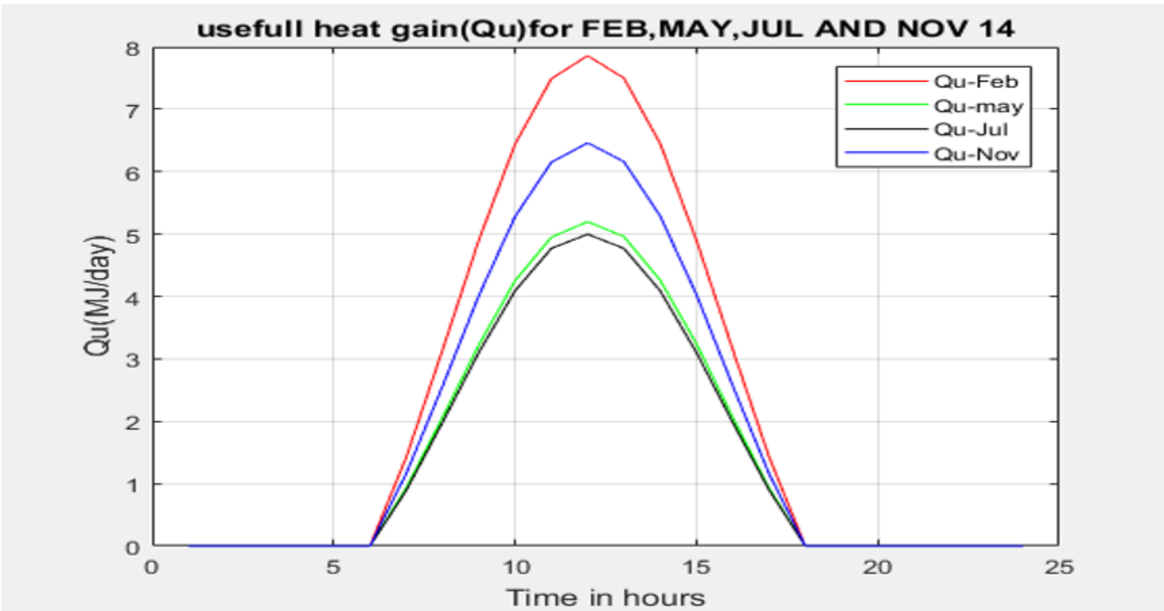

Figure 8.3: Hourly distribution daily useful heat gain

8.4 Over all discussion:

According to hourly distribution of daily useful heat harvesting in figure 8.3, February month energy harvesting capacity from single collector is maximum and equals to $54.717603 \frac{\text{MJ}}{\text{day}}$ and from load estimation total energy required to fuilfill the hospital demand equals to $2820.3 \frac{\text{MJ}}{\text{day}}$

Solar fraction:

Is the ration of energy gain from solar energy to the total energy (solar energy + auxiliary energy) requirement for water heating for different appliance in daily usages of hospital and is given as $\text{SF} = \frac{Q_s}{Q_s + Q_{aux}}$, Figure 8.4 shows the solar fraction which is calculated based on Febraury month with equating solar fraction equal to one (1) and the minimum value on June equals to 0.6261933

So maximum auxiliary energy required to fulfil daily energy demand in the month of June about 1054.25 MJ/day

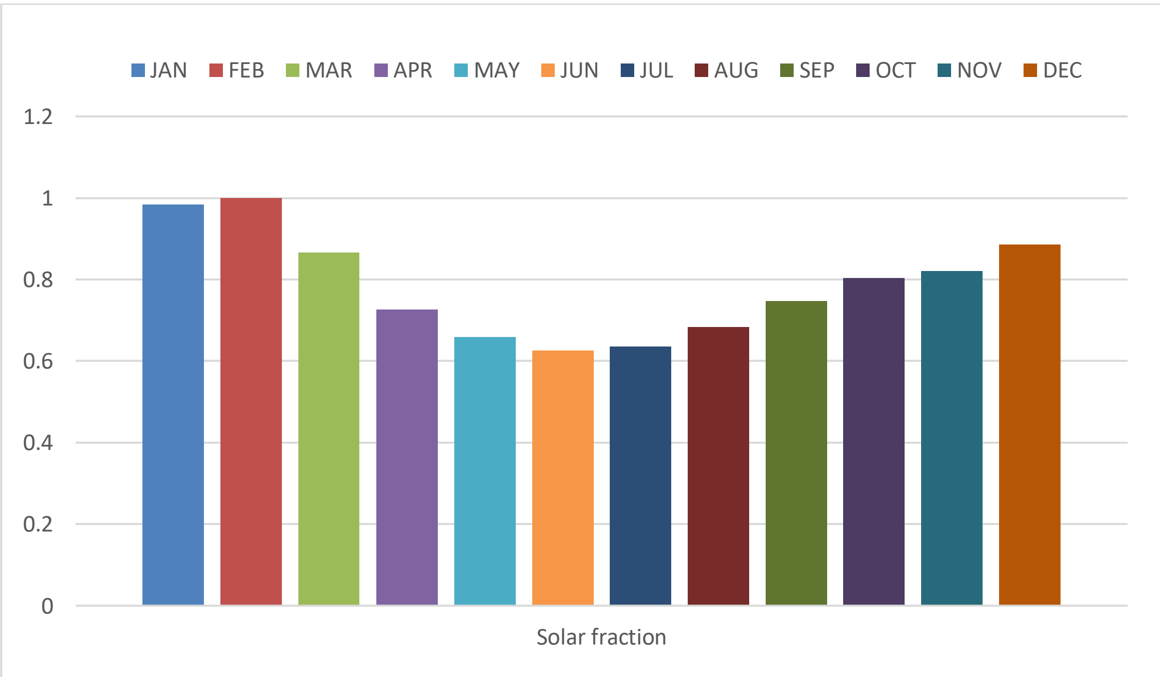

Figure 8.4: Monthly average daily fraction of solar gain

CHAPTER 9

PUMP AND CONTROL SYSTEM SELECTION

According to the result of computer simulation for February month, the daily hot water demand of Adama general hospital is fulfil by the use of 52 collectors. Collector modules in the arrays connected in parallel and detail layout in annex D-1.

Pump selection: This is the heart of a hydraulic system, converts mechanical energy into hydraulic energy, in this section shows the fundamentals of fluid mechanics necessary to understand and determine pressure losses in the system. There are two types of friction losses in pipes: main and minor losses. The first type deals with the resistance to flow offered by straight pipe section while the second one refers to bends, fittings, and other elements present in the pipe system. U-type evacuated tube solar collector are shown in figure 9.1

Non-positive displacement pump used generally for low pressure and high volume flow application. Manly used for transporting fluids from one location to another.

Knowing the pressure losses in a piping system and the pumping power required allows for sizing considerations of pumps.

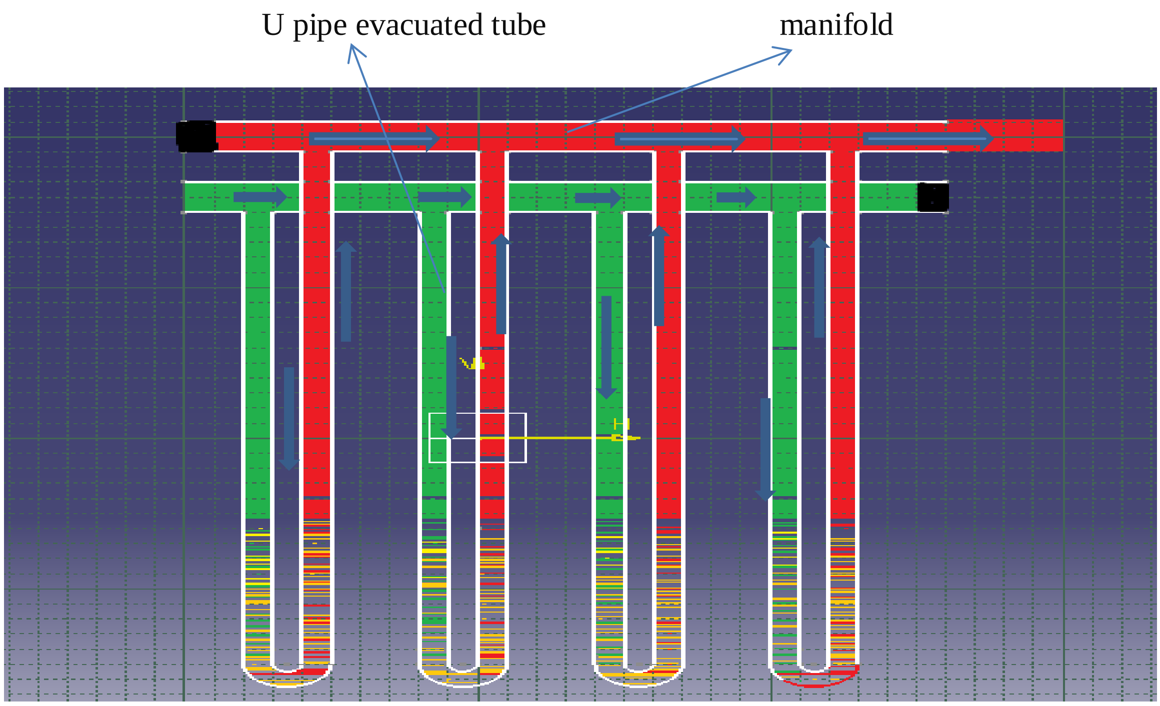

Figure 9. 1: U-type evacuated tube solar collector (CATIA V-5 R19)

A quantity of interest in the analysis of pipe flow is the pressure drop since it is directly related to the power Requirements of the pump to maintain flow.

In practice, it is found convenient to express the pressure loss for all types of fully development internal flows, Engineering design handbook [1973].

$$\Delta P = f\left(\frac{L}{d}\right)\left(\frac{\rho * {V_{av}}^2}{2}\right)$$

9.1 Pressure drop inside U pipe evacuated tube solar collector

P = 101325 pa

$\rho = 985.65 \ \frac{Kg}{m^3}$

$\mu = 0.000504 \ \frac{kg}{m.s}$

$\dot{m} = 0.0227 \ \frac{Kg}{s}$

$\dot{Q} = \frac{\dot{m}}{\rho} = \frac{0.0227}{985.65} = 0.0000230304875 \ \frac{m^3}{sec}$

Volume flow rate in single tube (Q)

$Q = \frac{0.0000230304875 \ \frac{m^3}{sec}}{15} = 1.54 * 10^{-6} \ \frac{m^3}{sec}$

Velocity of fluid in side U-pipe in tubes (V_{av})

$$V_{av} = \frac{\dot{Q}}{A_{cu}} = 0.01956 \ \frac{m}{sec}$$

Reynolds number (R_e)

$R_e = \frac{\rho * V_{av} * d}{\mu} = \frac{985.65 \frac{Kg}{m^3} * 0.01956 \ \frac{m}{sec} * 0.01 \ m}{0.000504 \ \frac{Kg}{m.s}} = 383$

Since $383 < 2300$ the flow is under laminar and the pressure drop for Circular cross section tubes are calculated as

$$\Delta P = f\left(\frac{L}{d}\right)\left(\frac{\rho * {V_{av}}^2}{2}\right)$$

$ƒ = \frac{64}{R_e} = 0.167101827$

$\Delta P1 = ƒ\left(\frac{L}{d}\right)\left(\frac{\rho * V_{av}{}^2}{2}\right)$ =0.167101827* $\left(\frac{3.5}{0.01}\right) * \left(\frac{985.65 * (0.01956\ )^2}{2}\right)$ =10.0276 Pa

Total pressure drop 4300.75 Pa

9.2 Pressure drop in collector bending ($180°$)

For bending it is defined a total loss coefficient (K) and the value K depends on length and diameter of pipe [34].

$\Delta p2 = k * \frac{\rho * v_{av}{}^2}{2}$ =7.9 * $\left(\frac{985.65 * (0.01956\ \ )^2}{2}\right)$ = 1.49 Pa

Total pressure drop because of $180°$ bend = 581 Pa

9.3 Pressure drop in fluid Entrance

$\Delta p3 = k * \frac{\rho * v_{av}{}^2}{2} = 7.6 * \left(\frac{985.65 * (0.01956\ )^2}{2}\right)$= 1.433 Pa

Total pressure drop also happen when fluid inter into collector (smaller diameter) than intake manifold and equals to 558.8 Pa

9.4 Pressure drop in fluid Existing

$\Delta p4 = k * \frac{\rho * v_{av}{}^2}{2} = 7.583 * \left(\frac{985.65 * (0.01956\ )^2}{2}\right)$ = 1.43 Pa

Pressure drop also happen when fluid flows from collector to manifold and equals to =557 Pa.

9.5 Due to Inclination from horizontal pressure drop

$\Delta p5 = \rho g h = 985.65 * 9.81 * 0.7 = 6768.46\ Pa$

9.6 pressure drop in the manifold

9.6.1 Length of intake manifold

Seen from appendix D: 1

0ne collector widths = 1.178 m

There are 12 collectors in 2 arrays and the total length = 14.136 m

And there are also 14 collector in 2 arrays and the total length = 16.492 m

9.6.2 Length of return manifold

Same as intake manifold

9.6.3 Length From Storage tank to Collector arrays

Total length =4*1.8 m + 4*0.2 m +2m = 10 m

Intake manifold pressure drop

For diameter of 22 mm manifold tube the pressure drop for intake manifold calculated

$$\Delta P = f\left(\frac{L}{d}\right)\left(\frac{\rho * {V_{av}}^2}{2}\right)$$

Area of intake manifold $A_{im} = \pi * r^2 = 0.00037994\ m^2$

The total Volume flow rate rates, $\dot{Q} = 26 * 0.0000230304875\ \frac{m^3}{sec}$

Velocity inside intake manifold

$V_{im} = \frac{\dot{Q}}{A_{im}}$ = 1.576 $\frac{m}{sec}$

Reynolds number

$R_e = \frac{\rho * V_{im} * d}{\mu} = \frac{985.65 \frac{Kg}{m^3} * 1.576\ \frac{m}{sec} * 0.022\ m}{0.000504\ \frac{Kg}{m.s}}$ =67,807.3

Since 2300 $< 67{,}807.3$ the flow is under turbulent and the pressure drop for Circular cross section tubes are calculated as

$$\Delta P = f\left(\frac{L}{d}\right)\left(\frac{\rho * {V_{av}}^2}{2}\right)$$

For the material of galvanized iron cast, equivalent roughness(ε) 0.15 mm with pipe diameter of 0.022 mm

$\frac{\varepsilon}{d}$ =0.00682

Therefore, from the moody chart (appendix D:2) with corresponding Reynolds number f =0.032

$f, friction\ factor$

$\Delta P6 = ʄ\left(\frac{L}{d}\right)\left(\frac{\rho * V_{av}{}^2}{2}\right)$ = 0.032* $\left(\frac{7.1}{0.022}\right) * \left(\frac{985.65 * (1.576\ )^2}{2}\right)$ = 12,641.4 Pa

There are 2 arrays and the total pressure drop equals to 25,282.76 Pa

$\Delta P7 = ʄ\left(\frac{L}{d}\right)\left(\frac{\rho * V_{av}{}^2}{2}\right)$ = 0.032* $\left(\frac{8.246}{0.022}\right) * \left(\frac{985.65 * (1.576)^2}{2}\right)$ = 14,681.75 Pa

There are 2 arrays and the total pressure drop equals to 29,363.51 Pa

Return manifold pressure drop

Same as intake manifold pressure drop

9.7 Pressure drop from storage tank to collector arrays

Take volume flow rates, $\dot{Q} = 4 * \dot{Q}$ = 0.0023952 $\frac{m^3}{sec}$

For diameter of 37 mm tube the pressure drop calculated

Area of intake manifold $A_{im} = \pi * r^2 = 0.001074665\ m^2$

Velocity inside tube

$V_{im} = \frac{\dot{Q}}{A_{im}}$ = 2.228 $\frac{m}{sec}$

Reynolds number

$R_e = \frac{\rho * V_{im} * d}{\mu} = \frac{985.65\frac{Kg}{m^3} * 2.228\ \frac{m}{sec} * 0.037m}{0.000504\,\frac{Kg}{m.s}}$ = 161,271.37

Since 2300 $< 161{,}271.37$the flow is under turbulent and the pressure drop for Circular cross section tubes are calculated as

$$\Delta P = ʄ\left(\frac{L}{d}\right)\left(\frac{\rho * V_{av}{}^2}{2}\right)$$

For the material of galvanized iron cast the equivalent roughness(ε) is 0.15 mm with the pipe diameter 37 mm

$\frac{\varepsilon}{d}$ =0.004054054

Therefore, from the moody chart (appendix D:2) with corresponding Reynolds number ʄ =0.026

$\Delta P8 = ʄ\left(\frac{L}{d}\right)\left(\frac{\rho * V_{av}{}^2}{2}\right)$ = 0.026* $(\frac{10}{0.037}) * \left(\frac{985.65 * (2.228\ )^2}{2}\right)$ = 17,190.74 Pa

Total pressure drop from storage tank to collector arrays = 34,381.5 Pa

9.8 Pressure drop in bending

Seen from Appendix D:1, there are 8 bends

Pressure drop in fluid entrance, one 90° bends and three tee bends

For three tee bends

$\Delta p9 = 3 * k * \frac{\rho * v_{av}{}^2}{2} = 3 * 0.45 * \left(\frac{985.65 * (1.576)^2}{2}\right)$ = 1652.5 Pa

For one 90° bends

$\Delta p10 = k * \frac{\rho * v_{av}{}^2}{2} = 0.85 * \left(\frac{985.65 * (1.576)^2}{2}\right)$ =1040.46 Pa

Pressure drop in fluid existing

Pressure drop in fluid existence, one 90° bends and three tee bends

For three tee bends

$\Delta p11 = k * \frac{\rho * v_{av}{}^2}{2} = 3 * 0.45 * \left(\frac{985.65 * (2.228\ )^2}{2}\right)$ = 3302.61 Pa

For one 90° bends

$\Delta p12 = k * \frac{\rho * v_{av}{}^2}{2} = 0.85 * \left(\frac{985.65 * (2.228\ )^2}{2}\right)$ = 2079.42 pa

9.9 Total pressure drop

Total pumping pressure needed for design is the sum of all the above pressure drops

$\Delta p = \Delta p1 + \Delta p2 + \Delta p3 + \Delta p4 + \Delta p5 + \Delta p6 + \Delta p7 + \Delta p8 + \Delta p9 + \Delta p10 + \Delta p11 + \Delta p12$

= 164,510 Pa

In the analysis of piping systems, pressure losses are commonly expressed in terms of the equivalent fluid column height, called the head loss H

9.10 Total specific work (Y)

Once the pressure loss is known, the required pumping power to overcome the pressure loss is determined from

Specific work $= \frac{\text{Total pressure drop}}{density} = 164.51 \ \frac{m^2}{s^2}$

Head loss (H) $= \frac{\text{Specific work}}{\boldsymbol{g}} \cong 17$ m

Total volume flow rate for the pump equals to 0.0023952 $\frac{m^3}{sec}$

The proper centrifugal electric drive pump satisfying the requirement of head = 17 m and flow rate = 8.623 $\frac{m^3}{h}$

Table 9. 1: Pump performance specification, Electrical pump catalogues (NOCCHI)

CODE	MODEL	NORMAL POWER (kW)	VOLTAGE (V)	AMP 3×400 V	Motor type	Frequency	Weight (KG)
PA021010	NRB2 32×120 B	1.1 kW	230/400	4.7/2.7	80 B2	50 Hz	63

9.11 Control element

Valves are used in hydraulic circuits to control pressure, flow direction, or flow rate. They utilize mechanical motion to control the distribution of hydraulic energy within the system.

9.11.1 Pump Control

Active systems use electric pumps to circulate water or other heat transfer fluids through the collectors. However the operation of the pump should be designed only when solar energy collection is feasible. To determine whether solar energy collection is feasible or not, measuring collector outlet water temperature and comparing it with the storage tank bottom water temperature is necessary. If the energy obtained from solar collection is not relatively greater than the pumping cost, the pump should be off until sufficient energy is obtained.

The RTD is a temperature sensing device whose resistance changes with temperature. Typically built from platinum, though devices made from nickel or copper are common, RTDs can take many different shapes like wire wound, thin film.

Table 9. 2 : Typical temperature sensor characteristics

Typical temperature sensor characteristics				
Characteristics	**Thermistor**	**RTDs**	**Thermocouples**	**Semi-conductor**
Temperature range	-55℃ to 125℃	-200℃ to 850℃	-600℃ to 2000℃	-50℃ to 150℃
linearity	exponential	Fairly linear	Fairly linear	best
Sensitivity	high	low	medium	highest
Response time	Fast	low	Fast to low depends on construction	Slow
Excitation or power	Needed	Needed	Not needed	Needed
Long-term stability	Low	High	High	Medium
Self-heating	Yes	Yes	No	Yes
Cost	low	Low to high	Moderate to high	Low to moderate

The RTD which is present for maximum and minimum temperature difference closes or opens the electric pump circuit. For this model one end of the RTD sensors is placed at the bottom of the storage tank and the other end at the collector outlet pipe and set to start the pump. The pump will stop its operation when the temperature difference is nearly zero. In order to avoid continuous off and on operation of the pump, 1– 3 minutes delay increases the life of the motor. Other RTD is present in outlet from storage tank to adjust actuator and control flow rate in the system. Figure 9.2 shows the arrangement of the component in the system.

9.11.2 Pressure Relief Valve

A pressure relief valve is a valve used in liquid systems that opens whenever the pressure in the system is greater than some safe maximum. It guards against destructive pressures that could build up if the system is overheated.

9.11.3 Air Vent

The amount of air which can be contained in water decreases with the temperature of the water. Therefore, a large amount air from the water may develop a higher pressure in the storage tank and the pipes. Therefore this air should be vented through an air vent, air vent designed at the header and top of the storage tank is in coincidence with a lighter density of air.

9.11.4 Flow control valves for limiting the fluid flow rate in a line, which in turn limits the extension or retraction.

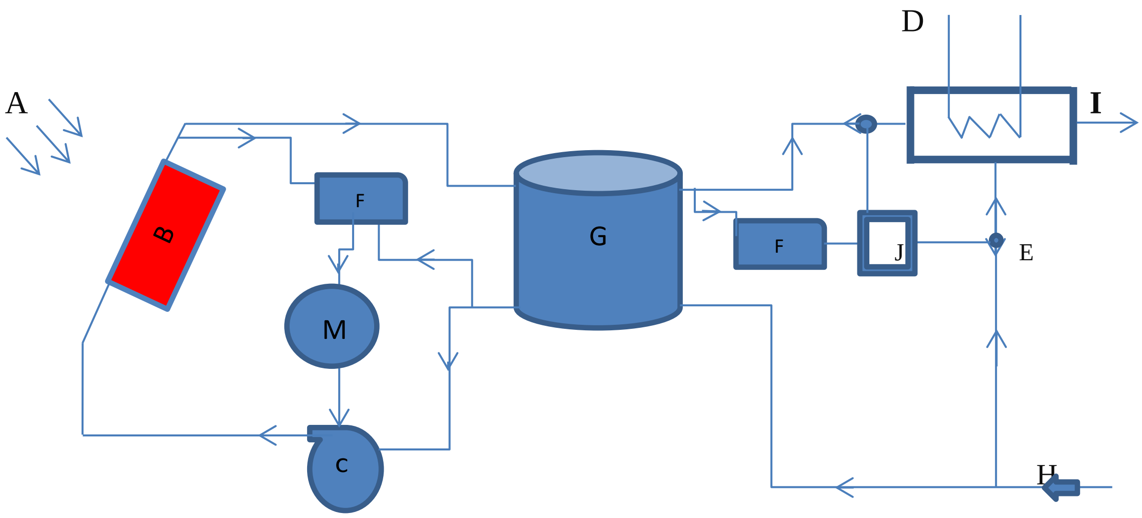

Figure 9. 2: Overall system layout

Keys

J-Actuator, H-Main water stream, B-Solar collector, I-Load D-Auxiliary heater,

C-Pump, F-RTD Sensor, G-Tank, A-Solar radiation, E- flow control Valve, M- Motor,

CHAPTER 10

ECONOMIC ANALYSIS

In this chapter economics of solar water heater system will be analysed. Economic analysis plays a vital role in the decision of using these systems after the technical feasibility is identified.

10.1 Costs associated with solar water heater system: the costs associated with solar water heater system can be divided
Mainly in two categories:

- Capital costs: include equipment purchases cost and installation work of the system.
- Operation and maintenance costs: include labour and other varies spending funds during the life time of the project after the system is installed.

10.1.1 Capital Costs

The capital costs represent all costs associated with the buys of equipment and installation works of the project.

These costs are classified as direct and indirect costs.

10.1.1.1 Direct Capital Cost: the direct capital cost represents costs for specific equipment or installation service. The direct costs for solar water heater system are solar collector field, storage tank, other system components and labour costs. The direct capital costs associated with solar thermal systems are listed in Table 10.1 (All costs referred in this thesis are in Birr)

10.1.1.2 Indirect Capital Cost: Indirect cost is normally not identified in a specific term like the direct cost of equipment and installation services; rather it includes all other costs that can be included throughout the operation period, this costs includes; Engineer, Procure, Project, Miscellaneous and Sales taxes, indirect capital costs associated with solar thermal systems are listed in Table 10.2:

Table 10.1: Direct Costs for solar water heater system components

No	Item description	Specification	Unit cost(birr)	Total cost(birr)
1	Solar collector	U-tupe evacuated solar collector	9,000.00	468,000.00
2	Frame	Aluminum	700.00	36,400.00
3	Collector stamp		100.00	5,200.00
4	Labour and instalation	15 % of collector cost		72,930.00
5	Storage tank	cylinder		
	Inside material	3 mm mild steel glass W=1m and L=2m	750.00	11,009.00
	Insulation	10 mm fiber glass W=1m and L=2m	4,133.00	66,670.40
	Insulation cover	0.8 mm thickness galvanized pre painted steel	200.00	6,405.30
	manufacture	50% of material cost		39,042.00
6	Pump	MEC-A 1/40A	17,000.00	34,000.00
7	controller	RTD	20,000.00	
		Pressure relief valve	15,000.00	
		Air vent	10,000.00	
		Flow control valve	15,000.00	60,000.00
8	Galvanized iron cast	D=22mm D=37mm	250.00 333.00	5,105.00 4,439.00
9	Elbow	Tee elbow 90 degree elbow	137.50 100.00	1,650.00 400.00
10	Contingency	10 %		81,125.03
Total				892,375.3

Table 10. 2: Indirect capital costs of solar water heater systems

No	Item description	Total Cost (Birr)
1	Engineer, procure and construction-16% of direct cost.	142,780.04
2	Project, land and miscelanious-3.5% of direct cost	31,233.14
3	Total	174,013.14

The Total capital cost of the system will be the sum of direct and indirect capital costs

$T_C = d_c + id_c$………………………………………………………………………. 10.1

10.2 Operation and Maintenance Costs:

The cost associated with solar water heater system after installation is operation and Maintenance costs. These represent all costs on services throughout the project life, mainly cost of maintenance (repair and replace) and pumping cost.

Pumps are the solar water heater components most frequently replaced. Various companies working with solar water heaters recommended that the average age of pumps replaced varies between 7-10 years.

Collectors from various companies manufacturing solar collectors certified that the solar collector would last for at least 25-30 years.

Storage tanks various companies recommend the average age of tanks replacement varies between 10-15 years.

The Annual operational and maintenance costs associated with solar thermal systems are listed in table 10.3:

Table 10.3: Annual Operation and maintenance of solar water heater system

	Unit cost	Total cost(Birr)
Annual Operation Cost (maintenance and pumping cost)	10 % of system cost	106,638.81

10.3 Life Cycle Cost:

The Life cycle cost (LCC) analysis make up an economics tool to help in making investment decisions mainly by identifying the breakeven point or payback period over the project life time. For renewable energy solutions like solar and wind comparisons with that of conventional energy solutions, the life cycle cost (LCC) approach is very important as most of these renewable energy projects require high initial investment.

Mostly renewable energy solutions require high initial investment and low operational cost, whereas conventional energy solutions require low investment cost and high operational cost. Hence renewable solutions have low payback period over conventional solutions due to costs associated with fossil fuel.

The LCC accounts capital cost, operational and maintenance cost throughout the project life time as follows

$$LCC = CI + C_m \frac{1}{i}\left(1 - \frac{1}{(1+i)^n}\right) \qquad \text{10.2}$$

CI is the investment cost of solar water heating system

C_m is annual maintenance and pumping cost

Economic analysis: Life time of the investment is 25 years; most of them certified that the solar collector would last for at least 25-30 years, pumps 7-10 years, storage tank 10-15 years.

Table 10. 4: Economic analysis parameters

Parameters	**Value**
Inflation rate	10%
Discount rate	10%
Salvage rate	10%
Dept interest rate	8.5%
Rate of energy escalation	15%
Cost of electricity	1.674 Birr/kWh

From equation 10.2 the life cycle cost of solar water heating system of the project is

LCC = 2,003,254.00

10.4 Life cycle saving of energy

The life cycle saving of solar water heater is the energy cost saved due to replacement of electricity and diesel fuel by solar thermal. The annual energy saving is,

ES = $f_a Q_a$……………………………………………………………….…………………10.3

The life cycle saving of energy

LCS =$P_e f_a Q_a (\frac{1+i_e}{i-i_e})$*[1-$(\frac{1+i_e}{1+i})^n$]……………………………………………………….. 10.4

Where

LCS is the life cycle saving of a solar water heating system (kWh)

f_a is annual fraction of load supplied by solar energy

Q_a is the annual heating load (kWh)

i is the annual market discount rate

i_e is the annual market rate of energy escalation

Solar fraction

Table 10. 5: Solar fraction for each month's

Months	Jan	Feb	Mar	Apr	Ma y	Jun	Jul	Aug	Sep	Oct	Nov	Dec
Solar fraction	0.98	1	0.86	0.73	0.66	0.63	0.635	0.68	0.75	0.80	0.82	0.88

Annual solar contribution to heating load 0.78622

Annual heating load

365*783.4172934 kWh = 285,947.32 kWh

10.5 Unit price of solar energy

To determine the unit price of solar energy cost, P_e the life cycle cost has to be equal to the life cycle savings of the solar water heater during its life time

To determine the unit price equate equations and then determine unit price of solar energy for water heating.

LCS = LCC ……………………………………………………………………………….10.5

$$CI + C_m \frac{1}{i}\left(1 - \frac{1}{(1+i)^n}\right) = P_e f_a Q_a \left(\frac{1+i_e}{i-i_e}\right) * [1-\left(\frac{1+i_e}{1-i}\right)^n]$$

$$P_e = \frac{CI + C_m \frac{1}{i}\left(1 - \frac{1}{(1+i)^n}\right)}{f_a Q_a \left(\frac{1+i_e}{i-i_e}\right) * [1-\left(\frac{1+i_e}{1+i}\right)^n]}$$

= 0.24 Birr/kWh

Since unit price of solar water heater is less than that off electricity and fossil fuel economical aspect also viable.

10.6 payback period

To determine the payback period, the replacement cost for system is consider. Hence the investment of the solar water heater has to be pay backed by the life cycle saving of electricity or fuel cost.

LCCS = $C_f f_a Q_a \left(\frac{1+i_e}{i-i_e}\right)$*[1-$\left(\frac{1+i_e}{1-i}\right)^n$] …………………………………………………… 10.6

Where, LCCS = CI + RC at n = N_p

LCCS is the life cycle saving of electric and fuel cost (Birr)

RC is replacement cost equals to 207,127.298 Birr

C_f is the unit cost of electricity and fuel for the first years of analysis (Birr/kWh)

CI + RC = $C_f f_a Q_a \left(\frac{1+i_e}{i-i_e}\right)$*[1-$\left(\frac{1+i_e}{1-i}\right)^{N_P}$]………………………………………………… 10.7

For adama general hospital 70% of energy source for water heating is electric city and Seen from table 10.4 unit cost of electricity 1.674 Birr/kWh also the rest 30 % from fuel (diesel oil).

Unit cost of fuel

The price of diesel is 0.59 U.S. Dollar per litter (source global petrol price.com, last seen September 2, 2018)

United states Dollar ($1) to Ethiopia Birr equals to 27.75 Birr (last seen October 2, 2018)

The heating value of diesel fuel 48 MJ/kg =48,000 kJ/Kg

Since density of diesel fuel equals to 0.832 kg/L So one litter diesel oil has a heating value 11.11 kWh

Unit cost of fuel = 16.50 Birr/11.11 kWh = 1.482 Birr/kWh

The efficiency of a boiler is normally expressed as a percentage. Most of the boiler are between 88% to 91%, https://www.which.co.uk.

Take 88 % efficiency and total unit cost of the fuel 1.4852/0.88 = 1.7 Birr/kWh

Generally unit cost of conventional hot water generation system equals

= 0.3(1.7 Birr/kWh) + 0.7(1.674 Birr/kWh) ………………………………………….. 10.8

Then payback period is calculated as

$$N_p = \frac{\ln[1+\frac{(CI+RC)\left(\frac{i_e-i}{1+i_e}\right)}{C_f f_a Q_a}]}{\ln(\frac{1+i_e}{1+i})} = 5.7 \text{ years}$$

CHAPTER 11

CONCLUSIONS AND RECOMMENDATIONS

11.1 Conclusions

From the foregoing, the following conclusion can be drawn from the study; shows that solar water heater with evacuated tube solar collector has been done for Adama general hospital. A survey was carried out to establish the daily hot water demand of adama general hospital which was estimated to be 30.022 m^3 per day. An assessment of solar energy potential has been developed for Adama city and result shows that there exist high potential resources through the year, average solar irradiance 745 W/m^2. The result from technical feasibility study shows that evacuated tube solar collector can meet the hot water demand of the hospital by 52 Collectors on holding space 82.46 m^2 with two storage tank each capacity of 15.011 m^3 are uses to partially 84 % substitute diesel fuel and electricity. Similarly the economic analysis shows that initial investment cost 1,066,388.44 Birr and life cycle cost 2,003,254.14 Birr also unit cost per kWh equals to 0.24 Birr and the payback period of the project 5 years and 6 months.

11.2 Recommendations for further works

In the study of renewable energy sources appropriator weather data for specific location is essential but unfortunately this device is not available mainly so the only chance to get those data from satellite or empirical correlation so the concerned parts should give attention.

As we know this study and other at time also world focus on renewable energy especially solar energy and this transient energy form need commercials and programing software's for analysis so the university should licence at least populate software's like MAT-LAB, TRNSYS, etc.

Assessment of Ethiopia's solar thermal resource indicates that the country has huge potential for solar energy application. There are, however, challenges like low purchasing power, unfavourable public attitude towards the private sector.it is thus recommended that the government, nongovernment organization and public make coordinated effort to overcome the challenges.

The following point can be recommended for the further works

- More study should be conducted further in the area of solar thermal system and PV in the future.
- The same study can be done by consider thermos-physical property of fluids.
- Improving efficiency of evacuated tube collector with mini-compound reflector.
- Techo-econonical comparison of three most common collector types for different solar thermal areas.

REFERENCES

[1] Adel A.Ghoneim, Hany M.Shabana, Mohamed S.Shaaban and Adel M.Mohammedein, "performance of evacuated tube solar collector in hot climate" European international journal of science and technology, Volume 5, Issue 3, April 2016.

[2] Addisu Bekele "large scale application of solar water heating system in Ethiopia" MSc. thesis, department of mechanical engineering, Addis Abeba university, July 2007.

[3] Aman Sharma and Pathak A.K., "Evacuated tube solar collector importance and innovations in wide range applications," International journal of science and technology advancements, Volume 2, Issue 4, pp.39-44, 2016.

[4] Boiler energy efficiency, https://www.which.co.uk.

[5] Budihardjo, G.L. Morrison, "Performance of water- in-glass evacuated tube solar water heaters," International journal of science and technology advancements, Volume 8, Issue 3, pp. 49-56, 2009.

[6] Chien C. C., Kung C. K., Chang C. C., Lee W. S., Jwo C. S. and Chen S. L. "Theoretical and experimental investigation of a two-phase thermo-syphon solar water heater," Energy 36 (2011) 415-423.

[7] Chong K. K., Chay K. G. and Chin K. H. "Study of a solar water heater using stationary V-trough collector," Renewable Energy 39 (2012) pp-207-215**.**

[8] Dagim kebede **"**Design and analysis of solar thermal system for hot water supply to Minilk II hospital new building," department of mechanical engineering, Addis Abeba university, June 2016.

[9] Delfin silio salcines, carlos renedo estebanez and valentin castanera herrero" simulation of a solar domestic water heater system, with different collector efficiencies and different volume storage tanks"Avda. Los castros s/n, 39005 santander (spain), 2015.

[10] Dejene Assefa,"Techno-Economical Assessment of Parabolic trough steam Generation for Hospital," MSc. Thesis EGI-2011-031 mscekv839, KTH Industrial Engineering and Management,

[11] Demba Ndiaye, "Simplified model for Dynamic Simulation of Solar Systems with Evacuated Tube Collector," UNC Charlotte, 9201 University City Blvd, Charlotte, NC 28223, U.S.A, 2014.

[12] Dilip Mishra and Saikhedkar N.k., “a study and theoretical analysis of evacuated tube collectors as solar energy conversion device for water heating,” advance physics letter, Volume 1, Issue 3, pp. 26-35, 2014.

[13] Dimensioning and design of solar thermal system.”AEE-Institute for sustainable technologies (www.aee-intec.at), Austria development cooperation.

[14] Doerte Laing and Dorothea Lehmann, ”Concrete storage for solar thermal power plant and industrial process heat, ”International renewable energy conference, 24-25.11.2008 berlin.

[15] Electrical pumps catalogue, NOCCHI pentairy water

[16] Engineering design handbook, [1973] (laminar or turbulent flow, circular or noncircular pipes, smooth or rough surfaces horizontal or inclined pipes)

[17] Ethiopia national energy agency.[2013]

[18] Guidelines for energy efficiency in hospital, LIFE-ENVIROMENT,LIFE04 ENN/GR/000114,Athens,Greec, 2007.

[19] Hernandez E. and Reguzman,”Comparision of three system of solar water heating by thermosiphon,” Journal of physics series: Conference Series 687(2016)012007.

[20] http://www.alibaba.com/trade/search?fsb=y&IndexArea=producten&CatId=&SearchText=u+type+15+tubes+evacuated+solar+collector+cost&isPremium=y. (last seen September 3,2018.(Alibaba.com, global trade))

[21] Hydraulic fluid,”engineering design handbook”,U.S. Army material command, feb 12/1973.

[22] International energy agency, Renewables, 2017.

[23] Lingkai kong, Weixing yuan and Ning zhu, ”CFD simulation of thermal stratification heat storage water tank with an inside cylinder with opening,” 8th international cold climate HVAC 2015 conference, CCHAV 2015.

[24] John A. Duffie and William A. Beckman,”solar engineering of thermal process,” solar energy laboratory, university of Wisconsin-Madison, fourth edition, 2013.

[25] Luigi Mongibello, Nicola Bianco, Martina Caliano, Adriano de luca and Giorgio Graditi, ”transient analysis of a solar domestic hot water system using two different solvers,” 69th conference of the thermal machines engineering association, 2016.

[26] Maxi brochure 05 “saving energy with energy efficiency in hospitals” international energy agency December 2015.

[27] Ministry of water irrigation and electricity “federal democratic republic of Ethiopia” berlin energy transition dialogue, march 2017.

[28] Mishara D.,”A study and theoretical analysis of evacuated tube collectors as solar energy conversion device for water heating,” ICFAI University, 2014.

[29] Pumping selection considerations, pumping system tips sheet # 2, October 2005.

[30] Rokas valancius, andrius jurelionis, rolandas jonynas, vladislovas katinas and eugenijus perednis,”analysis of medium-scale solar thermal systems and their potential in Lithuania” energies 2015,8,5725-5737;doi:10.3390/en8065725.

[31] Sabiha M.A.,“Progress and latest development of evacuated tube solar collector” International journal of science and technology advancements, Volume 5, Issue , pp.27-38, 2016.

[32] Sadik kakac and hongtan liu, “heat exchanger selection, rating and thermal design, second edition,” university of Miami in 2002.

[33] Selvan Bellan, Jose Gonzalez-Aguilar, Manuel Romero, Muhammad M. Rahman, D. Yogi Goswami and Elias K.Stefanakos, “Numerical investigation of PCM-based thermal energy storage system,” Energy Procedia 69 (2015) 758 – 768.

[34] Selvakumar P., Somasundaram P. and Thangavel P., “Solar collector using thermionol D-12 as heat transfer fluid coupled with parabolic trough” international journal of engineering and technology, Volume 6, Issue 1, pp.110-117, 2014.

[35] Siva kumar, Mohan Kumar, Sanjeev kumar, and Charles, ”Experimental and theoretical investigation of evacuated tube solar collector with heat pipe,” International journal of innovative research in science, engineering and technology, Volume 6, Issue 3, pp.4050-4054, 2017.

[36] Soulayman S. and Sabbagh W. “Optimum tilt angle at tropical region,” International journal on renewable energy development,4(1) 2015:48-54.

[37] Soteris A. Kalogirou, “Solar thermal collectors and applications.” Progress in Energy and Combustion Science 30 (2004) 231–295.

[38] Tewolde Berhan G Egziabher ”Renewable energy projects in Ethiopia,” 2016.

[39] Tiwari G.N and Arvind Tiwari and Shyam, “Hand book of solar energy; theory, analysis and applications” http://www.springer.com/series/13509, 2016.

[40] Vishal G. Shelke1, Chinmay V. Patil2, Kishor R. Sontakke, Solar Water Heating Systems: A Review ISSN (Online): 2347-3878, Impact Factor (2014): 3.05.

[41]Xinyu Zhang, Shijun You, Wei Xu, Min Wang, Tao He and Xuejing Zheng, “Experimental investigation of the higher coefficient of thermal performance for water-in-glass evacuated tube solar water heaters in China,” Energy Conversion and Management 78(2014) 386-392.

[42] Xun yang,yong wang, and teng xiong, ”numerical and experimental study on a solar water heating system in lhasa,” energy 2017,10,963,doi:10.3390/en10070963.

[43] Zahedi H. R., Adam N. M., Sapuan S. M. and Ahmed M. H., ”Effect of storage tank geometry on performance of solar water heater,” Journal of Science and Industrial Research, Volume 6, Issue 6, pp. 146-151, 2007.

[44] Zambolin E. and Del Col D. “Experimental analysis of thermal performance of flat plate and evacuated tube solar collectors in stationary standard and daily conditions,” Solar Energy. 2010, 84: 1382-1396.

LIST OF PUBLICATIONS

Journal articles

Chandrabrabu V. and Gedlu S., " Evacuated tube solar collectors: A review," International journal of scientific Engineering and Research, Volume 6 Issue 12, pp 138-141, December 2018.

Chandrabrabu V., Samuiel G. and Gedlu S., "Dataset of Solar energy potential assessment for Adama City (Ethiopia)," journal of data in brief," www.elsevier.com/locate/dip

ANNEX A

Table A- 1: Property of different storage tank materials

Property of 300 K						Property of $\frac{K}{C_p}$ $(\frac{W/Km}{J/KgK})$
substance	**Melting point[K]**	$\rho\ [\frac{kg}{m^3}]$	$C_p\ [\frac{J}{kgK}]$	**K[W/Km]**	$\alpha * 10^6[\frac{m^2}{s}]$	**At 400 K**
Copper	1358	8933	385	401	117	393
aluminum	933	2702	903	237	97.1	240
Mild steel	1810	7832	434	63.9	18.8	58.7
Stainless steel	1670	7913	477	14.6	3.95	16.6
Lead	601	11,340	129	35.3	24.1	34
nickel	1728	8900	444	90.7	23	80
Iron	1810	7870	447	80.2	23.1	69.5

Table A- 2: Property of different Insulation materials

material	**K(W/Km)**	**Maximum service temperature(**℃)	$\rho[\frac{kg}{m^3}]$	$C_p\ [\frac{J}{kg\ K}]$
Glass fiber	0.032	343	56-72	38-39
Mineral fiber	0.036-0.055	649-1037	4.8-32	710-960
Calcium silicate	0.055	649	2330	712
Perlite	0.048	816	16	1260
Foamed Glass	0.058	565	144	1000
Polystyrene foam	0.029-0.039	74	16	1200
Polyurethane Foam	0.023	104	24 - 40	1600
Isocyanate foam	0.025	121	70	1045
Phenolic Foam	0.033	135	136	1000
Cellular plastic	0.040	100	37-51	39-46

Table A- 3: Solar radiation calculation for representative day of the months

9.35	9.38	8.9	7.32	6.86	6.8	7.96	8.23	8.4	9	9.25	8.73	**ns**
1367	1367	1367	1367	1367	1367	1367	1367	1367	1367	1367	1367	**Is**
8.558	8.558	8.558	8.558	8.558	8.558	8.558	8.558	8.558	8.558	8.558	8.558	**ϕ**
344	318	288	258	228	198	162	135	105	75	47	17	**n**
-23.05	-18.91	-9.59	2.22	13.45	21.18	23.09	18.79	9.41	-2.42	-12.95	-20.92	**δ**
86.33	87.04	88.54	90.33	92.06	93.34	93.67	92.94	91.43	89.64	88.07	86.70	**ωs**
31807817	33123618	35503313	37176696	37348471	36709602	36564497	37230083	37848225	37127604	35081609	32664744	**Ho**
11.5	11.6	11.8	12.0	12.2	12.4	12.5	12.4	12.2	12.0	11.7	11.5	**NS**
0.38	0.37	0.36	0.31	0.30	0.29	0.32	0.33	0.34	0.36	0.37	0.36	**a**
0.35	0.36	0.39	0.50	0.53	0.54	0.47	0.46	0.44	0.39	0.37	0.39	**b**
21493213	22366006	23662630	23148255	22460320	21857085	23176423	23942442	24631505	24739019	23591963	21780148	**H**
5798576	6108610	7509082	10099461	10693185	10628121	9557380	9346254	9109811	7867514	6827499	6885876	**Hd**
24	24	24	24	24	24	24	24	24	24	24	24	**β**
86.33	87.04	88.54	90.33	92.06	93.34	93.67	92.94	91.43	89.64	88.07	86.7	**1, ω's**
96.75	95.43	92.67	89.39	86.21	83.85	83.23	84.60	87.37	90.66	93.64	96.06	**2, ω's**
86.32	87.04	88.54	89.78	88.69	88.78	87.67	88.14	89.09	89.63	88.07	86.70	**min ω's**
1.043	1.043	1.02	0.94	0.84	0.74	0.72	0.77	0.88	0.98	1.03	1.04	**Num Rb**
0.82	0.86	0.93	0.99	1.07	1.00	0.99	1.01	1.01	0.97	0.91	0.84	**den Rb**
1.27	1.21	1.09	0.94	0.83	0.74	0.72	0.77	0.87	1.00	1.13	1.24	**Rb**
1.46	1.46	1.46	1.46	1.46	1.46	1.46	1.46	1.46	1.46	1.46	1.46	**Rd**
0.54	0.54	0.54	0.54	0.54	0.54	0.54	0.54	0.54	0.54	0.54	0.54	**Rr**
0.4	0.2	0.2	0.2	0.2	0.2	0.2	0.2	0.2	0.4	0.7	0.7	**ρ**
1.6E+07	1.6E+07	1.6E+07	1.3E+07	1.2E+07	1.1E+07	1.4E+07	1.5E+07	1.6E+07	1.7E+07	1.7E+07	1.5E+07	**Hb**
33.09	31.02	31.1	29.62	27.74	26.19	26.28	27.44	29.45	33.75	37.88	36.78	**HT**

Table A- 4: Ambient temperature for the representative day of the months

T(H)JAN17	T(H)FEB 16	T(H)MAR1	T(H)APR15	T(H)MAY1	T(H)JUN11	T(H)JUL17	T(H)AUG1	T(H)SEP15	T(H)OCT15	T(H)NOV1	T(H)DEC10
17.3186	20.9728	20.6924	22.51034	20.41034	16.7661	16.12305	19.97281	19.7974	19.81277	23.81649	20.6023
16.9386	19.7782	20.15508	22.22289	19.96257	16.10583	15.59368	19.6782	19.41982	19.31892	23.37947	20.41882
16.55859	19.4836	19.61777	21.93543	19.5148	15.44557	15.0643	19.3836	19.04224	18.82508	22.94245	20.23534
16.17858	19.189	19.08045	21.64798	19.06704	14.7853	14.53492	19.08899	18.66466	18.33123	22.50543	20.05187
15.79857	18.8955	18.54313	21.36052	18.61927	14.12503	14.00554	18.79438	18.28708	17.83738	22.06841	19.86839
15.41857	18.4598	18.00581	21.07307	18.17151	13.46477	13.47617	18.49977	17.9095	17.34353	21.63139	19.68492
15.03856	18.2056	17.46849	20.78561	17.72374	12.8045	12.94679	18.20516	17.53193	16.84969	21.19437	19.50144
14.65855	17.9999	16.93117	20.49816	17.27598	12.14424	12.41741	17.91056	17.15435	16.35584	20.75735	19.31796
14.27855	17.6211	16.39385	20.2107	16.82821	11.48397	11.88803	17.61595	16.77677	15.86199	20.32033	19.13449
14.98967	18.0957	17.13105	20.93311	17.24225	12.20174	12.3907	18.23415	17.27052	16.48967	20.87656	19.67156
18.6124	22.10658	21.27131	24.34883	19.9593	16.60077	15.65116	21.28759	20.09108	20.1124	24.08527	22.12984
21.91316	25.761	25.04362	27.46098	22.43487	20.60884	18.62185	24.06967	22.66096	23.41316	27.0088	24.36965
24.66156	28.80387	28.18464	30.05233	24.49617	23.94618	21.09541	26.38617	24.80079	26.16156	29.4431	26.23463
26.66574	31.02278	30.47513	31.94198	25.9993	26.37983	22.89917	28.07541	26.36118	28.16574	31.21823	27.59461
27.7858	32.26285	31.7552	32.99804	26.83935	27.7399	23.90722	29.01946	27.23323	29.2858	32.21028	28.35465
27.94356	32.43751	31.93549	33.14678	26.95767	27.93146	24.0492	29.15243	27.35605	29.44356	32.35001	28.4617
27.128	31.53457	31.00343	32.37783	26.346	26.94114	23.3152	28.46503	26.72108	28.628	31.62766	27.90828
25.39605	29.61706	29.02406	30.74485	25.04704	24.83806	21.75645	27.00524	25.37264	26.89605	30.09365	26.73304
21.54554	25.22173	24.3454	26.95011	22.00863	19.97215	18.35614	23.64422	22.9845	22.85171	26.56501	24.01385
20.77478	24.59525	23.9415	26.50513	21.68875	19.36263	17.5507	23.19285	22.6154	22.41342	26.08505	23.67323
20.00402	23.96878	23.5376	26.06015	21.36887	18.75311	16.74525	22.74147	22.1574	21.97512	25.60509	23.33262
19.23327	23.3423	23.1337	25.61517	21.04899	18.14359	15.93981	22.2901	21.6798	21.53683	25.12513	22.992
18.46251	22.71582	22.7298	25.17019	20.72911	17.53406	15.13436	21.83873	21.1245	21.09853	24.64517	22.65139
17.69175	22.08935	22.3259	24.72521	20.40923	16.92454	14.32892	21.38735	20.7705	20.66023	24.16521	22.31077

Table A- 5: Constant for calculation of local Nu for circular Tubes With constant Heat Rate

Brandt Number	a	b	m	n
0.7	0.00398	0.0114	1.66	1.12
10	0.00236	0.00857	1.66	1.13
∞	0.00172	0.00281	1.66	1.29
NU_{∞}=4.4				

ANNEX B

Appendix B: 1 Determine heat lost coefficient

```
function[ul]=outer(tog)
eog=0.08;        % emisivity of outer glass
a=5.6697e-8;     % steven boltzman constant [w/m^2*k^4]
ta=21.8+273;     % average ambient temperature[K]
ts=0.0552*ta^1.5; % sky temperature
vw=3.5;          % average wind speed[m/s]
eig=0.01;        % emisivity of inner glass
tig=120+273;     % inner glass intilization[K]
l=1.8;           % length of collector[m]
do=0.058;              %outer tube diameter[m]
di=0.048;              %inner tube diameter[m]
eff=[1/eog+1/eig-1]^-1;     % effective emisivity
Aog=pi*do*l;               % lateral area of outer glass
Aig=pi*di*l;               % lateral area of inner glass
hradog=eog*a*((tog^4-ts^4)/(tog-ta));    % coefficient of radiation heat transfer from outer
glass
hradig=eff*a*((tig^4-tog^4)/(tig-tog));  % coefficient of radiation heat transfer from inner
glass
hw=5.7*3.8*vw;               % convection heat transfer coefficient[m/s]
hwp=(Aog/Aig)*0.6*hw;        % Outer glass convection
ul=1/[1/(hradig+hwp)+(1/hradog)];   %  heat loss coefficient
top1 = tig - [(ul/hradig)*(tig-ts)] % outlet temperature[K]
end
```

Published with MATLAB® R2017a

Appendix B: 2 Variation of outlet water temperature with mass flow rate steady state analysis

```
% variation of outlet water temperature withh mass flow rate
% steady state analysis
clear all
clc
cpw =4200;              % specific heat of water[J/kg*K]
ti=295.8;               % water inlet temperature[K]
I=745;                  % Average irradiance [w/m^2]
Aog=4.91724;            % area of absorber tube[m^2]
n=0.9;                  % collector efficiency
mf=(0.005:0.001:0.03);          % input mass flow rate range[Kg/s]
two=((n*I*(Aog))./(mf*cpw))+ti;   % outlet water temperature[k]
twoc=two-273;                   % outlet water temperature[c^0]
plot(mf,twoc)
grid on
xlabel('mass flow rate')
ylabel('temperature in degree celcius')
title('outlet temperature variation with respective mass flow rate')
```

Published with MATLAB® R2017a

Appendix B: 3 Transient analysis of solar water heating system

```
% Transient analysis of temperature
% hourly temperature variation of water stream and storage tank
% given global radiation and ambient temperature value for a year
% consider u-type evacuated tube solar collector
% design parameters
clear all
clc
tms= 0.005;                 % thickness of storage tank [m]
tfg= 0.016;                 % thickness of fiber glass [m]
Lt =1.8;                    % length of collector [m]
di=0.01;                    % inner diameter of copper tube [m]
ds=2.2;                     % diameter of storage tank [m]
Aog=4.91724;                % area of outer glass [m^2]
Aig=4.06944;                % area of inner glass [m^2]
Aw=1.6485;                  % copper tube surface area [m^2]
Ast=36.9578;                % storage tank surface area [m^2]
Vs=15.011;                  % storage tank volume [m^3]
Gabso=0.01;                 % absorivity of glass
Pabso=0.96;                 % absorivity of plate
```

```
Tabso=0.9;                    % absorivity of riser tube
Gtrans=0.92;                  % transmissivity of glass
Ep=0.01;                      % emisivity of plate
Eg=0.08;                      % emissivity of glass
Vw=3.5;                       % wind speed [m/s]
sigma=5.67e-8;                % Boltzman constant[w/m^2.K^4]
phi= 8.558*(pi/180);          % latitude of adama city[rad]
beta=24*(pi/180);             % collector slope(south facing) [rad]
mg=4.768875;                  % mass of glass[kg]
mp=2.89502976;                % mass of plate[kg]
mw=4.05172451;                % mass of water[kg]
mf=0.0227;                    % mass flow rate of a water[kg/s]
mfs=2.361;                    % mass flow rate of storage tank[kg/s]
Cpg =830;                     % specific heat of glass [J/kg*K]
Cpp =8933;                    % specific heat of plate [J/kg*K]
Cpw =4185;                    % specific heat of water [J/kg*K]
kw =0.625;                    % thermal conductivity of water [w/m^2.k]
ks=63.9;                      % thermal conductivity of mild steel [w/m*K]
ksin=0.032;                   % thermal conductivity of fiber glass [w/m.k]
prw=3.374784;                 % prandtl number of water
Re=249.15;                    % Reynolds number
Nuinf =4.4;                   % nusselt number at infinity
a =0.00398;                   % nusselt number constant
b =0.0114;                    % nusselt number constant
m=1.6;                        % nusselt number constant
n=1.12;                       % nusselt number constant
N=15;                         % number of riser tube
wdens=988;                    % density of water[kg/m^3]
deltt=60;                     % time step
H=4.25;                       % height of storage tank[m]
Dh =0.01;                     % hydraulic diameter
r1=0.005;                     % radius of copper tube[m]
r2=0.02;                      % radius of aluminium fin[m]
r3=0.024;                     % radius of inner glass[m]
r4=0.029;                     % radius of outer glass[m]
KAl=237;                      % thermal conductivity of aluminium [w/m*K]
kcu=401;                      % thermal conductivity of copper [w/m*K]
Kig=1.14;                     % thermal conductivity of borosilicate glass [w/m*K]
pl=58.5216;                   % perimeter of selective coating[m]
pith=340.875;                 % perimeter of the n surface[m]

% solar radiation data input with ambient temperature
load raddata2.m;
data1= zeros(24,2);
for j=1:365
    data1(:,:,j) = raddata2(j+(23*(j-1)):j*24,:);
end
%%%%%
Tp=zeros(24,365);Tp1=zeros(24,365);Tp2=zeros(24,365);Tp3=zeros(24,365);
```

```
Tg=zeros(24,365);Tg1=zeros(24,365);Tg2=zeros(24,365);Tg3=zeros(24,365);
Two=zeros(24,365);Two1=zeros(24,365);Two2=zeros(24,365);Two3=zeros(24,365);
Upw2=zeros(24,365);Ts=zeros(24,365);Ts1=zeros(24,365);Ts2=zeros(24,365);
Ts3=zeros(24,365);Upw1=zeros(24,365);Uls1=zeros(24,365);Ic1=zeros(24,365);
Uls2=zeros(24,365);It1=zeros(24,365);It2=zeros(24,365);Ic2=zeros(24,365);
Qu1=zeros(24,365);
%%%%%%
% This Approximates the Plate, Glass, Water and Storage Temperature
 for j=1:365
    Grr=data1(:,1,j);
    Taa=data1(:,2,j);
    for i=1:24
        Gr=Grr(i);
        T=Taa(i);
% Incident radiation
 It=Gr;
 Ic=It*Gtrans*Pabso ;
 Tsky=0.0552*(Ta0)^1.5;        % sky temperature
 hradog = Eg*sigma*(Tg0^4-Tsky^4)/(Tg0-Ta0);
 hw=5.7*3.8*Vw;
 hwp=(Aog/Aig)*0.6*hw;
 F=Re*prw*(Dh/Lt);
 G=Re*prw*(Dh/Lt);
 Ulms= ks/tms;
 Ulfg= ksin/tfg;
 Ulcfg=2.8+3.5*Vw;
 hradp = Ep*sigma*(Tp0^4-Tg0^4)/(Tp0-Tg0);
 Uga = ((1/hradog)+ (1/hwp))^-1;
 Nud = Nuinf+((a*(F)^m))/(1+b*(G)^n);
 Upw = (Nud*kw)/di;
 Uls = 1/[1/( Ulfg+ Ulcfg)+1/ Ulms];

% initial temperature assumption
 Ta0=T+273;           % ambient temperature [K]
 Tg0=Ta0+0.25;        % initial glass temperature [K]
 Tp0=Ta0+1.0;         % initial plate temperature [K]
 Twi0=Ta0;            % initial inlet water temperature [K]
 Two0=Ta0+0.75;       % initial outlet water temperature [K]
 Ts0=Ta0+0.75;        % initial storage tank temperature [K]

% calculation of Tg1,Tp1,Tw1 and Ts1 for each day in the year
 Tg1=((Aog*It*Gabso*deltt)/(mg*Cpg))+((deltt*Aog*hradp*Tp0)/(mg*Cpg)+...
    ((deltt*Aog*Uga*Ta0)/(mg*Cpg))+((1-(((Aog*hradp)+(Aog*Uga))*...
    (deltt/(mg*Cpg))))*Tg0));
 Tp1=Tp0+((Gtrans*Pabso*Aig*It*deltt)/(mp*Cpp))-((Aig*hradp*Tp0*deltt)/...
    (mp*Cpp))+((Aig*hradp*Tg0*deltt)/(mp*Cpp))-((Aw*Upw*Tp0*deltt)/...
    (mp*Cpp))+((Aw*Upw*((Two0+Twi0)/2)*deltt)/(mp*Cpp));
 Two1=Two0+((Aw*Upw*Tp0*deltt)/(mw*Cpw))-((Aw*Upw*Two0*deltt)/...
  (2*(mw*Cpw)))-((Aw*Upw*Twi0*deltt)/(2*(mw*Cpw)))-((mf*Cpw*Two0*deltt)/...
```

```
 (mw*Cpw))+((mf*Cpw*Twi0*deltt)/(mw*Cpw));
Ts1=(1-((Uls*Ast*deltt)/(wdens*Cpw*Verse)))*Ts0+((mfs*Cpw*deltt*Two0)/...
    (wdens*Cpw*Verse))+((Uls*Ast*deltt*Ta0)/(wdens*Cpw*Verse))-...
    ((mfs*Cpw*deltt*Twi0)/(wdens*Cpw*Verse));
    end

%%% temperature for each day of the year are stored as:
Tp2(j,i)=Tp1;
Tg2(j,i)=Tg1;
Two2(j,i)=Two1;
Ts2(j,i)=Ts1;
Upw1(j,i)=Upw;
Uls1(j,i)=Uls;
It1(j,i)=It;
Ic1(j,i)=Ic;
end

%%%%%%%%%%% main program %%%%%%%%%%%
for j=1:365
   grr=data1(:,1,j);
   taa=data1(:,2,j);
   for i=1:24
       gr=grr(i);
       t=taa(i);
       Ta0=t+273;

% define input varation
Lr =3.5;                % length of riser tube (COPPER TUBE)[m]
Hs =4.25;               % height of storage tank[m]
n =50;                  % number of nodes
del_i=Lr/(n-1);         % collector length input
del_s=Hs/(n-1);         % storage length input

% initial temperature assumption
Tw_i=Ta0;
T_s=Ta0;
% time gradient
t_2=60;
del_t=t_2/(n-1);
t(1)=0;
% temperature variation of glass cover, absorber plate and water stream
Tp3=Tp2(i,j);
Upw2=Upw1(i,j);
Uls2=Uls1(i,j);
It2=It1(i,j);
Ic2=Ic1(i,j);
% initial temperature
Two(n,:)=Ta0;        % inlet water temperature[K]
Ts(n,:)=Ta0;         % inlet storage temperature[K]
```

```
% loop to generate(x) position matrix
for z=1:n
    x(z)=del_i*(z-1)
    x(z)=del_s*(z-1)
end
% initiate iteration variable
m=1;              % time count
mm=1;             % plot count
% start while loop to run until convergence it met
while t(m)<t_2
% loop to calculate updated temperature based on governing equation
    for k=1:n
        if k==1
   Two(k,m+1)=Two(k,m)+((pi*di*N*(del_i)*It2*Tabso*Gtrans*del_t)/...
  (Cpw*wdens*N*(del_i)*((pi*(di^2))/4)))+(((Upw2*del_t*pi*...
   di*N*(del_i))/(Cpw*wdens*N*(del_i)*((pi*(di^2))/4)))*(Tp3-...
  ((Two(k,m)+Tw_i)/2)))-(((mf*del_t)/(wdens*(del_i)*N*...
  ((pi*(di^2))/4)))*(Two(k,m)-Tw_i));

   Ts(k,m+1)=Ts(k,m)+(((mfs*Cpw*9. *del_t)/(Cpw*wdens*del_s*...
 ((pi*(ds^2))/4)))*(Two(k,m)-Tw_i))-(((Uls2*9. *del_t*pi*ds*...
   (del_s))/(Cpw*wdens*del_s*((pi*(di^2))/4)))*(T_s-Ta0));

elseif k==n
        Two(k,m+1)= Two(k,m)+((pi*di*N*(del_i)*It2*Tabso*Gtrans*del_t)/...
        (Cpw*wdens*N*(del_i)*((pi*(di^2))/4)))+(((kw*Upw2*del_t*pi*...
         di*N*(del_i))/(Cpw*wdens*N*(del_i)*((pi*(di^2))/4)))*(Tp3-...
         ((Two(k,m)+Two(k-1,m))/2)))-(((mf*del_t)/(wdens*N*(del_i)*...
         ((pi*(di^2))/4)))*(Two(k,m)-Two(k-1,m)));

        Ts(k,m+1)=Ts(k,m)+(((mfs*Cpw*9.*del_t)/(Cpw*wdens*del_s*...
        ((pi*(ds^2))/4)))*(Two(k,m)-Tw_i))-(((k*Uls2*9.*del_t*pi*ds*...
        (del_s))/(Cpw*wdens*del_s*((pi*(ds^2))/4)))*(Ts(k,m)-Ta0));

        else
      Two(k,m+1)=Two(k,m)+((pi*di*N*(del_i)*It2*Tabso*Gtrans*del_t)/...
     (Cpw*wdens*N*(del_i)*((pi*(di^2))/4)))+(((k*Upw2*del_t*pi*...
      di*N*(del_i))/(Cpw*wdens*N*(del_i)*((pi*(di^2))/4)))*(Tp3-...
      ((Two(k,m)+Two(k-1,m))/2)))-(((mf*del_t)/(wdens*N*(del_i)*...
      ((pi*(di^2))/4)))*(Two(k,m)-Two(k-1,m)));

      Ts(k,m+1)=Ts(k,m)+(((mfs*Cpw*9. *del_t)/(Cpw*wdens*del_s*...
     ((pi*(ds^2))/4)))*(Two(k,m)-Tw_i))-(((k*Uls2*9.*del_t*pi*ds*...
     (del_s))/(Cpw*wdens*del_s*((pi*(ds^2))/4)))*(Ts(k,m)-Ta0));

      Qu=(mf*Cpw*(Two(k,m)-Ta0));
        end
    end
```

```
    t(m+1)=t(m)+del_t;
    %important to put all the (m+1) variable before the m=m+1 line
    m=m+1;                  % update time counter
    mm=mm+1;                % update plot counter
    %condition statement to check and make sure while loop does not run
    %indefinitily (use control C to stop infinite loop)
    if m==2001
       fprintf('Autobreak')
       break
    end
 end
 %Temperature for each day of the years are stored as
 Two3(i,j)=Two(k,m+1);
 Ts3(i,j)=Ts(k,m+1);
 Qu1(i,j)=Qu;
   end
end
%generate figure and results
figure(1)
plot(Two3)
plot(Ts3)
plot(Qu1)
%This stores for the selected day for plotting
%water stream
TwJ17=Two3(:,17); TwF16=Two3(:,47); TwM16=Two3(:,75); TwA15=Two3(:,105);
TwM1=Two3(:,121); TwJ11=Two3(:,162); TwJu17=Two3(:,199); TwA16=Two3(:,228);
TwS15=Two3(:,258); Tw015=Two3(:,288); TwN14=Two3(:,318); TwD10=Two3(:,344);
%storage tank
TsJ17=Ts3(:,17); TsF16=Ts3(:,47); TsM16=Ts3(:,75); TsA15=Ts3(:,105);
TsM1=Ts3(:,121); TsJ11=Ts3(:,162); TsJu17=Ts3(:,199); TsA16=Ts3(:,228);
TsS15=Ts3(:,258); Ts015=Ts3(:,288); TsN14=Ts3(:,318); TsD10=Ts3(:,344);

%useful heat gain
QuJ17=Qu1(:,17); QuF16=Qu1(:,47); QuM16=Qu1(:,75); QuA15=Qu1(:,105);
QuM1=Qu1(:,121); QuJ11=Qu1(:,162); QuJu17=Qu1(:,199); QuA16=Qu1(:,228);
QuS15=Qu1(:,258); QuO15=Qu1(:,288); QuN14=Qu1(:,318); QuD10=Qu1(:,344);
i=1:24;
% plot the water temperature, storage tank temperature and useful heat gain
plot(i,real(TwF16),'r',i,real(TwM1),'b',i,real(TwJu17),'k',i,real(TwN14),'g','linewidth',2)
xlabel('Time in hours','fontsize',12)
ylabel('Temperature in Degree celcius','fontsize',12)
title('temperature variation of water stream','fontsize',12)
legend('Two-Feb','Two-may','Two-JUl','Two-Nov')
grid
pause
clf
plot(i,real(TsF16),'r',i,real(TsM1),'b',i,real(TsJu17),'k',i,real(TsN14),'g','linewidth',2)
xlabel('Time in hours','fontsize',12)
ylabel('temperature in degree celcius','fontsize',12)
```

```
title('temperature variation of storage tank','fontsize',12)
legend('Ts-Feb','Ts-may','Ts-Jul','Ts-Nov')
grid on
pause
clf
plot(i,real(QuJu17),'r',i,real(QuN14),'b','linewidth',2)
xlabel('Time in hours','fontsize',12)
ylabel('Qu(MJh)','fontsize',12)
title('usefull heat gain(Qu) for JUY.17 and NOV. 14','fontsize',12)
legend('Qu-Feb','Qu-may','Qu-Jul','Qu-Nov')
grid on
pause
clf
```

Published with MATLAB® R2017a

ANNEX C

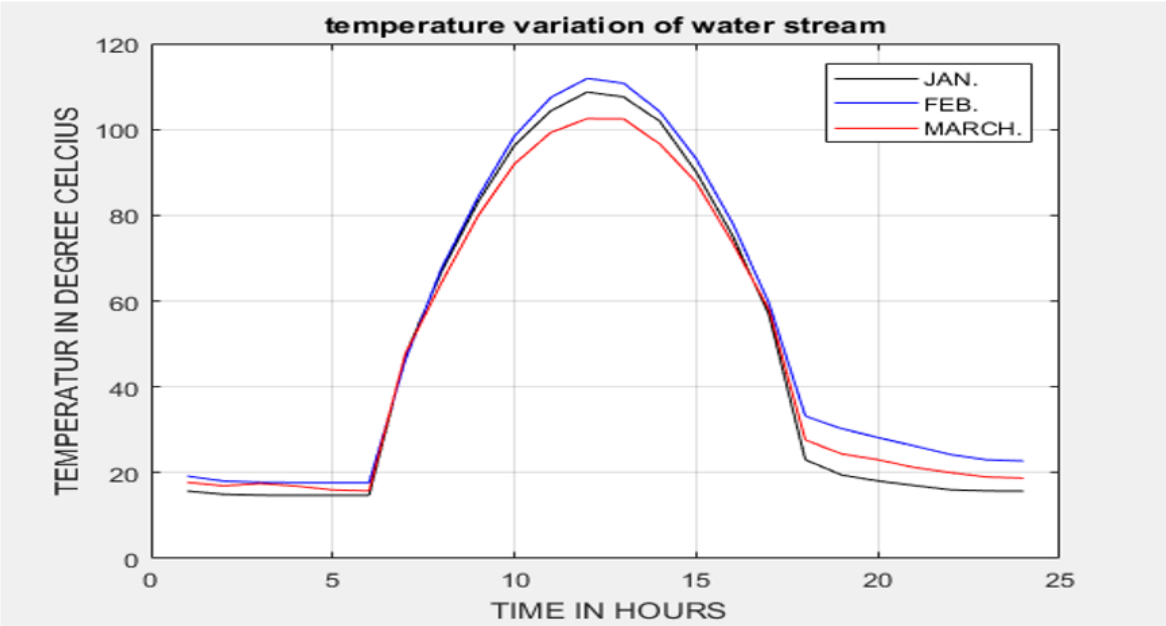

Figure C- 1: Collector outlet water temperature in winter

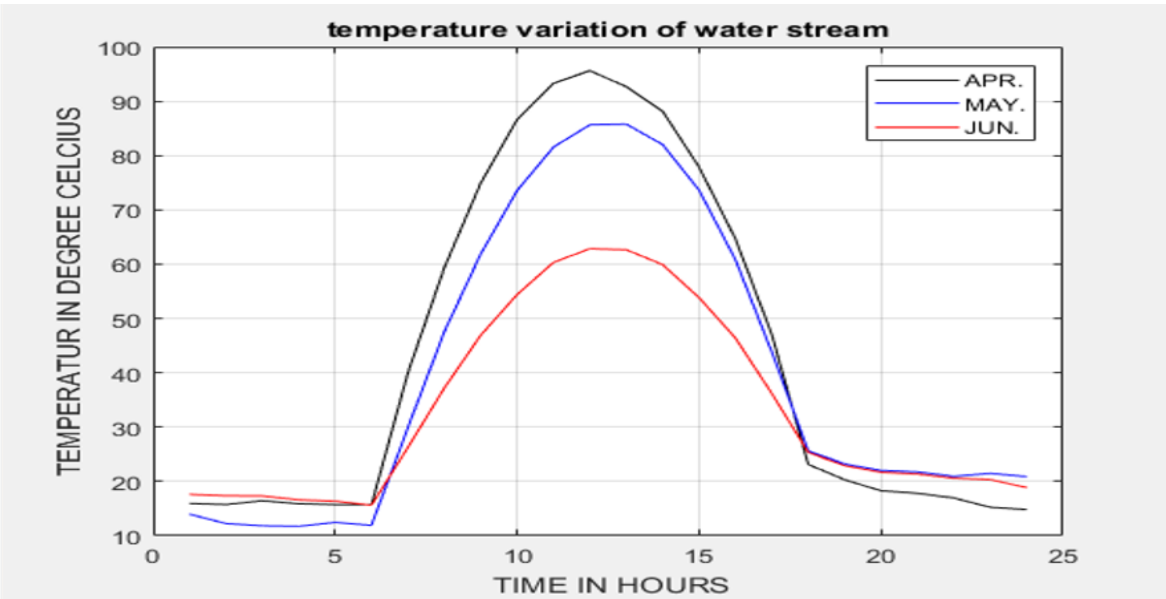

Figure C- 2: Collector outlet water temperature in spring

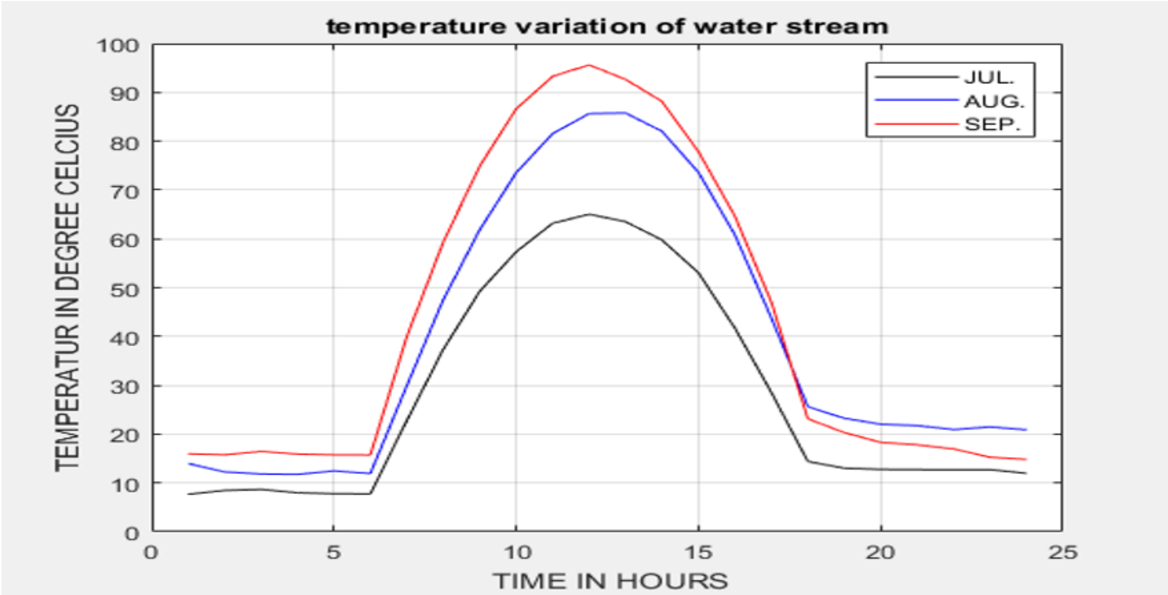

Figure C- 3: Collector outlet water temperature in summer

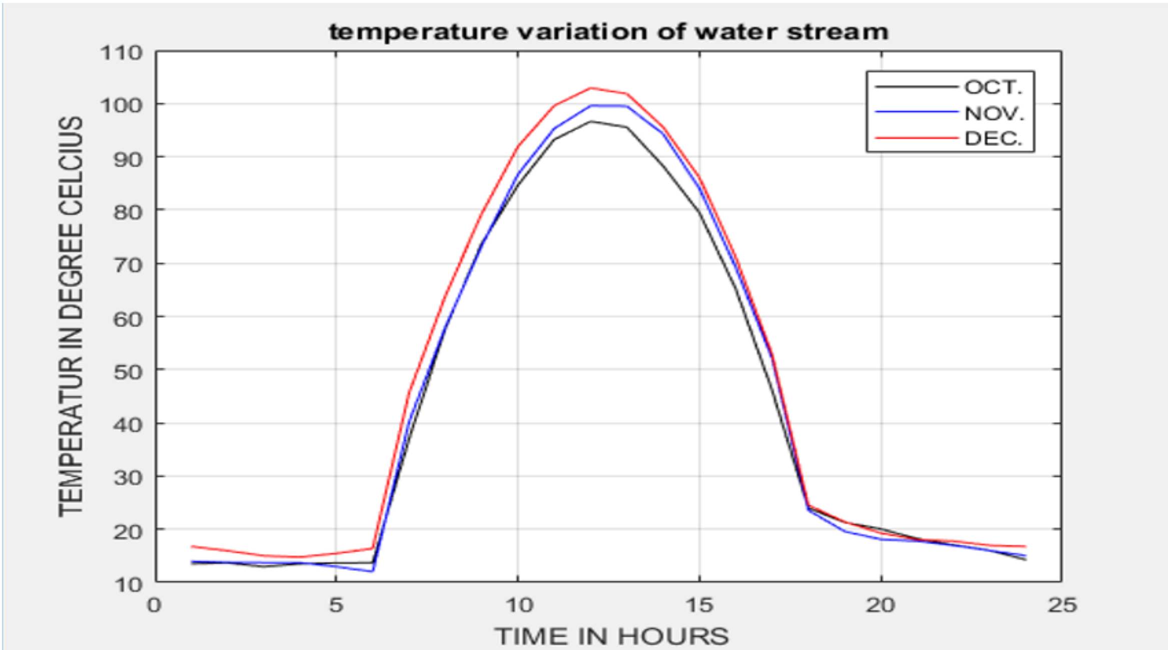

Figure C- 4: Collector outlet water temperature in autumn

ANNEX D

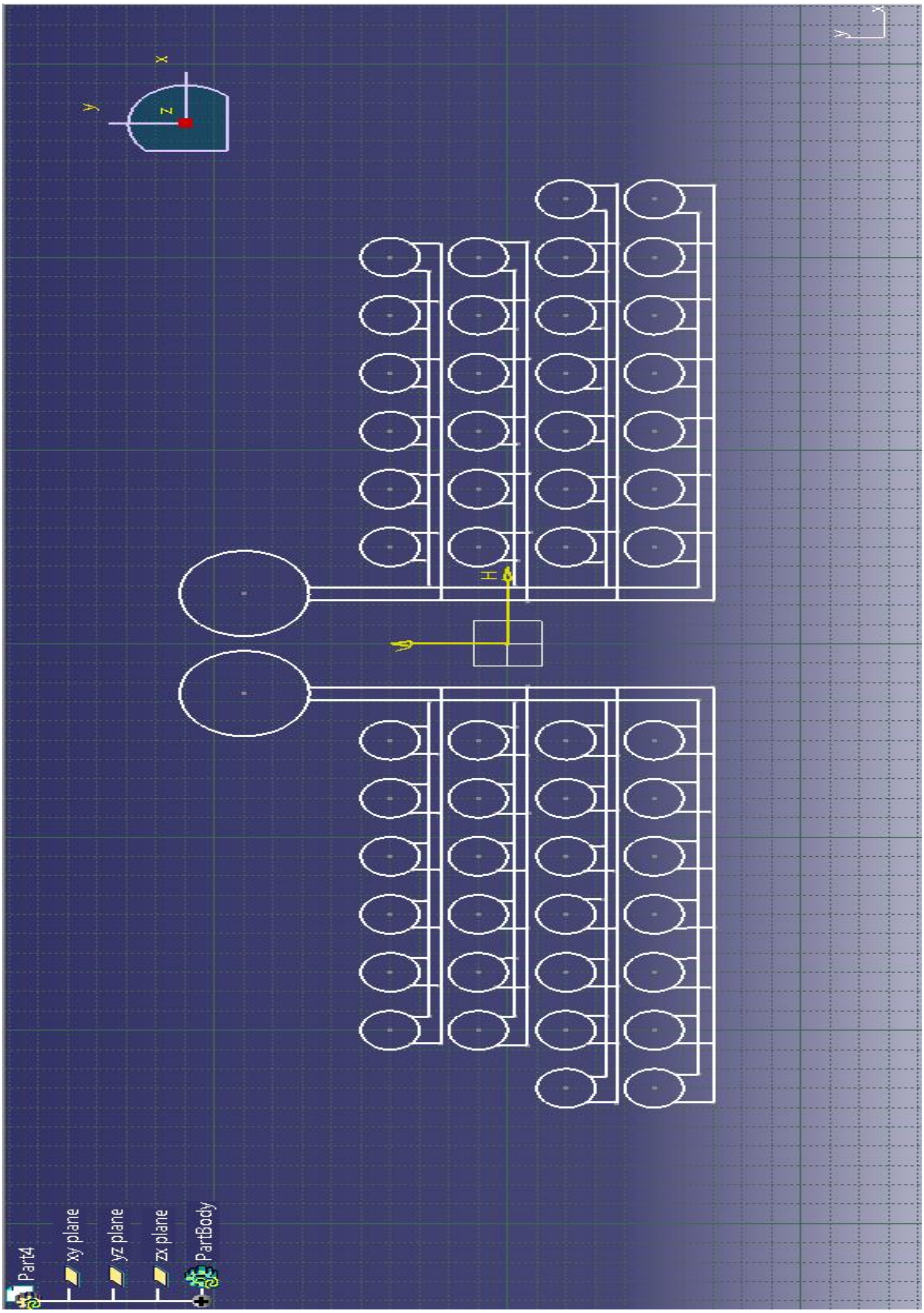

Figure D- 1: Solar water heating system layout (CATIA V5 R19)

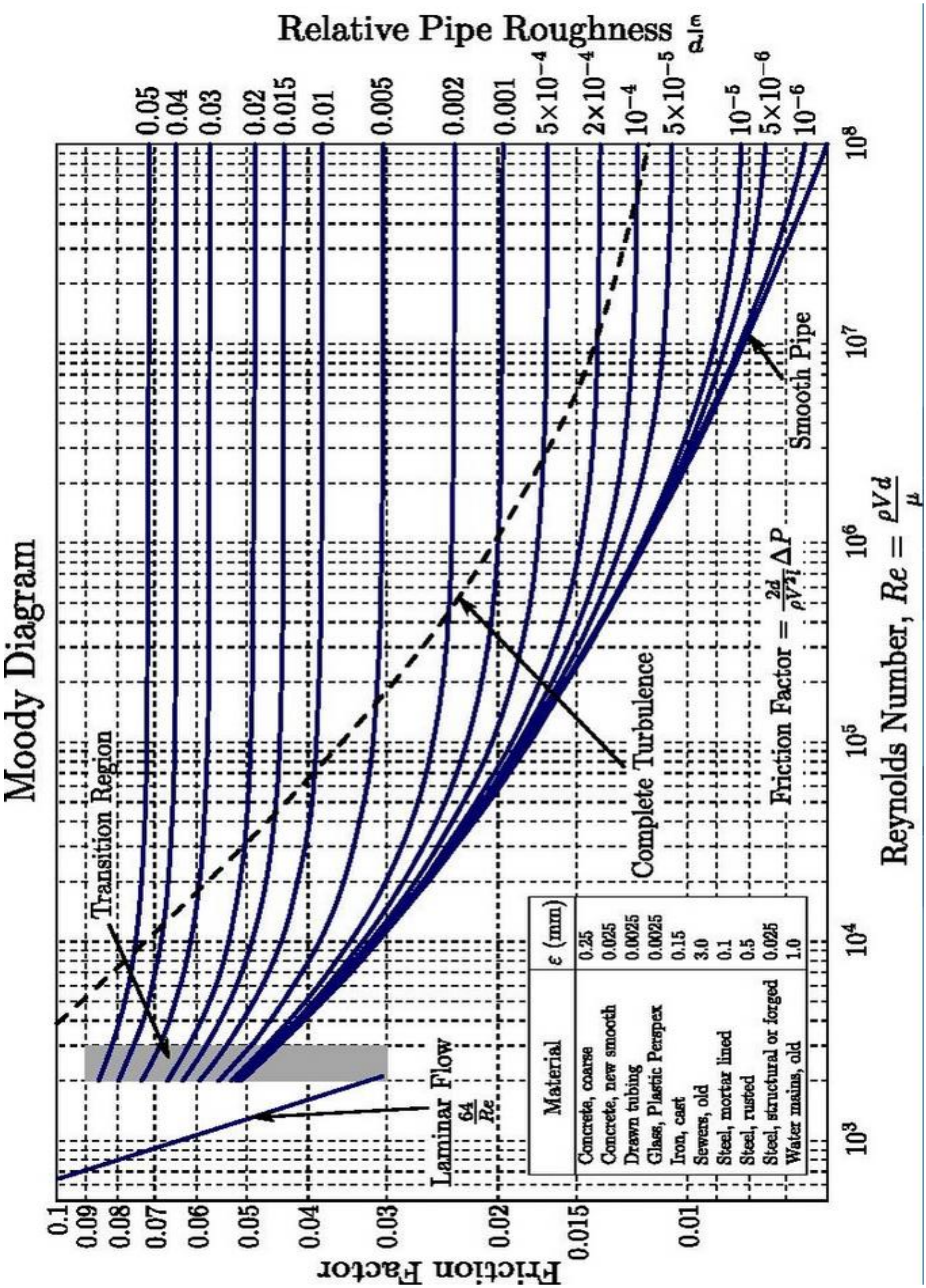

Figure D- 2: Moody chart

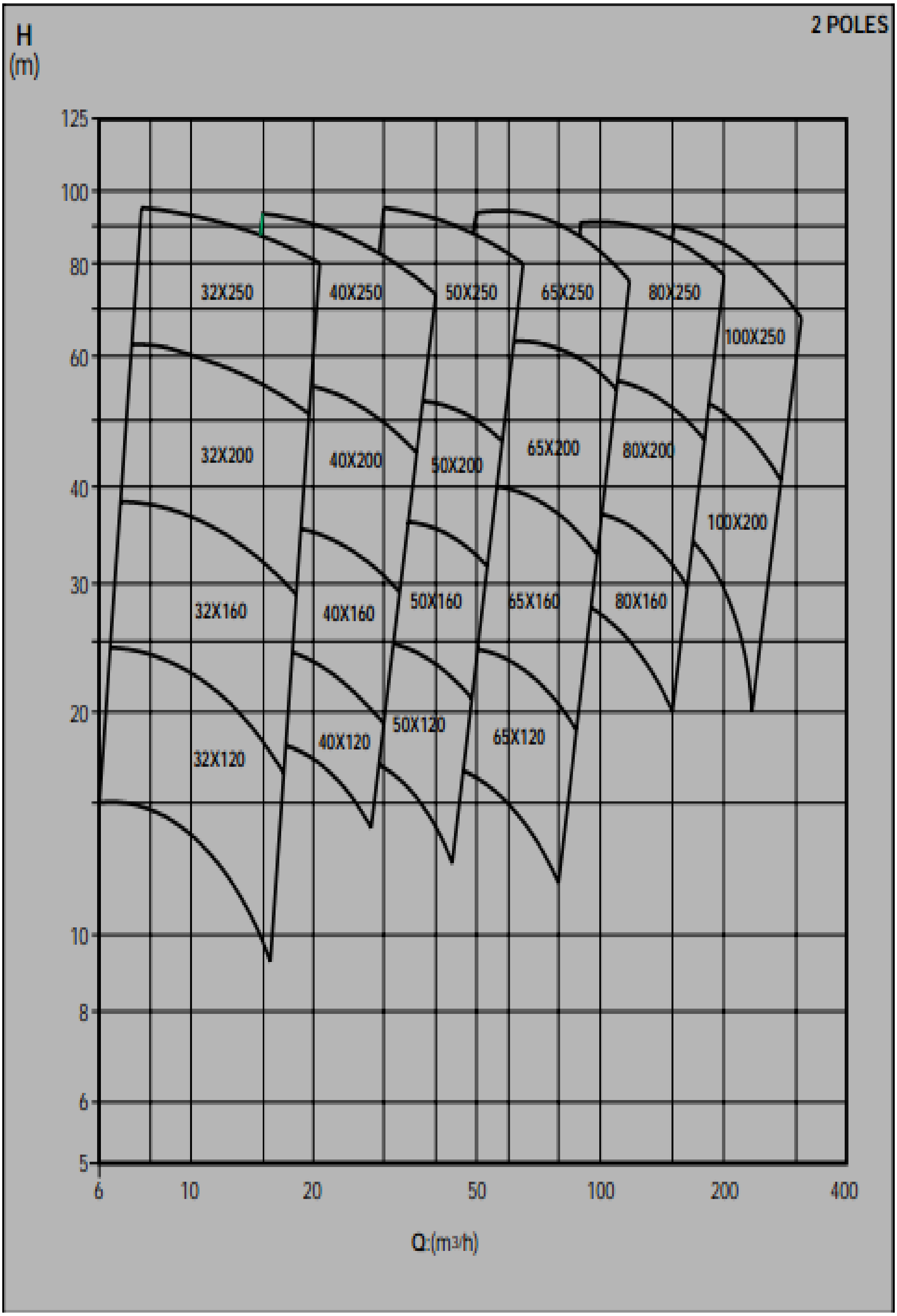

Figure D- 3: Pump performance range